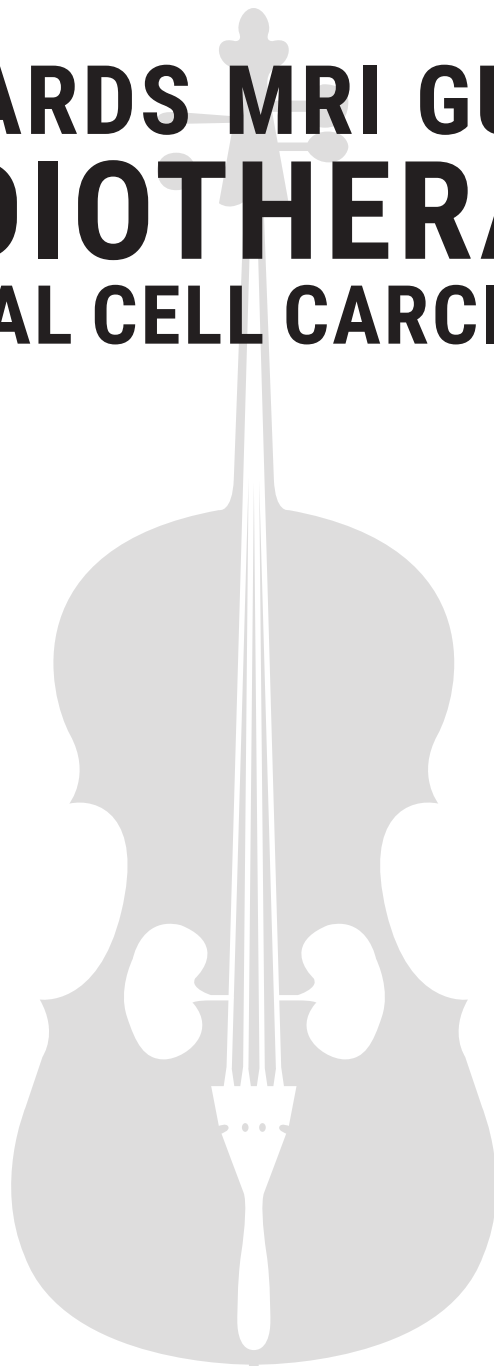


# TOWARDS MRI GUIDED RADIOTHERAPY OF RENAL CELL CARCINOMA



FIEKE PRINS

## **Towards MRI guided radiotherapy of renal cell carcinoma**

PhD thesis, Utrecht University, The Netherlands

© Fieke M. Prins, Utrecht, 2018

All rights reserved. No part of this thesis may be reproduced or transmitted in any form or by any means without prior written permission from the author. The copyright of the papers that have been published or have been accepted for publication has been transferred to the respective journals.

Publication of this thesis was financially supported by Department of Radiation Oncology UMC Utrecht, Elekta B.V., Chipsoft B.V., RT-IDea B.V., Pfizer B.V., Astellas Pharma B.V., Ipsen B.V., Sectra Benelux and Pap&Mam.

Layout and cover design

Printing

ISBN

Design Your Thesis, [www.designyourthesis.nl](http://www.designyourthesis.nl)

Ridderprint B.V. [www.ridderprint.nl](http://www.ridderprint.nl)

978-94-6299-977-0

# **Towards MRI guided radiotherapy of renal cell carcinoma**

Vorbereiding voor de ontwikkeling van MRI gestuurde  
radiotherapie van nierceltumoren

(met een samenvatting in het Nederlands)

Proefschrift

ter verkrijging van de graad van doctor aan de Universiteit Utrecht  
op gezag van de rector magnificus, prof. dr. G.J. van der Zwaan,  
ingevolge het besluit van het college voor promoties  
in het openbaar te verdedigen  
op donderdag 31 mei 2018 des middags te 2.30 uur

door

**Fieke Maria Prins**

geboren op 18 juli 1987  
te Bedum

**Promotoren:** Prof. dr. J.J.W. Lagendijk  
Prof. dr. C.H.J. Terhaard

**Copromotoren:** Dr. L.G.W. Kerkmeijer  
Dr. M.M. Barendrecht

## TABLE OF CONTENTS

Chapter 1	Introduction and outline of the thesis	7
Chapter 2	Renal cell carcinoma: alternative nephron-sparing treatment options for small renal masses, a systematic review	21
Chapter 3	Superior target delineation for stereotactic body radiotherapy of bone metastases from renal cell carcinoma on MRI compared to CT	49
Chapter 4	Development and evaluation of a MRI based delineation guideline for renal cell carcinoma	63
Chapter 5	Intrafraction motion management of renal cell carcinoma with MRI guided stereotactic body radiotherapy	77
Chapter 6	A dual-purpose MRI acquisition to combine 4D-MRI and Dynamic Contrast-Enhanced imaging for abdominal stereotactic body radiotherapy planning	91
Chapter 7	Ablative treatment of inoperable renal cell carcinoma using stereotactic body radiotherapy (ARREST-study): study protocol and first clinical experience	109
Chapter 8	Summary	123
Chapter 9	General discussion and future perspectives	129
Addenda	Samenvatting	147
	Review committee	151
	List of publications	153
	Dankwoord	155
	Curriculum Vitae	161



## **Introduction and outline of the thesis**

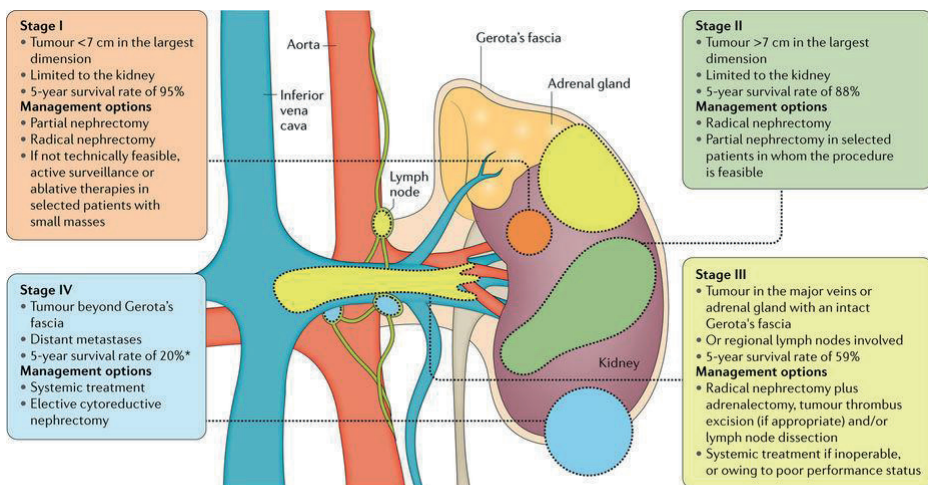
---





## RENAL CELL CARCINOMA

Malignancies of the kidney account for 2-3% of all cancers: 90% of these are renal cell carcinomas (RCC)(1). In the last decade, the incidence of RCC in Europe is increasing, due to improved imaging techniques and their increased use and accessibility(2). RCC is discovered incidentally in 60-70% of the cases, when imaging is used to detect other pathology. The 'incidental' tumors are called incidentalomas and are often small renal masses (SRM). SRM are renal lesions less than 4 cm in largest diameter with contrast enhancement on abdominal imaging(3). The lesions are either solid or cystic, of which the Bosniak III or IV classified lesions are potentially malignant(4). SRM's are mostly asymptomatic and have a good prognosis if treated on time(5). Long-term prognosis depends, among other factors, on the stage of the tumor. Within the group of RCC, only a small group (non-growing tumors < 3 cm) does not need treatment, and is monitored by active surveillance. If the tumor shows radiographic signs of growth or exceeds 3 cm in diameter, treatment is indicated(6).



Nature Reviews | Disease Primers

**Figure 1:** stages of RCC. Hsieh JJ et al. Renal cell carcinoma. Nat Rev Dis Primers 2017 Mar 9;3:17009(6)

## CURRENT TREATMENT OF RCC

The current standard treatment of RCC is (partial-) nephrectomy (1). Although in most cases curative, with a risk of recurrence of up to 4%(7), it is nevertheless an invasive treatment option including inherent risks like parenchyma bleeding or urine leakage. Over time, less

invasive alternative treatment options, such as radio frequency ablation (RFA), cryoablation (CA), microwave ablation (MWA), and stereotactic body radiotherapy (SBRT) have been developed, although the gold standard remains surgery. These alternative techniques effectively induce necrosis and apoptosis of tumor cells, either by heating, freezing, the use of electromagnetic microwaves or irradiation. The most important complications of RFA, CA and MWA are bleeding and hematuria. Incomplete treatment of the tumor is also reported, especially in the larger lesions. The currently used SBRT radiotherapy technique has a low rate of severe complications (<5% of patients). The most important severe complications of SBRT are renal function loss, duodenal ulceration and skin toxicity(8). The different alternative treatment techniques and outcome results are further discussed in **chapter 2**. So far, only (minimally) invasive treatment options of RCC have been shown to be curative. A completely non-invasive curative approach would be desirable. Radiotherapy could be an eligible non-invasive treatment option for primary RCC.

## **DEVELOPMENT OF RADIOTHERAPY FOR RCC**

Radiotherapy for RCC has been used for decades, with external beam radiotherapy (EBRT) in the treatment of RCC first reported in 1966. In that report, a study on preoperative palliative irradiation in large tumors was described (including case series dating since 1935), using a dosage of 3000 rads (30 Gy) on a 240 kV orthovoltage machine(9). In 1987 it was shown that preoperative radiotherapy did not change the overall survival or local tumor control after 5 years(10). Years later, conformal radiotherapy was introduced as a primary treatment, although still using large fields and relatively low doses. The use of low-dose radiotherapy led to the assumption that RCC was radioresistant(11). The assumed radioresistance resulted in the use of EBRT for RCC only in inoperable patients or for treatment of metastatic tumor localations, and not as a primary treatment modality for operable patients(12).

The use of large radiation fields was required in historical series as conventional radiotherapy techniques could not compensate for kidney motion, and this motion could not be visualized before or during treatment. In these large fields, a large volume of healthy kidney as well as other radiation-sensitive surrounding healthy tissue (such as small bowel) was irradiated, which limited the radiation dose that could be prescribed to the tumor. The dose administered for primary kidney tumors was lower than for tumor sites located elsewhere in the body, and this moderate dose level led to moderate cure rates(12). The former assumption that RCC is radioresistant may therefore have been incorrect(13). In recent literature higher biological effective doses with a stereotactic body radiotherapy (SBRT) approach were used, using conventional linear accelerators (linacs) with on-board cone beam computed tomography (CBCT)(14-21). RCC is shown to be sensitive to radiotherapy, when adequate doses are applied.

SBRT treatment is currently used mostly for inoperable patients(21). Due to lack of randomized controlled trials of SBRT versus surgery in operable patients, surgery is still considered the treatment of choice for operable patients (suspected of) having RCC.

## **PRESENT-DAY STEREOTACTIC BODY RADIATION THERAPY FOR RCC**

SBRT is a high precision radiation technique that, in its modern form, makes use of online (mostly CBCT) image guidance to deliver the dose precisely at the location of the tumor with steep dose fall off around the tumor. SBRT treatment enables delivery of a high dose in one or a few fractions (hypofractionation) and ensures a high biological effective dose to the tumor compared with previous conventional fractionated radiotherapy schemes. SBRT treatment for RCC is currently used in trials for inoperable patients or patients refusing surgery. The doses and fractionation schemes used in the different clinical studies and case reports are very heterogeneous. An overview of the current limited literature about SBRT, including the different dose schemes, toxicity and local control rates for inoperable renal cell carcinoma, is described in chapter 2 of this thesis.

## **RADIOTHERAPY MARGINS AND KIDNEY MOTION**

As the tumor is surrounded by organs at risk (particularly healthy kidney tissue and small bowel), the targeting of radiotherapy to the gross tumor volume (GTV) should be very precise. A considerable margin around the kidney is required for SBRT for RCC on conventional linacs, as the kidney is moving during breathing, particularly in the cranio-caudal direction. The kidneys can move by up to 2.4 cm in normal breathing and up to 6.6 cm in deep breathing(22).

In previous studies of SBRT for primary RCC, several methods were used for defining radiation margins(14-21). Pham et al.(15) defined the irradiation margin by means of an internal target volume (ITV) to take the motion of the tumor throughout the breathing cycle into account. This ITV margin approach is used to make sure the target (tumor) will receive the prescribed dose, irrespective of the phase of the breathing cycle during irradiation. When the ITV margin concept is used, a significant amount of normal tissue (both renal cortex and other surrounding healthy tissues) will be irradiated (23).

Staeher et al.(18) and Ponsky et al.(16) used the Cyberknife system to track the tumor during breathing. This system uses a motion model and X-ray cameras in combination with fiducial markers in the kidney to track (follow) the kidney in real-time. The system delivers high radiation dose, which closely conforms to the shape of the actual target.

Besides using the ITV margin concept or tracking the tumor, it is also possible to irradiate during midventilation/mid-position. Compared to the ITV concept, the midventilation approach leads to a decrease of margins and of healthy tissue irradiated. It is also more robust than tumor tracking, because there is less chance of error(24). In **chapter 7** the first results of a study conducted at the UMC Utrecht (ARREST-study) on SBRT treatment of inoperable RCC patients is described, applying a midventilation technique with the use of fiducial markers.

Fiducial markers can also be used on conventional linacs. The on-board CBCT does not allow for an adequate soft-tissue contrast and cannot be used during beam-on (irradiation). The lack of soft tissue contrast is in some studies circumvented by using fiducial markers, which are visible on CBCT (or electronic portal imaging device (EPID)) to guide radiation treatment(25). Without these markers, the kidney itself would be hard to visualize before treatment and targeting the tumor would be challenging and imprecise, requiring larger PTV margins to account for the inaccuracy.

Although in the last decade large improvements have been made on the SBRT treatment of RCC, there is still a need for improvement towards more accurate online (during treatment) imaging and online adaptive radiotherapy in order to reduce the margins around the tumor. This reduction will reduce toxicity to the surrounding organs at risk and allow for an increase of the dose to the tumor, with the possibility to also reduce the number of fractions. The ultimate goal of improving the image-guided SBRT technique would be to increase recurrence free survival and overall survival with lower (or at least) equal toxicity rates, compared to the first experiences in SBRT of RCC. MRI-guided radiation therapy has the potential to achieve state-of-the-art image-guided online adaptive radiotherapy for RCC, as RCC is clearly visible on MRI.

## **MRI IN RCC**

MRI-sequences dedicated to radiotherapy for RCC are not readily available, as MRI has rarely been used for radiotherapy purposes in RCC patients. Diagnostic MRI of the kidney however, was first described in 1984(26). In the last decade, MRI for RCC developed rapidly resulting in a feasible alternative to CT for imaging and monitoring of RCC(27). Contrast enhanced MRI-scans are important to differentiate between tissues that give the same contrast-free MRI signal but are histologically different. In diagnostic studies, contrast-enhanced MRI is mainly used for tumor characterization(28). Although the quality and use of MRI-scans for renal tumors are rapidly improving, MRI-scans are nowadays most frequently used in radiology to diagnose RCC in patients not suitable for multiple CT-scans (for example in patients with a single kidney or Von Hippel Lindau disease).

Gold standard in diagnostic imaging of RCC is multi-phasic contrast enhanced CT imaging, due to a high sensitivity and specificity for characterization and detection of RCC(1). Although recent literature suggests MRI has a slightly higher sensitivity and specificity in detecting SRMs(1). In addition to T1 and T2 weighted imaging, contrast enhanced and diffusion weighted sequences can also be used in MRI for characterization of lesion vascularity and diffusion restriction. It may discriminate RCC from benign lesions and allow for classification of RCC subtypes. In particular T2 weighted images have proven to be successful in differentiating benign pathologies from RCC.

For treatment (radiotherapy) purposes, there are different requirements for the MRI sequences than for diagnostic purposes. Geometric accuracy is critical. For example, in radiotherapy, the tumor should be contoured precisely and it is important to differentiate between tumor, healthy kidney tissue and to visualize the location of the surrounding healthy organs. Thus when used for radiotherapy, the MRI-sequences should be scanned with a smaller slice thickness (3 mm instead of 7 mm used in diagnostic scans). Also, the patients must be scanned in the radiotherapy position with arms up and deformations should be minimized as much as possible. For diagnostic purposes, the size of the tumor, stage and differentiation between different pathologies are most important.

In **chapter 3, 4, 5 and 6**, optimized MRI-sequences dedicated for radiotherapy are used for various purposes in order to work towards MRI-guided radiotherapy of RCC.

## MRI-GUIDED RADIOTHERAPY

Image (CT)-guided SBRT for RCC has dramatically improved treatment outcome with local control rates comparable to other minimally invasive alternative treatment options. The next step in image guided SBRT, in order to improve radiotherapy precision and outcome for RCC, would be MRI-guided radiotherapy. There are different MRI-guided radiotherapy systems available or in development. The main differences between the systems are in field strength of the MRI (ranging between 0.35 and 1.5T (Tesla)), and radiation source used (7 MV linac and Co-60)(29). The UMC Utrecht, in collaboration with Elekta and Philips, has designed a hybrid diagnostic quality 1.5 T MRI and 7 MV linear accelerator (MRI-linac)(30). The system provides real-time MRI imaging during radiation delivery and therefore enables tumor tracking for better targeting precision(31). Better targeting allows for dose escalation in order to increase cure rates, but it may also reduce the dose to the surrounding healthy tissues, and therefore decrease the toxicity in the organs at risk (OAR). The MRI-linac has the potential to offer high precision radiotherapy as a non-invasive treatment of complex tumor sites and moving targets such as the kidney(32). The MRI-linac shows excellent soft-tissue visualization during radiation delivery for improved targeting. This enables on-line treatment optimization for precise radiation delivery (accuracy better than 1 mm). The MRI-

linac makes 'seeing exactly what you treat' a reality. Seeing the tumor and the surrounding healthy tissues, at the exact moment of treatment, makes it possible to give the required dose to the tumor while optimally sparing normal tissues.

The first technical prototype of the MRI-linac was developed and installed at the UMC Utrecht and has been used to develop, evaluate and validate clinical procedures. An international MRI-linac consortium (The Atlantic Consortium) has been formed in order to ensure the clinical introduction of the MRI-linac(33). All consortium sites installed clinical prototypes of the MRI-linac. The first clinical prototype has been installed in Utrecht and has been used for First-in-Man treatments in patients with bone metastases. The treatment was successfully conducted and is the first treatment on the MRI-linac worldwide(34).

Treatment protocols for many different tumor sites are currently being developed within the Atlantic Consortium and will be introduced within the upcoming years (including treatment of RCC).

## **MRI-GUIDED RADIOTHERAPY IN RCC**

Previous research showed that MRI, from a technical point of view, is suitable for MRI-guided radiation of RCC(35,36). However, the studies performed were mainly a proof of concept on the technical part of the development of MRI in irradiation of RCC and further clinical development of the procedures and protocols is warranted.

As described above, the clinical introduction of image-guided radiotherapy initiated a paradigm shift in the treatment of RCC, from highly fractionated treatment series, using large fields and suboptimal doses, towards a more ablative approach, using small fields in a few fractions. The MRI-linac is anticipated to deliver an online adaptive, ablative and truly non-invasive radiation treatment of RCC, without the need for fiducial markers. RCC is particularly suitable for treatment on a MRI-linac, considering it is a high-amplitude moving tumor, surrounded by soft tissue organs at risk. The MRI-linac is capable to track this motion and to treat RCC with smaller margins, higher dose on the tumor, lower dose to the healthy surrounding tissues, and a reduction of number of fractions, ideally to a single fraction. While a more precise dose delivery is anticipated than in CBCT-guided SBRT, the MRI-linac has the potential to have equal oncologic outcomes but with fewer complications compared to invasive treatments like (partial-) nephrectomy, which could lead towards better quality of life. MRI-guidance also makes a better evaluation of the treatment of RCC possible (both the technical aspects to review the delivered dose, as well as studies in prediction of tumor control by acquiring functional imaging) as imaging prior to and during treatment is available. In the end, the goal is to move from a CT-based approach towards a MRI-guided clinical radiotherapy treatment for RCC.

The ultimate goal is to develop a non-invasive treatment option for operable and inoperable patients with RCC with minimal toxicity and local control rates comparable to surgery.

## RATIONALE AND OUTLINE OF THIS THESIS

The present thesis focuses on the necessary developments towards MRI-guided radiotherapy of RCC. Ranging from clarifying the position of curative radiotherapy for the treatment of RCC, optimization of MRI-sequences for radiotherapy, optimization of the contouring, optimization of the techniques necessary and gaining experience in treating RCC with radiotherapy in the Netherlands.

**Chapter 2** reviews all recent studies on alternative (nephron sparing) treatment modalities in primary T1 RCC, other than the gold standard (partial-) nephrectomy. The efficacy, safety, and outcome for each treatment modality are summarized and discussed, including radiotherapy. It describes the demand for a truly non-invasive treatment option and the benefits and disadvantages of SBRT for RCC compared to the other alternative treatment modalities.

Despite local treatment for primary RCC, occasionally metastatic disease can be found during or after initial presentation of RCC. **Chapter 3** describes the differences in MRI-based and CT-based contouring for bone metastases of RCC. The benefit of the use of MRI for contouring of the metastatic lesion is discussed. It seems that MRI has a clear benefit over CT in delineations of RCC bone metastases. It may be possible that the local control rates of SBRT treatment of RCC bone metastases can be optimized when using MRI for contouring.

Development and evaluation of MRI-based delineation for MRI-only radiotherapy for RCC are described in **chapter 4**. The main topic of this chapter is the contouring agreement of MRI-only delineation of primary RCC lesions between different observers. This chapter includes a recommendation for MRI-sequences to be used and proposes how to introduce MRI-only contouring for RCC.

A challenging part of accomplishing MRI-only radiotherapy is to encompass motion of the kidney during treatment. Different suggestions in literature have been made to handle interfraction motion, based on CT or CBCT only, and a few studies describe the intrafraction motion. The 3D drift during actual treatment time has not been characterized yet. In **chapter 5**, the intrafraction motion based on respiratory movement and drift of the tumor during actual treatment time were simulated, to be taken into account in future MRI-only treatments. Also, a recommendation for the PTV margin based on the simulated intrafraction motion and treatment technique is described.

**Chapter 6** describes the development of a dual purpose MRI-sequence that combines the DCE and 4D-MRI acquisitions. The reconstructions can potentially provide complementary information for tumor characterization, accurate delineations and mid position volume generation. These are all key elements in the development of MRI-only radiotherapy of RCC.

In order to successfully develop a MRI-only treatment it is essential to gain experience in the current CBCT guided SBRT technique of radiation treatment of RCC, which is already used in several institutes, for example in Toronto and Melbourne(14,21). **Chapter 7** describes the study protocol and the first clinical experience of a clinical phase 1-2 trial at the UMC Utrecht to treat inoperable patients with primary RCC. Additional MRI scans are performed in order to prepare for future MRI-only treatment of RCC and to study MRI-based response prediction and evaluation.



## REFERENCES

1. Ljungberg B, Bensalah K, Bex A, Canfield S, Dabestani S, Giles RH, et al. Guidelines on Renal Cell Carcinoma. European Association of Urology 2015.
2. Ferlay J, Steliarova-Foucher E, Lortet-Tieulent J, Rosso S, Coebergh JW, Comber H, et al. Cancer incidence and mortality patterns in Europe: estimates for 40 countries in 2012. *Eur J Cancer* 2013 Apr;49(6):1374-1403.
3. Volpe A, Panzarella T, Rendon RA, Haider MA, Kondylis FI, Jewett MA. The natural history of incidentally detected small renal masses. *Cancer* 2004 Feb 15;100(4):738-745.
4. Bosniak MA. The current radiological approach to renal cysts. *Radiology* 1986 Jan;158(1):1-10.
5. Hollingsworth JM, Miller DC, Daignault S, Hollenbeck BK. Rising incidence of small renal masses: a need to reassess treatment effect. *J Natl Cancer Inst* 2006 Sep 20;98(18):1331-1334.
6. Hsieh JJ, Purdue MP, Signoretti S, Swanton C, Albiges L, Schmidinger M, et al. Renal cell carcinoma. *Nat Rev Dis Primers* 2017 Mar 9;3:17009.
7. Uzzo RG, Novick AC. Nephron sparing surgery for renal tumors: indications, techniques and outcomes. *J Urol* 2001 Jul;166(1):6-18.
8. Siva S, Kothari G, Muacevic A, Louie AV, Slotman BJ, Teh BS, et al. Radiotherapy for renal cell carcinoma: renaissance of an overlooked approach. *Nat Rev Urol* 2017 Jun 20.
9. Riches E. The place of radiotherapy in the management of parenchymal carcinoma of the kidney. *J Urol* 1966 Mar;95(3):313-317.
10. deKernion JB, Mukamel E. Selection of initial therapy for renal cell carcinoma. *Cancer* 1987 Aug 1;60(3 Suppl):539-546.
11. Ning S, Trisler K, Wessels BW, Knox SJ. Radiobiologic studies of radioimmunotherapy and external beam radiotherapy in vitro and in vivo in human renal cell carcinoma xenografts. *Cancer* 1997 Dec 15;80(12 Suppl):2519-2528.
12. Siva S, Pham D, Gill S, Corcoran NM, Foroudi F. A systematic review of stereotactic radiotherapy ablation for primary renal cell carcinoma. *BJU Int* 2012 Dec;110(11 Pt B):E737-43.
13. De Meerleer G, Khoo V, Escudier B, Joniau S, Bossi A, Ost P, et al. Radiotherapy for renal-cell carcinoma. *Lancet Oncol* 2014 Apr;15(4):e170-7.
14. Chang JH, Cheung P, Erler D, Sonier M, Korol R, Chu W. Stereotactic Ablative Body Radiotherapy for Primary Renal Cell Carcinoma in Non-surgical Candidates: Initial Clinical Experience. *Clin Oncol (R Coll Radiol)* 2016 Apr 27.
15. Pham D, Thompson A, Kron T, Foroudi F, Kolsky MS, Devereux T, et al. Stereotactic ablative body radiation therapy for primary kidney cancer: a 3-dimensional conformal technique associated with low rates of early toxicity. *Int J Radiat Oncol Biol Phys* 2014 Dec 1;90(5):1061-1068.
16. Ponsky L, Lo SS, Zhang Y, Schluchter M, Liu Y, Patel R, et al. Phase I dose-escalation study of stereotactic body radiotherapy (SBRT) for poor surgical candidates with localized renal cell carcinoma. *Radiother Oncol* 2015 Sep 8.
17. Siva S, Jackson P, Kron T, Bressel M, Lau E, Hofman M, et al. Impact of stereotactic radiotherapy on kidney function in primary renal cell carcinoma: Establishing a dose-response relationship. *Radiother Oncol* 2016 Mar;118(3):540-546.

18. Staehler M, Bader M, Schlenker B, Casuscelli J, Karl A, Roosen A, et al. Single fraction radiosurgery for the treatment of renal tumors. *J Urol* 2015;203(3):771-775.
19. Sun MR, Brook A, Powell MF, Kaliannan K, Wagner AA, Kaplan ID, et al. Effect of Stereotactic Body Radiotherapy on the Growth Kinetics and Enhancement Pattern of Primary Renal Tumors. *AJR Am J Roentgenol* 2016 Mar;206(3):544-553.
20. Yamamoto T, Kadoya N, Takeda K, Matsushita H, Umezawa R, Sato K, et al. Renal atrophy after stereotactic body radiotherapy for renal cell carcinoma. *Radiat Oncol* 2016 May 26;11(1):72-016-0651-5.
21. Siva S, Pham D, Kron T, Bressel M, Lam J, Tan TH, et al. Stereotactic ablative body radiotherapy for inoperable primary kidney cancer: a prospective clinical trial. *BJU Int* 2017 Feb 10.
22. Moerland MA, van den Bergh AC, Bhagwandien R, Janssen WM, Bakker CJ, Lagendijk JJ, et al. The influence of respiration induced motion of the kidneys on the accuracy of radiotherapy treatment planning, a magnetic resonance imaging study. *Radiother Oncol* 1994 Feb;30(2):150-154.
23. Teh B, Bloch C, Galli-Guevara M, Doh L, Richardson S, Chiang S, et al. The treatment of primary and metastatic renal cell carcinoma (RCC) with image-guided stereotactic body radiation therapy (SBRT). *Biomed Imaging Interv J* 2007 Jan;3(1):e6.
24. Wolthaus JW, Schneider C, Sonke JJ, van Herk M, Belderbos JS, Rossi MM, et al. Mid-ventilation CT scan construction from four-dimensional respiration-correlated CT scans for radiotherapy planning of lung cancer patients. *Int J Radiat Oncol Biol Phys* 2006 Aug 1;65(5):1560-1571.
25. van der Heide UA, Kotte AN, Dehnad H, Hofman P, Lagenijk JJ, van Vulpen M. Analysis of fiducial marker-based position verification in the external beam radiotherapy of patients with prostate cancer. *Radiother Oncol* 2007 Jan;82(1):38-45.
26. Choyke PL, Kressel HY, Pollack HM, Arger PM, Axel L, Mamourian AC. Focal renal masses: magnetic resonance imaging. *Radiology* 1984 08/01; 2017/09;152(2):471-477.
27. Sankineni S, Brown A, Cieciera M, Choyke PL, Turkbey B. Imaging of renal cell carcinoma. *Urol Oncol* 2016 Mar;34(3):147-155.
28. Ramamurthy NK, Moosavi B, McInnes MD, Flood TA, Schieda N. Multiparametric MRI of solid renal masses: pearls and pitfalls. *Clin Radiol* 2015 Mar;70(3):304-316.
29. Menard C, van der Heide U. Introduction: Systems for magnetic resonance image guided radiation therapy. *Semin Radiat Oncol* 2014 Jul;24(3):192.
30. Raaymakers BW, Lagendijk JJ, Overweg J, Kok JG, Raaijmakers AJ, Kerkhof EM, et al. Integrating a 1.5 T MRI scanner with a 6 MV accelerator: proof of concept. *Phys Med Biol* 2009 Jun 21;54(12):N229-37.
31. Crijns SP, Raaymakers BW, Lagendijk JJ. Proof of concept of MRI-guided tracked radiation delivery: tracking one-dimensional motion. *Phys Med Biol* 2012 Dec 7;57(23):7863-7872.
32. Lagendijk JJ, Raaymakers BW, Raaijmakers AJ, Overweg J, Brown KJ, Kerkhof EM, et al. MRI/linac integration. *Radiother Oncol* 2008 Jan;86(1):25-29.

33. Kerkmeijer LG, Fuller CD, Verkooijen HM, Verheij M, Choudhury A, Harrington KJ, et al. The MRI-Linear Accelerator Consortium: Evidence-Based Clinical Introduction of an Innovation in Radiation Oncology Connecting Researchers, Methodology, Data Collection, Quality Assurance, and Technical Development. *Front Oncol* 2016 Oct 13;6:215.
34. Raaymakers BW, Jurgenliemk-Schulz IM, Bol GH, Glitzner M, Kotte ANTJ, van Asselen B, et al. First patients treated with a 1.5 T MRI-Linac: clinical proof of concept of a high-precision, high-field MRI guided radiotherapy treatment. *Phys Med Biol* 2017 Nov 14;62(23):L41-L50.
35. Kerkhof EM, Raaymakers BW, van Vulpen M, Zonnenberg BA, Bosch JL, van Moorselaar RJ, et al. A new concept for non-invasive renal tumour ablation using real-time MRI-guided radiation therapy. *BJU Int* 2011 Jan;107(1):63-68.
36. Stam MK, van Vulpen M, Barendrecht MM, Zonnenberg BA, Crijns SP, Lagendijk JJ, et al. Dosimetric feasibility of MRI-guided external beam radiotherapy of the kidney. *Phys Med Biol* 2013 Jul 21;58(14):4933-4941.



# **Renal cell carcinoma: alternative nephron-sparing treatment options for small renal masses, a systematic review**

---

Fieke M. Prins  
Linda G.W. Kerkmeijer  
Anne A. Pronk  
Evert-Jan P.A. Vonken  
Richard P. Meijer  
Axel Bex  
Maurits M. Barendrecht

*J Endourol. 2017 Jul 25*

## ABSTRACT

*Background.* The standard treatment of T1 renal cell carcinoma (RCC) is (partial) nephrectomy. For patients where surgery is not the treatment of choice, for example in the elderly, in case of severe comorbidity, inoperability, or refusal of surgery, alternative treatment options are available. These treatment options include active surveillance (AS), radiofrequency ablation (RFA), cryoablation (CA), microwave ablation (MWA), or stereotactic body radiotherapy (SBRT). In the present overview, the efficacy, safety, and outcome of these different options are summarized, particularly focusing on recent developments.

*Methods and Materials.* Databases of MEDLINE (through PubMed), EMBASE, and the Cochrane Library were systematically searched according to the Preferred Reporting Items for Systematic Reviews and Meta-Analyses (PRISMA) criteria. The search was performed in December 2016, and included a search period from 2010 to 2016. The terms and synonyms used were renal cell carcinoma, active surveillance, radiofrequency ablation, microwave ablation, cryoablation and stereotactic body radiotherapy.

*Results.* The database search identified 2806 records, in total 73 articles were included to assess the rationale and clinical evidence of alternative treatment modalities for small renal masses. The methodological quality of the included articles varied between level 2b and level 4.

*Conclusion.* Alternative treatment modalities, such as AS, RFA, CA, MWA, and SBRT, are treatment options especially for those patients who are unfit to undergo an invasive treatment. There are no randomized controlled trials available comparing surgery and less invasive modalities, leading to a low quality on the reported articles. A case-controlled registry might be an alternative to compare outcomes of noninvasive treatment modalities in the future.

## INTRODUCTION

Kidney cancer occurs frequently and accounts for 2-3% of all cancers; 90% of these are renal cell carcinomas (RCC)(1). In Europe, the incidence RCC is increasing(2), partially due to improved imaging techniques. Of all RCC diagnoses, 60-70% are incidentalomas, often classified as small renal masses (SRM,  $\leq 4$ cm)(3). SRMs are asymptomatic and usually have a good prognosis, although SRMs will grow over time(4). T1 tumors encompass tumors  $< 7$ cm(1). Treatment of T1 tumors is focused on nephron sparing therapy and subsequent preservation of renal function. The preferred treatment of SRMs  $< 4$  cm, in order to preserve renal function and avoid unnecessary removal of the entire kidney, are minimal invasive techniques as described by the European Association of Urology (EAU) guidelines.

The current standard treatment of T1 tumors is (partial-) nephrectomy(1). Alternative treatments are active surveillance (AS), radiofrequency ablation (RFA), cryoablation (CA), microwave ablation (MWA) and stereotactic body radiation therapy (SBRT) (for inoperable patients). In this systematic review, we will give an overview of the alternative treatment modalities for small renal masses. The aim is to summarize efficacy, safety and outcome for each alternative therapeutic method available, focusing on nephron sparing treatment for T1 renal cell carcinoma (RCC).

This review can be considered an update on the review of Cutress and colleagues(5), without the surgical options. The added value of this review is that the focus is solely on alternative treatment options, including SBRT, the most recent development in the treatment of RCC.

## MATERIAL AND METHODS

The protocol for this systematic review was registered on PROSPERO (CRD42016052946) and can be assessed at [http://www.crd.york.ac.uk/PROSPERO/display\\_record.asp?ID=CRD42016052946](http://www.crd.york.ac.uk/PROSPERO/display_record.asp?ID=CRD42016052946).

### ***Search strategy***

A systematic search was performed in the databases Medline, Embase and the Cochrane library, according to the Preferred Reporting Items for Systematic Reviews and Meta-Analysis (PRISMA) criteria(6). The last update was on December 1<sup>st</sup> 2016. Details of this search strategy are provided in Table 1.

**Table 1.** Search strategy performed in Medline (through PubMed).

<b>Search strategy (Medline through Pubmed)</b>	
#1	"carcinoma, renal cell"[Mesh terms] OR "renal cell carcinoma"[tiab] OR "kidney cancer"[tiab] OR "small renal mass"[tiab] OR "renal cortical tumor*"[tiab] OR "renal cortical tumour*"[tiab] OR "small renal tumor*"[tiab] OR "small renal tumour*"[tiab]
#2	"active surveillance"[tiab] OR "organ sparing treatment"[tiab] OR "RFA"[tiab] OR radiofrequency ablation* [tiab] OR "thermal ablation"[tiab] OR "MWA"[tiab] OR microwave ablation*[tiab] OR "cryosurgery" [Mesh terms] OR cryoablation*[tiab] OR "radiotherapy"[Mesh terms] OR radiotherapy*[tiab] OR "radiation oncology"[Mesh terms] OR "radiation oncology"[tiab] OR "stereotactic body radiotherapy" [tiab] OR "SBRT" [tiab]
#3	#1 AND #2

Comparable search strategies have been conducted for EMBASE and the Cochrane Library.

### **Study inclusion**

Articles reporting on alternative treatment options for RCC (AS, RFA, CA, MWA, SBRT) were eligible for inclusion. Articles were excluded if the title/abstract did not report primary treatment with AS, RFA, MWA, CA or SBRT in patients with primary RCC/SRM, or if it was not an original article (i.e. review, abstract, commentary, case report, animal studies), or not written in English or Dutch. The resulting titles and abstracts were reviewed by the researchers. The search covered a period from 2010- December 2016.

### **Selection of studies and data extraction**

After removal of duplicates, all articles were screened on title and abstract. Full text articles assessed for eligibility were all reviewed by one investigator (F.M.Pr) and, to retrieve a second independent review opinion, divided among all researchers. Disagreement among team members was resolved by discussion and consensus. A pre-defined data-extraction form was used to obtain all relevant information, including a level of evidence according to the Oxford Centre for Evidence-based Medicine Levels of Evidence 2009 (<http://www.cebm.net/oxford-centre-evidence-based-medicine-levels-evidence-march-2009/>).

## **RESULTS**

The database search identified 2806 records. After removal of duplicates, 2534 articles were screened on title/abstract. A flowchart of this search is reported in Figure 1. In total 73 articles were included in this review, divided among the different treatment modalities.



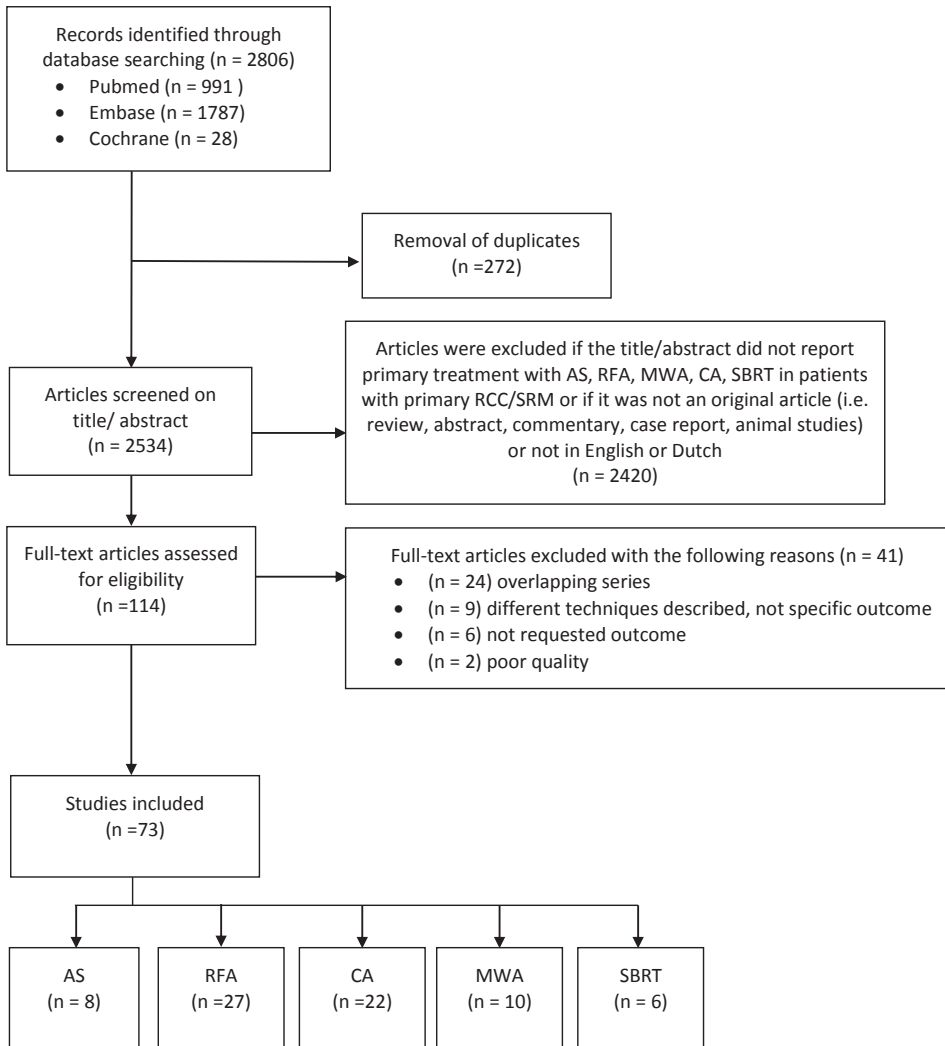


**Figure 1.** PRISMA flow chart of the systematic review.

PRISMA = Preferred Reporting Items for Systematic Reviews and Meta-Analysis.

### **Active surveillance (AS)**

Active surveillance (AS) involves monitoring tumor size by different imaging techniques over a period of time. In case progression occurs, delayed intervention will be performed(1). The goal of AS is to prevent unnecessary treatment-related morbidity and monitor the tumor progression in such manner that timely intervention with curative intent is assured.

As is shown in table 2, the level of evidence in all studies is 2b, the studies are all retrospective or prospective cohort studies. AS is mainly used for small renal masses, i.e. renal masses  $\leq$  4 cm. The mean and median tumor diameters in these studies varied between 1.8 and 2.8 cm with a mean tumor growth between 0.11 and 0.7 cm/year. Although the range of tumor growth is not wide, evidence concerning the relationship between tumor size and tumor growth was inconclusive. One study did not report any association between tumor size and growth rate(4). Three studies reported an association with an increased growth rate for larger tumors(7-9). Manson and colleagues reported that larger tumors ( $\geq$ 2.45 cm) grow faster than smaller lesions(7). However, all studies concluded that a faster growth rate was related to worse outcome, and a higher risk of developing metastatic disease.

Based on the growth rate, delayed intervention can be necessary in patients on AS(8,9). Delayed intervention varied between 5% to 26%. Indeed, fast growth rate was the major indication to start invasive treatment, most often surgery(4,7,9-13). Even so, two studies showed delayed intervention with RFA or CA as well(10,13). The goal of delayed intervention is to assure local control and prevent metastatic disease, which occurred in 0% - 3.2% of the AS population(4,7-13). Patel and colleagues did not observe any metastatic progression in tumors showing negative or zero tumor growth during follow-up(FU)(8). Moreover, they proposed to intervene if SRM's are  $>$ 3.5 cm in size or show mean tumor growth of  $>$ 0.5cm/year(8).

Interestingly, only a small proportion of patients in FU for active surveillance underwent a biopsy either at the start or during FU. As such, the percentage of biopsy proven RCC in these studies of the total number of patients varied from 8.5-50%. Therefore the results presented are possibly not an accurate reflection of the actual study population, i.e. patients with RCC proven SRM (table 2: biopsy proven RCC). In groups with delayed intervention, more often a biopsy was performed shown to be positive for RCC; patients with benign or unknown pathology were more likely to be scheduled for AS(10-12).

Several outcome measures have been used in the aforementioned studies. Cancer specific survival (CSS) varied from 97 % - 100% in a median FU period between 25 and 92 months (range 6-208). Nevertheless, in most studies, AS was mainly considered for the elderly, patients with comorbidities preventing an invasive treatment approach or patients refusing surgery(4,7-13).

In conclusion, a small proportion of patients will need to undergo delayed intervention during AS. AS is considered a safe treatment option for patients with SRMs. However, as there is no curative treatment for metastatic disease, developing metastatic disease during surveillance remains a rare but nonetheless potential risk.

**Table 2.** Summary of studies reporting on Active surveillance in primary Renal Cell Carcinoma

References	Level of evidence	NP/NT <sup>a</sup>	Initial median tumor diameter in cm (range)	Mean tumor growth (cm/year)	Median follow-up in months (range)	Delayed intervention (%)	CSS <sup>a</sup> (%)	Progress to metastatic disease (%)	Biopsy proven RCC (%) <sup>a</sup>
Rosales and colleagues <sup>(6)</sup>	2b	212/223	2.8 (0.5–13.7)	0.34	35 (6–137)	5	99.5	2	19
Mason and colleagues <sup>(7)</sup>	2b	82/84	2.3 (0.8–5.4)	0.25	36 (6–96)	15	99	1.2	8.5
Jewett and colleagues <sup>(10)</sup>	2b	178/209	2.1 (0.4–4.0)	0.13	29 (NR <sup>9</sup> )	5	99	1.1	50
Patel and colleagues <sup>(8)</sup>	2b	71/93	2.2 (NR) mean	0.21	34 (NR)	20	99	1.4	10
Brunocilla and colleague <sup>(11)</sup>	2b	62/64	2.6 (1.6–4.3)	0.70	92 (8–208) mean	26	97	3.2	40
Schiavina and colleague <sup>(12)</sup>	2b	70/72	2.7 (1.8–3.7)	0.50	61 (38–150)	25	99	1	40
Pierorazio and colleague <sup>(13)</sup>	2b	223	1.9 (NR) mean	0.11	25 (10–45)	9	100	0	9.4
Bahouth and colleague <sup>(9)</sup>	2b	70/78	1.8 (0.5–4.0)	0.17	34 (12–112)	10	100	0	8

<sup>a</sup>Biopsy proven RCC; percentage of RCC proven of total NP

CSS= cancer specific survival; NP= number of patients; NR= not reported; NT= number of tumors.

### **Radio frequency ablation (RFA)**

The first study describing the treatment of renal cell carcinoma by RFA was published in 1997 by Zlotta and colleagues(14). Radiofrequency energy can be used to create heat causing necrosis of tumor cells. The local effects are obtained by implanting single or clustered needles in the tumor tissue through which the radiofrequency energy is applied. Operating temperatures range from 50°C-100°C. Placement of these needles can be achieved both laparoscopically or via a percutaneous approach(1).

Percutaneous treatment is most frequently used, usually ultrasound (US) or CT-guided, under general anesthesia or intravenous (IV) sedation(15,16).

Table 3 summarizes the studies reviewed on RFA. The level of evidence in all studies varied between 2b and 4. The described techniques of RFA were either percutaneous or laparoscopic, both US- or CT-guided. Most tumors treated by RFA were classified as T1a or T1b tumors. RCC was 100% proven in 13 studies, in the other 15 studies RCC was partly biopsy proven benign or suspected for RCC on CT or MRI.

Tumor diameter is an important predictor for success in RFA treatment. In the reviewed studies, tumor diameter ranged between 2.1-5.1 cm (range 0.5-7.6). Zagoria and colleagues concluded that for RCCs less than 4 cm long-term tumor control can be achieved since no recurrences were reported for lesions < 4 cm(17). Iannuccilli and colleagues reported an increased risk of residual tumor for lesions  $\geq 3.5$  cm(18). In US-guided percutaneous RFA of tumors  $\geq 4$  cm, 40% showed incomplete ablation, whereas in CT-guided percutaneous RFA there was an incomplete ablation of 16.7%(19). Each centimeter increase in tumor diameters greater than 3.6 cm, appeared to be associated with a decreased disease free survival by a factor of 2.19(17). In accordance with other studies, it was concluded that for RCC >4 cm other treatment options should be considered(17). Or, as McClure et al stated, smaller lesions may require a single ablation (median size 2.1 cm), but larger lesions (3.6 cm) need more than one ablation (20).

Another independent predictor of successful RFA is the location of the tumor. An exophytic localization is considered beneficial, with a decrease in risk of residual disease (20-23). Larger diameter and central localizations were associated with an increased risk of major complications(16), and a risk of incomplete ablation(20,24). Therefore a laparoscopic RFA approach has been proposed as the treatment of preference when the renal tumor is in the proximity of critical structures(25). Beside tumor location, clear cell subtype and maximum treatment temperature  $\leq 70^\circ\text{C}$  were factors related to an increased risk of residual lesions(23). Several complications have been reported after RFA treatment. Complication rates varied between 5.1% and 37% in different studies. Most of these complications were minor, i.e. Clavien Dindo grade I-II. Minor complications included perirenal hematoma(16,18-21,26-31), postoperative fever (19,27,32,33), gross hematuria(19,26,29,34), asymptomatic

pneumothoraxes(16,17,21,28,34), paresthesias(16,18,19,21,27,33), thermal injury in skin, psoas muscle and liver(16,21,26,33), and arterial hypertension(16,18). Major complications (Clavien Dindo grade III-IV) included fistula in the abdominal tract (with or without urinoma and infection)(16,21,25,28), bowel injury (which required diverting ileostoma) or duodenal perforation(16,26,35), abscess(16,21,24,29), acute kidney failure and dialysis(16,20,21,33), urethral stenosis, stricture, obstruction or urine leak(16,18,20,21,24,25,27,30,33).

A few studies also reported on kidney function pre- and post-procedural. Most find no significant decrease in eGFR(19,28,36,37), or an increase in creatinine(35,38). Three studies reported a better preservation of renal function after a RFA procedure, compared to a partial nephrectomy(22,29,39). Impaired baseline kidney function tended to deteriorate after RFA(22).

Median FU varied between 15 and 79 months (range 1 – 131 months); only four studies reported results after a median FU time > 60 months(15,23,37,40). In most studies recurrence was defined as contrast enhancement of >10 Hounsfield units (HU)(17,25,27), >15 HU(15,16), >20 HU(26,41), based on a CT-scan, a >15% increase of the signal on MRI(17,21)(21,26), or presence of viable tumor cells(26). FU was set at 1, 3, 6 months and biannually thereafter for all studies.

Tumor recurrence was usually seen within the first 2 years after treatment(18,23). Recurrence free survival between 67.6% and 100% was reported at a median FU between 15 and 79 months (range 1 – 131 months). A higher tumor stage correlated with a decreased RFS and disease free survival (DFS) in patients treated with RFA(15,17). Stage T1a tumor was a positive predictor for overall and cancer specific survival(24). In addition to tumor size, the technical success and RFS are dependent on the experience of the operator, and more experienced physicians can achieve RFS rates up to 100%(21). In case incomplete ablation or recurrence occurred, patients were considered candidates for a second RFA treatment(20,24).

Median survival and overall survival rates were higher for tumors  $\leq$  3 cm than for tumors >3 cm(16,23). Tumor size diameter over 4 cm was also mentioned as being the only risk factor associated with residual tumor or recurrence of the tumor(16,19). Indeed, in T1b tumors a significantly higher risk of residual disease was reported compared to T1a lesions(15). In Veltri and colleagues T1a is mentioned as a positive predictor for complete ablation(24). Balageas and colleagues reported a relative risk of recurrence or residual disease for each centimeter increase of 9.35(16).

In conclusion, RFA is considered to be an effective treatment option in small renal tumors <4cm with a beneficial localization and is mostly used in poor surgical candidates(17,25,29,31,35,36), although a few studies do report the possibility in healthy patients in T1a tumors(22,27,37,40). In the last few years studies with longer FU are presented and therefore RFA can also be considered as an alternative treatment for durable local control(15).

**Table 3.** Summary of studies reporting on Radiofrequency Ablation in primary Renal Cell Carcinoma

References	Level of evidence	NP/NT <sup>a</sup>	Mean tumor diameter in cm (range)	RFS (%) <sup>a</sup>	Complications (%)	Median follow-up in months (range)	CSS (%) <sup>a</sup>	Biopsy proven RCC (%) <sup>a</sup>
Tracy and colleagues <sup>(63)</sup>	2b	208/243	2.4 (1.0–5.4)	90	NR	27 (1.5–90) (mean)	99	79
Zagoria and colleagues <sup>(17)</sup>	4	41/48	2.6 (1.7–3.6) median	88	8	56 (36–64)	83	100
Zhao and colleagues <sup>(19)</sup>	4	73/73	3.4 (1.7–5.8)	90.4	12.3	22 (12–42) (mean)	100	100
Olweny and colleagues <sup>(40)</sup>	4	37/37	2.1 (1.8–2.8)	91.7	NR	78 (69.6–85.2)	97.2	100
Sung and colleagues <sup>(22)</sup>	4	40/45	2.4 (1.0–7.6)	94.7	NR	36.6 (1–65) (mean)	NR	12.5
Sommer and colleagues <sup>(28)</sup>	4	22/28	2.5 (1.3–3.9)	93	22.7	15.2 (3–31)	NR	14.3
Psutka and colleagues <sup>(15)</sup>	4	185/185	3.0 (1.0–6.5) median	95.2	NR	77 (63–92)	99.4	100
Kim and colleagues <sup>(26)</sup>	2b	47/48	2.3 (1.0–3.0)	89.6	35.8	49.6 (12–81) (mean)	100	16.7
Balagtas and colleagues <sup>(16)</sup>	2c	62/71	2.3 (0.8–4.6) median	61.9	5.9	36.5 (18–78)	96.8	100
Leveillee and colleagues <sup>(41)</sup>	2b	273/292	2.5 (0.7–5.3)	94.3	37	20 (1–98)	98.6	67.5
Seklehner and colleagues <sup>(32)</sup>	4	40/44	2.6 (1.5–4.2)	92.3	27	23.8 (3–59) (mean)	100	68.6
Karam and colleagues <sup>(60)</sup>	2b	150/150	2.6 (0.9–7.1) median	96.7	NR	40.1 (mean)	100	72
Wah and colleagues <sup>(21)</sup>	2b	165/200	2.9 (1.0–5.6)	93.5	13.9	46.1 (2.6–96) (mean)	97.9	100
Ma and colleagues <sup>(37)</sup>	2b	52/58	2.2 (NR)	94.2	NR	60.1 (48–90)	100	70
Yang and colleagues <sup>(27)</sup>	4	51/51	5.1 (4.1–6.4)	98	11.8	31.5 (12–60) (mean)	NR	100
Veltri and colleagues <sup>(24)</sup>	2c	137/203	3.0 (1.2–7.5)	97.8	10.4	39 (1–109) (mean)	91	95
Takaki and colleagues <sup>(29)</sup>	4	21/21	4.6 (4.1–6.5)	100	24	46.1 (6–122)	95.2	47.6
Ramirez and colleagues <sup>(25)</sup>	4	79/111	2.2 (0.9–4.2) median	93.3	8.8	59 (2–120)	100	77.2
McClure and colleagues <sup>(20)</sup>	2b	84/100	2.3 (0.7–6.0) median	NR	13	24 (1–106)	100	100
Andersson and colleagues <sup>(33)</sup>	2c	60/61	2.5 (1.3–5.0) median	98	13	19 (2–46) (mean)	NR	38
Forauer and colleagues <sup>(34)</sup>	2b	39/46	2.6 (1.2–4.0)	98	7.7	35.5 (12–83) (mean)	97.4	100
Pleper and colleagues <sup>(35)</sup>	4	38/38	2.1 (NR)	67.6	5.1	54.6 (1–127) (mean)	NR	76.3
Iannuccilli and colleagues <sup>(18)</sup>	2b	203/203	2.5 (1.0–6.0)	87	14.7	34.1 (1–131) (mean)	NR	86.7
Zhang and colleagues <sup>(23)</sup>	4	122/122	3.4 (NR)	94.2	NR	64.9 (NR)	98.3	100
Zachos and colleagues <sup>(31)</sup>	4	32/32	2.3 (0.6–3.5)	90.6	9.4	24 (NR)	NR	100
Kim and colleagues <sup>(30)</sup>	2b	51/51	2.1 (1.0–3.9) median	96	5.8	26 (4–60)	NR	100
Pantelidou and Colleagues <sup>(61)</sup>	4	63/63	2.1 (0.5–5.2)	90.5	7.9	47.5 (11.8–80.2)	NR	100

<sup>a</sup>Biopsy-proven RCC; percentage of RCC proven of total NP.

CSS = cancer specific survival; NP = number of patients; NR = not reported; NT = number of tumors; RFS = recurrence free survival.

### **Cryoablation (CA)**

In 1995, Uchida and colleagues were the first to report on percutaneous renal cryoablation(42). Both laparoscopic (LCA) and percutaneous cryoablation (PCA) are used in clinical practice. Patients with a localized SRM ( $\leq 4$  cm) are selected for treatment by CA based on operator preference, presence of multiple masses, previous renal surgery and medical comorbidity(43-46). PCA is most often used in clinical practice and is preferred in posterior and lateral tumors, with a clear window for probe placement(47). Aron and colleagues suggested to use the PCA for posterior and posteromedial tumors ; for anterior and lateral tumors they prefer LCA, although it is a more invasive approach(48). LCA is preferred if bowel or solid organs are close to the tumor(49). The exact mechanism of cryotherapy is not entirely known, but it relies on the assumption that temperatures  $< -20^{\circ}\text{C}$  induce cell death(45,49). A nitrogen-based liquid is guided through the tip of the cryoprobe in order to create an ice-ball extending 1 cm beyond the margins of the tumor. There is a rapid freeze at the tip with working temperatures between  $-185^{\circ}\text{C}$  and  $-195^{\circ}\text{C}$ .

In table 4 the reviewed studies on CA are summarized. The level of evidence in all studies is 2b. The mean tumor diameter varied between 2.1 and 4.8 cm. Although most tumor sizes were rather small, treatment failure was significantly associated in tumor size  $> 4$  cm as was reported by Kim and colleagues. Even so, two studies reported no association between tumor size and complication rate(50,51). In all studies the majority of tumors within the study group were pathologically proven RCC, varying between 49% and 100%.

The cause of treatment failures mentioned in the different studies were divers. One technical failure occurred during treatment of a 4.3 cm large centrally situated RCC(52,53). A broad based contact with the renal sinus led to a clinical treatment failure in seven out of eight patients (53). Ice-ball formation under 6 mm around the tumor was related to incomplete local control(45,54). An increased skin to tumor distance was also mentioned as a risk factor of treatment failure(50). Location of the tumor also plays an important role in treatment success, where central location of the tumor was associated with an increased risk in treatment failure(52-54).

Renal clamping in surgical treatment is necessary, but causes a period of ischemia and therefore it influences renal function post-operatively. Ischemia is not used in ablative procedures, which is a potential benefit of ablative therapies(49,55). Most studies reported on kidney function after treatment. The results were heterogeneous. Most studies showed no difference in serum creatinine levels and eGFR, pre- and post-ablation(43,45-48,51,55-59), while others showed a minimal impact (44,48,57). It is even stated that CA has superior

outcomes compared to surgery in regard to preserving renal function, especially in single kidneys(45,49). Interestingly, Tanagho and colleagues stated that a smaller tumor size and hilar location contributes to improved renal function outcomes after CA(44).

The complication rates in the different studies varied from 0%-23%. The occurrence of major complications appeared to be associated with tumor size(50,52,60). Atwell and colleagues reported a significant higher complication rate in higher T-stages, in which they advise that CA for >T1b is technically feasible, although complications are more frequent(60). Bleeding was also significantly increased in T1b tumors(59). Breen and colleagues reported that upper pole location was a predictive factor for complications(52).

Most reported minor complications (Clavien grade I-II) were perirenal hematoma (44,45,50,52,57,59,61), pneumothorax (48,50,52,55,62), pneumonia (48,55,62), hematuria (54,59), and persistent flank pain (45,52,60,62).

Most reported major complications (Clavien grade III-IV) were cardiopulmonary decompensation and myocardial infarct (44,47,48,60,62), ureteropelvic junction obstruction/injury(47,52,55,60,63), post-procedural bleeding (47,48,52,57,60,64), and blood transfusion (52,59,62,63). One of the causes of bleeding during CA treatment was ice ball fracture, especially in treatment with larger tumor diameter (52).

The recurrence free survival (RFS) varied between 81% and 99%, with a median FU period between 12.7 and 97.9 months. Recurrence free survival was defined as no evidence of radiographic recurrence or increasing tumor size > 6 months after the procedure(43,50), although the definition of recurrence in the reviewed studies is not always clear. Four studies reported a FU of 10 years(48,57,63,64), in which Johnson and colleagues described an average time to recurrence of 39.9 months, Larcher and colleagues reported a median time to recurrence of 18 months, and Caputo and colleagues reported a time to recurrence of 27.6 months with the latest recurrence after 53.3 months. The cancer specific survival (CSS) varied between 92% and 100%, although it was not reported in nine studies. Even so, several short FU studies show adequate oncological control and limited morbidity indicating that the use of CA in renal tumors is acceptable. However, more recent results on ablative treatment of T1 lesions in long-term studies suggested that CA is possibly associated with poorer outcomes, such as reduced overall, cancer-specific and disease free survival(48,60,62). However, CA may be safely used in patients groups not suitable for surgical treatment(45,46,57).

In conclusion cryoablation is considered a safe and effective treatment for patients with small renal masses who are poor surgical candidates due to significant comorbidities(51,52,60,65). The RFS and CSS are favorable on the short term. Whether results in the long term are acceptable is up for debate, since several studies suggest a poorer outcome(48,60,62), whereas other studies do show a beneficial outcome in a longer FU period (48,57,63,64).



**Table 4.** Summary of studies assessing Cryoablation in primary Renal Cell Carcinoma

References	Level of evidence	NP/NT <sup>a</sup>	Mean tumor diameter in cm (range)	RFS (%) <sup>a</sup>	Complications (%)	Median follow-up in months (range)	CSS (%) <sup>a</sup>	Biopsy proven RCC (%) <sup>a</sup>
Yoost and colleagues <sup>(53)</sup>	2b	45/47	2.7 (1.2–5.4)	83	NR	13 (NR)	NR	49
Ko and colleagues <sup>(43)</sup>	2b	39/45	2.5 (0.7–3.9)	96.7	0	23.5 (6–53)	100	60
Aron and colleagues <sup>(48)</sup>	2b	80/88	2.3 (0.9–5.0)	81	8	93 (60–132)	92	69
Park and colleagues <sup>(58)</sup>	2b	14/15	2.8 (1.7–3.7)	93.3	0	32.6 (12–51) mean	NR	100
Vricella and colleagues <sup>(51)</sup>	2b	52/54	2.5 (0.6–6.2)	96.2	12	18.5 (9–40)	100	51.9
Haber and colleagues <sup>(49)</sup>	2b	30/35	2.6 (NR)	86.7	10.2	60.2 (NR) mean	93	83.3
Duffey and colleagues <sup>(62)</sup>	2b	116/116	2.8 (1.1–5.5)	89	19.8	27.4 (1–112) mean	NR	65.3
Guillotreau and colleagues <sup>(65)</sup>	2b	220/234	2.2 (NR)	89	12	44.5 (8.7–66.8)	NR	77
Blute and colleagues <sup>(50)</sup>	2b	139/139	2.4 (1.0–6.5)	93	12.9	24 (NR)	NR	56
Breen and colleagues <sup>(62)</sup>	2b	147/171	3.2 (1.1–6.7)	99	10.4	20.1 (NR)	NR	56
Georgiades and Rodriguez <sup>(47)</sup>	2b	134/134	2.8 (0.5–7.0)	97	6	NR (NR)	100	100
Tanagho and colleagues <sup>(44)</sup>	2b	267/267	2.5 (NR)	83.1	8.6	39.8 (NR) mean	96.4	52.3
Buy and colleagues <sup>(59)</sup>	2b	95/120	2.6 (1.0–6.8)	94	9.5	28 (6–63) mean	100	74
Emara and colleagues <sup>(55)</sup>	2b	56/56	2.5 (NR)	96.4	9	31.3 (NR)	100	69.6
Johnson and colleagues <sup>(63)</sup>	2b	92/112	2.3 (NR)	91	16.3	97.9 (NR) (mean)	98.5	76
Larcher and colleagues <sup>(64)</sup>	2b	174/174	2.1 (NR)	95	27	48 (1–156)	100	62
Kim and colleagues <sup>(56)</sup>	2b	68/79	2.3 (0.3–5.7)	83	19.1	59.8 (3–119) mean	100	65.8
Yan and colleagues <sup>(46)</sup>	2b	18/18	3.3 (1.4–4.6)	94.5	11	26.8 (12–56) mean	NR	100
Atwell and colleagues <sup>(60)</sup>	2b	46/46	4.8 (4.1–6.4)	96.4	17.2	24 (3.6–73.2)	94	85
Yamanaka and colleagues <sup>(64)</sup>	2b	61/61	2.4 (0.8–4.8)	93.4	NR	12.7 (6.1–25.9)	NR	87
Lai and colleagues <sup>(45)</sup>	2b	30/32	3.1 (1.4–4.9)	86.4	23.3	15.2 (1–47.4) mean	NR	93.8
Caputo and colleagues <sup>(57)</sup>	2b	138/142	2.4 (0.6–5.2)	91.4	10.6	92 (44.6–153)	96.8	70.4

<sup>a</sup>Biopsy-proven RCC; percentage of RCC proven of total NP.

### **Microwave ablation (MWA)**

MWA is a thermal ablation technique, which uses electromagnetic microwaves through one or multiple antennas placed in the tumor. Tumor cells are damaged by the mechanism of creating a thermal field by rotation of dipole water molecules, producing heat and causing tissue necrosis in solid tumors(66). The electrodes function as an antenna to concentrate the energy and are placed by a percutaneous (67-74) laparoscopic (67,75,76) or open approach(76) under general anesthesia. The number of antennas used depends on size and location of the tumor. The penetration depth of the energy can be adjusted by the frequency of the energy source. The different energies used vary between 1-100W, with a frequency of 915MHz or 2450MHz, depending on the system used.

Table 5 shows the reviewed studies on MWA. The level of evidence varied between 2b and 4. A few studies mention a potential benefit over RFA. A potential benefit can be that MWA is less effected by the heat-sink effect, as a result of less dependence on the electrical conductivity of tissue, higher thermal efficiency, thereby reaching higher intratumoral temperatures and thereby less ablation time(69,70,72,73,76). As such, possibly larger tumors can be ablated(69,70,76).

The mean diameter varied between 2.4 cm and 3.7 cm (range 0.6-8.4 cm). The size of the tumor is important. Gao and colleagues reported a significantly better ablation success in tumors <4 cm (100% success), compared to > 4 cm (75% success)(72). Guan and colleagues stated that only exophitic low grade tumors with a diameter <4 cm should be considered for treatment with MWA(76). A maximum diameter of 4 cm was recommended in most studies(68-70). However, several authors suggested that MWA can also be performed in tumors near the renal sinus (72), or in the collecting system(67); a clear benefit over other ablative techniques.

As opposed to surgical techniques renal clamping is not necessary in MWA procedures (75). A few studies in MWA reported on post-procedural renal functions. In some studies, the eGFR and post-procedural creatinine levels(70-72,74) did not significantly decrease (69). In other studies a small decline in kidney function had been seen(73,76). In patients with pre-existent chronic kidney disease function remained stable.(72,76).

The complication rate varied between 0% and 60%. Most complications were low grade complications (Clavien grade I-II): hematuria(67,72,73,76), numbness(67,76), flank pain (67,76), thermal injury (67,73), urine fistula(70-72), and subcapsular renal hemorrhage(69,74). High grade complications (Clavien III-IV) were also reported: urinoma (67), retained foreign body(67), urine leakage and abscess formation requiring drainage(72,76), hydrothorax in two patients(73), pleural effusion(74) and bowel injury(73). Two studies did not mention any complications (68,75).

**Table 5.** Summary of studies assessing Microwave Ablation in primary Renal Cell Carcinoma

References	Level of evidence	NP/NT <sup>a</sup>	Mean tumor diameter in cm (range)	RFS (%) <sup>a</sup>	Complications (%)	Median follow-up in months (range)	CSS (%) <sup>a</sup>	Biopsy proven RCC (%) <sup>a</sup>
Castle and colleagues <sup>(67)</sup>	4	10/10	3.7 (2.0–5.5)	62	60	17.9 (14–24) mean	NR	90
Muto and colleagues <sup>(72)</sup>	4	10/10	2.8 (1.3–4.2)	100	0	13 (1–25) mean	100	100
Guan and colleagues <sup>(76)</sup>	2b	48/48	3.1 (1.2–3.9)	91.3	12.5	32 (NR)	100	62.5
Li and colleagues <sup>(68)</sup>	4	79/83	3.2 (0.6–7.8)	91.6	NR	26 (3–74)	100	100
Moreland and colleagues <sup>(69)</sup>	4	53/55	2.6 (0.8–4.0)	100	11.3	8 (5–18.3)	100	100
Yu and colleagues <sup>(70)</sup>	3	98/105	2.7 (0.6–4.0)	96.2	1.7	25.8 (3.7–75.2)	97	100
Wells and colleagues <sup>(71)</sup>	4	29/30	3.1 (2.3–3.8) median	100	10.1	12.0 (6–18)	97	100
Chen and colleagues <sup>(74)</sup>	4	29/32	2.4 (1.8–2.9) median	100	6.5	17 (3–71)	100	100
Gao and colleagues <sup>(72)</sup>	4	41/41	3.6 (1.9–6.8)	83	26.8	37.6 (3.0–97.3)	92.7	100
Dong and colleagues <sup>(73)</sup>	4	101/105	2.9 (0.6–8.4)	NR	24.8	25 (1.1–93.2)	NR	87.6

<sup>a</sup>Biopsy-proven RCC; percentage of RCC proven of total NP.

The RFS varied between 62% and 100% in a median FU between 8 and 32 months (range 1 – 93.2 months). Castle and colleagues reported the highest recurrence (38%, median FU of 18 months) (67). Wells and colleagues reported a RFS of 100%, but recurrence to metastatic disease in one patient(71). Gao and colleagues reported a median time to recurrence of 34.1 months(72). In a few studies a second ablation session was necessary, due to residual tumor (68,70,71,74,76). The RFS ratios were reflected in a favorable CSS ratios (92% - 100%). In all studies RCC was biopsy proven in the largest part of the cohort. In Dong and colleagues a part of the studygroup was not pathologically proven due to the inability to take biopsies due to comorbidities(73). In Guan and colleagues 14 out of 38 treated tumors were benign(76). This raises the question whether not all SRM's should be biopsied in advance of ablative treatment, as was the case in most other studies(68-72,74,75).

In conclusion, MWA appears to be a safe and effective treatment option especially for tumors  $\leq 4$  cm, in elderly with associated comorbid diseases, and in poor surgical candidates(70,71). It is also a suitable treatment option in tumors near the renal sinus or in the collecting system(67,72); a clear benefit over other ablative modalities. Although these results are promising, the groups were relatively small and only short-time FU is available. MWA has a few theoretically advantages over other ablative techniques, but oncological control has to be proven during the long term FU. More and larger studies are required to more safely implement this technique.

### ***Stereotactic body radiation therapy (SBRT)***

The use of external beam radiotherapy (EBRT) has been limited before the last decade due to assumed radioresistance of RCC dating back to the time that conventional (too) low dosed fractionated radiotherapy for RCC was standard of care. Developments in SBRT within the last decade have allowed for precise delivery of high dose hypofractionated radiotherapy. Recent studies have shown that RCC is actually radiosensitive(77). Stereotactic body radiation therapy is a high precision radiation technique that enables delivery of a high radiation dose in one or a few fractions, making use of on-line image guidance. An additional advantage relative to conventional EBRT is a steep dose fall off from the planned target volume (PTV) to surrounding tissues and a high biological dose can be delivered with small margins surrounding the tumor volume and therefore low associated toxicity rates. The last few years there has been an improvement in imaging and therefore the margins are smaller and the dosage can be delivered even more precise(78). Another advantage is that this treatment is either non-invasive (without fiducial markers)(77,79), or minimal invasive (when fiducial markers are placed in the tumor or in the near parenchymal tissue)(78,80-82).

**Table 6.** Summary of studies assessing Stereotactic Body Radiation Therapy in primary Renal Cell Carcinoma

References	Level of evidence	NP/NT <sup>a</sup>	Mean tumor diameter in cm (range)	Dose (fractions)	RFS <sup>a</sup> (%)	Toxicity (%)	Median follow-up in months (range)	CSS <sup>a</sup> (%)	Biopsy proven RCC (%) <sup>a</sup>
Pham and colleagues <sup>(77)</sup>	2b	20/20	NR (3.0-9.0)	42 Gy (3) 26 Gy (1)	NR	60	6 (NR)	NR	NR
Staehler and colleagues <sup>(81)</sup>	2b	40/45	<4 cm (NR)	25 Gy (1)	98	30	28.1 (6 – 78)	100	100
Ponsky and colleagues <sup>(82)</sup>	2b	19/19	NR	24 Gy (4) 32 Gy (4) 40 Gy (4) 48 Gy (4)	63 – 84	37	14 (6 – 35)	100	95
Yamamoto and colleagues <sup>(80)</sup>	2b	14/14	3.0 (1.6-4.6)	70 Gy (10) 60 Gy (10) 50 Gy (10)	NR	NR	31.2 (16.2-54.2)	100	0
Sun and colleagues <sup>(78)</sup>	2b	40/41	3.9 (1.6-8.3)	21 Gy (3) 48 Gy (3)	93	NR	18.7 (3-46)	100	80
Chang and colleagues <sup>(79)</sup>	2b	16	4.0 (1.0-14.6)	40 Gy (5) 35 Gy (5) 32.5 Gy (5) 30 Gy (5)	100	18.7	19 (7-30)	100	56

<sup>a</sup>Biopsy-proven RCC; percentage of RCC proven of total NP.

An overview of the current literature about SBRT for inoperable renal cell carcinoma is described in table 6. The level of evidence in these studies is 2b. SBRT treatment for RCC is currently used in inoperable patients. All of the described studies used a high-dose per fraction external radiation, gross tumor volume (GTV) outline for treatment planning on CT-scan and the use of CT for position verification. In some studies the position verification before each treatment fraction was improved by the use of fiducial markers in the tumor/surrounding kidney tissue(78,80-82), or the patient is fixed in a body frame with vacuum stabilization(77,79). When using fiducial markers and therefore more precise targeting of radiotherapy, in one study a significant lower ratio of renal atrophy was reported(80). Although the radiotherapy techniques used in the different studies are comparable, the prescribed doses and fractionation schemes used were heterogeneous, sometimes even within studies as the fractionation scheme may be adapted to tumor size(77,79), or due to dose escalation(78,82).

The tumors treated in the different studies vary in diameter (mean 3-4 cm; range 1.0-14.6); two studies did not report a diameter of the treated tumors, although one stated that lesions had to be less than 4 cm due to technical limitations of the cyberknife(81). Successful treatment seems to be related to tumor size. Pham and colleagues use the size of the tumor to determine the dosage given to the tumor, 42 Gy in three fractions in tumors  $\geq 5$  cm, and 26 Gy in one fraction in tumors  $< 5$ cm(77). The more recent studies have shown the possibility to treat larger lesions. They stated that in SBRT treatment there are no limitations considering tumorsize and location of the tumor(78,79).

The fractionation schemes in literature varied between 25 Gy and 48 Gy, in 1 to 5 fractions. The recurrence free survival with these dosages was reported between 63 and 98%. The largest study so far including 40 patients with 45 tumors, 98% RFS was achieved after a mean FU of 28.1 months. This study did not include metastatic RCC(81). Overall the FU was relatively short, with a median FU varying between 6 – 31.2 months. The CSS is not reported in any of the studies.

The reported grade 1-2 toxicities varied between 30% and 60%, but were relatively mild. Most reported toxicities were nausea(77,79,81), fatigue(77,81,82), dermatitis(77,81), local pain(77). In one patient a duodenal ulcer (grade 4 toxicity) occurred(82). Ponsky and colleagues also reported renal toxicity in two out of 19 patients with pre-existing renal dysfunction(82), Chang and colleagues reported on grade 4 renal toxicities in two out of 16 patients(79), while two other studies described a stable kidney function pre- and post-treatment(80,81).

In conclusion, radiotherapy is considered to be a safe and effective treatment. Indications for the use of SBRT are patients not suitable for surgery due to comorbidity, so there is a need for non-invasive treatment alternatives (78,80,81). Although early results seem promising, most studies have used a small number of primary RCC, partially not pathologically proven and with a relatively short FU.

## CONCLUSION

There are several alternative treatment options for patients with RCC other than (partial) nephrectomy, especially for those patients who are unfit to undergo an invasive treatment. Most of these treatment modalities are minimal invasive (CA, RFA, MWA and SBRT with fiducial markers); radiotherapy can be completely non-invasive, when a technique without fiducial markers is used.

Active surveillance is by definition non-invasive during the 'surveillance' period. However, this modality also implies 'active' treatment in case of disease progression, with a limited risk of metastatic disease. It should be noted that in described series only a small fraction of patients underwent a biopsy. So whether these series indeed reflect studies concerning patients with RCC is debatable.

All alternative treatment modalities have been described as being safe and effective, based on phase I and II studies. Phase II studies with mean FU time longer than five years have been published for AS, RFA, CA, MWA and SBRT, although the number of patients treated in MWA and SBRT studies were small. For RFA, CA and MWA, limitations in the size (and sometimes location) of the tumor exist, as larger sizes or more central locations may interfere with local control rates and treatment-related morbidity. Despite the theoretical advantages of MWA on RFA and CA, more and larger studies are required to more safely execute this treatment. For SBRT there are in general no limitations to tumor size and location and the expected toxicity of SBRT is mostly related to the proximity of the surrounding healthy organs.

Radiotherapy treatment has improved dramatically throughout the last decade, moving from low radiation doses with large treatment fields, to more precise CT-guided radiotherapy, allowing for a higher biological effective dose, a smaller number of treatment fractions at stereotactic accuracy (therefore limiting the volume of healthy tissue treated and minimizing toxicity). Improvements are expected within the next years, when non-invasive (without fiducial markers) MRI-guided radiotherapy will become available, allowing for even more accurate radiation and dose escalation.

Randomised controlled trials (RCTs) comparing (partial) nephrectomy to less invasive treatment modalities have not been performed to date. However, an RCT comparing surgery and less invasive modalities may not be feasible any more due to patient preferences

leading to inability to randomize patients into treatment arms. Nevertheless, case-controlled registries may be alternatives to compare outcomes of minimal- to non-invasive treatment modalities to surgery in the future.



## REFERENCES

1. Ljungberg B, Bensalah K, Bex A, Canfield S, Dabestani S, Giles RH, and colleagues Guidelines on Renal Cell Carcinoma. European Association of Urology 2015.
2. Ferlay J, Steliarova-Foucher E, Lortet-Tieulent J, Rosso S, Coebergh JW, Comber H, and colleagues Cancer incidence and mortality patterns in Europe: estimates for 40 countries in 2012. *Eur J Cancer* 2013 Apr;49(6):1374-1403.
3. Hollingsworth JM, Miller DC, Daignault S, Hollenbeck BK. Rising incidence of small renal masses: a need to reassess treatment effect. *J Natl Cancer Inst* 2006 Sep 20;98(18):1331-1334.
4. Rosales JC, Haramis G, Moreno J, Badani K, Benson MC, McKiernan J, and colleagues Active surveillance for renal cortical neoplasms. *J Urol* 2010 May;183(5):1698-1702.
5. Cutress ML, Ratan HL, Williams ST, O'Brien MF. Update on the management of T1 renal cortical tumours. *BJU Int* 2010 Oct;106(8):1130-1136.
6. Moher D, Liberati A, Tetzlaff J, Altman DG, PRISMA Group. Preferred reporting items for systematic reviews and meta-analyses: the PRISMA statement. *PLoS Med* 2009 Jul 21;6(7):e1000097.
7. Mason RJ, Abdolell M, Trottier G, Pringle C, Lawen JG, Bell DG, and colleagues Growth kinetics of renal masses: analysis of a prospective cohort of patients undergoing active surveillance. *Eur Urol* 2011 May;59(5):863-867.
8. Patel N, Cranston D, Akhtar MZ, George C, Jones A, Leiblich A, and colleagues Active surveillance of small renal masses offers short-term oncological efficacy equivalent to radical and partial nephrectomy. *BJU Int* 2012 Nov;110(9):1270-1275.
9. Bahouth Z, Halachmi S, Meyer G, Avitan O, Moskovitz B, Nativ O. The natural history and predictors for intervention in patients with small renal mass undergoing active surveillance. *Adv Urol* 2015;2015:692014.
10. Jewett MA, Mattar K, Basiuk J, Morash CG, Pautler SE, Siemens DR, and colleagues Active surveillance of small renal masses: progression patterns of early stage kidney cancer. *Eur Urol* 2011 Jul;60(1):39-44.
11. Brunocilla E, Borghesi M, Schiavina R, Della Mora L, Dababneh H, La Manna G, and colleagues Small renal masses initially managed using active surveillance: results from a retrospective study with long-term follow-up. *Clin Genitourin Cancer* 2014 Jun;12(3):178-181.
12. Schiavina R, Borghesi M, Dababneh H, Bianchi L, Longhi B, Diazzi D, and colleagues Small renal masses managed with active surveillance: predictors of tumor growth rate after long-term follow-up. *Clin Genitourin Cancer* 2015 Apr;13(2):e87-92.
13. Pierorazio PM, Johnson MH, Ball MW, Gorin MA, Trock BJ, Chang P, and colleagues Five-year Analysis of a Multi-institutional Prospective Clinical Trial of Delayed Intervention and Surveillance for Small Renal Masses: The DISSRM Registry. *Eur Urol* 2015 Feb 16.
14. Zlotta AR, Wildschutz T, Raviv G, Peny MO, van Gansbeke D, Noel JC, and colleagues Radiofrequency interstitial tumor ablation (RITA) is a possible new modality for treatment of renal cancer: ex vivo and in vivo experience. *J Endourol* 1997 Aug;11(4):251-258.
15. Psutka S, McGovern F, Mueller P, McDougal WS, Gervais D, Feldman A. Long-term durable oncologic outcomes after radiofrequency ablation for t1a renal cell carcinoma. *J Urol* 2012 ;187(4):e452.

16. Balageas P, Cornelis F, Le Bras Y, Hubrecht R, Bernhard JC, Ferriere JM, and colleagues Ten-year experience of percutaneous image-guided radiofrequency ablation of malignant renal tumours in high-risk patients. *Eur Radiol* 2013 Jul;23(7):1925-1932.
17. Zagoria RJ, Pettus JA, Rogers M, Werle DM, Childs D, Leyendecker JR. Long-term outcomes after percutaneous radiofrequency ablation for renal cell carcinoma. *Urology* 2011 Jun;77(6):1393-1397.
18. Iannuccilli JD, Dupuy DE, Beland MD, Machan JT, Golijanin DJ, Mayo-Smith WW. Effectiveness and safety of computed tomography-guided radiofrequency ablation of renal cancer: a 14-year single institution experience in 203 patients. *Eur Radiol* 2016 Jun;26(6):1656-1664.
19. Zhao X, Wang W, Zhang S, Liu J, Zhang F, Ji C, and colleagues Improved outcome of percutaneous radiofrequency ablation in renal cell carcinoma: a retrospective study of intraoperative contrast-enhanced ultrasonography in 73 patients. *Abdom Imaging* 2012 Oct;37(5):885-891.
20. McClure TD, Chow DS, Tan N, Sayre JA, Pantuck AJ, Raman SS. Intermediate outcomes and predictors of efficacy in the radiofrequency ablation of 100 pathologically proven renal cell carcinomas. *J Vasc Interv Radiol* 2014 Nov;25(11):1682-8; quiz 1689.
21. Wah TM, Irving HC, Gregory W, Cartledge J, Joyce AD, Selby PJ. Radiofrequency ablation (RFA) of renal cell carcinoma (RCC): experience in 200 tumours. *BJU Int* 2014 Mar;113(3):416-428.
22. Sung HH, Park BK, Kim CK, Choi HY, Lee HM. Comparison of percutaneous radiofrequency ablation and open partial nephrectomy for the treatment of size- and location-matched renal masses. *Int J Hyperthermia* 2012;28(3):227-234.
23. Zhang F, Chang X, Liu T, Wang W, Zhao X, Ji C, and colleagues Prognostic Factors for Long-Term Survival in Patients with Renal-Cell Carcinoma After Radiofrequency Ablation. *J Endourol* 2016 Jan;30(1):37-42.
24. Veltri A, Gazzera C, Busso M, Solitro F, Piccoli GB, Andretto B, and colleagues T1a as the sole selection criterion for RFA of renal masses: randomized controlled trials versus surgery should not be postponed. *Cardiovasc Intervent Radiol* 2014 Oct;37(5):1292-1298.
25. Ramirez D, Ma YB, Bedir S, Antonelli JA, Cadeddu JA, Gahan JC. Laparoscopic radiofrequency ablation of small renal tumors: long-term oncologic outcomes. *J Endourol* 2014 Mar;28(3):330-334.
26. Kim SD, Yoon SG, Sung GT. Radiofrequency ablation of renal tumors: four-year follow-up results in 47 patients. *Korean J Radiol* 2012 Sep-Oct;13(5):625-633.
27. Yang R, Lian H, Zhang G, Wang W, Gan W, Li X, and colleagues Laparoscopic radiofrequency ablation with intraoperative contrast-enhanced ultrasonography for T1bN0M0 renal tumors: initial functional and oncologic outcomes. *J Endourol* 2014 Jan;28(1):4-9.
28. Sommer CM, Lemm G, Hohenstein E, Bellemann N, Stampfl U, Goezen AS, and colleagues CT-guided bipolar and multipolar radiofrequency ablation (RF ablation) of renal cell carcinoma: specific technical aspects and clinical results. *Cardiovasc Intervent Radiol* 2013 Jun;36(3):731-737.
29. Takaki H, Soga N, Kanda H, Nakatsuka A, Uraki J, Fujimori M, and colleagues Radiofrequency ablation versus radical nephrectomy: clinical outcomes for stage T1b renal cell carcinoma. *Radiology* 2014 Jan;270(1):292-299.

30. Kim HJ, Park BK, Park JJ, Kim CK. CT-Guided Radiofrequency Ablation of T1a Renal Cell Carcinoma in Korea: Mid-Term Outcomes. *Korean J Radiol* 2016 Sep-Oct;17(5):763-770.
31. Zachos I, Dimitropoulos K, Karatzas A, Samarinas M, Petsiti A, Tassoudis V, and colleagues Ultrasound-guided radiofrequency ablation for cT1a renal masses in poor surgical candidates: mid-term, single-center outcomes. *Ther Adv Med Oncol* 2016 Sep;8(5):331-338.
32. Seklehner S, Fellner H, Engelhardt PF, Schabauer C, Riedl C. Percutaneous radiofrequency ablation of renal tumors: a single-center experience. *Korean J Urol* 2013 Sep;54(9):580-586.
33. Andersson M, Hashimi F, Lyrdal D, Lundstam S, Hellstrom M. Improved outcome with combined US/CT guidance as compared to US guidance in percutaneous radiofrequency ablation of small renal masses. *Acta Radiol* 2015 Dec;56(12):1519-1526.
34. Forauer AR, Dewey BJ, Seigne JD. Cancer-free survival and local tumor control after impedance-based radiofrequency ablation of biopsy-proven renal cell carcinomas with a minimum of 1-year follow-up. *Urol Oncol* 2014 Aug;32(6):869-876.
35. Pieper CC, Fischer S, Strunk H, Meyer C, Thomas D, Willinek WA, and colleagues Percutaneous CT-Guided Radiofrequency Ablation of Solitary Small Renal Masses: A Single Center Experience. *Rofo* 2015 Jul;187(7):577-583.
36. Karam JA, Ahrar K, Vikram R, Romero CA, Jonasch E, Tannir NM, and colleagues Radiofrequency ablation of renal tumours with clinical, radiographical and pathological results. *BJU Int* 2013 May;111(6):997-1005.
37. Ma Y, Bedir S, Cadeddu JA, Gahan JC. Long-term outcomes in healthy adults after radiofrequency ablation of T1a renal tumours. *BJU Int* 2014 Jan;113(1):51-55.
38. Ofude M, Kitagawa Y, Koda W, Ueno S, Kadono Y, Konaka H, and colleagues Preserved renal function after percutaneous radiofrequency ablation for renal tumors: experience of a single institution. *Anticancer Res* 2013 Oct;33(10):4669-4673.
39. Chang X, Liu T, Zhang F, Ji C, Zhao X, Wang W, and colleagues Radiofrequency ablation versus partial nephrectomy for clinical T1a renal-cell carcinoma: long-term clinical and oncologic outcomes based on a propensity score analysis. *J Endourol* 2015 May;29(5):518-525.
40. Olweny EO, Park SK, Tan YK, Best SL, Trimmer C, Cadeddu JA. Radiofrequency ablation versus partial nephrectomy in patients with solitary clinical T1a renal cell carcinoma: comparable oncologic outcomes at a minimum of 5 years of follow-up. *Eur Urol* 2012 Jun;61(6):1156-1161.
41. Leveillee RJ, Castle SM, Gorbatiy V, Salas N, Narayanan G, Morillo-Burgos G, and colleagues Oncologic outcomes using real-time peripheral thermometry-guided radiofrequency ablation of small renal masses. *J Endourol* 2013 Apr;27(4):480-489.
42. Uchida M, Imaide Y, Sugimoto K, Uehara H, Watanabe H. Percutaneous cryosurgery for renal tumours. *Br J Urol* 1995 Feb;75(2):132-6; discussion 136-7.
43. Ko YH, Choi H, Kang SG, Park HS, Lee JG, Kim JJ, and colleagues Efficacy of laparoscopic renal cryoablation as an alternative treatment for small renal mass in patients with poor operability: experience from the Korean single center. *J Laparoendosc Adv Surg Tech A* 2010 May;20(4):339-345.

44. Tanagho YS, Bhayani SB, Kim EH, Figenshau RS. Renal cryoablation versus robot-assisted partial nephrectomy: Washington University long-term experience. *J Endourol* 2013 Dec;27(12):1477-1486.
45. Lai WJ, Chung HJ, Chen CK, Shen SH, Chou HP, Chiou YY, and colleagues Percutaneous computed tomography-guided cryoablation for renal tumor: Experience in 30 cases. *J Chin Med Assoc* 2015 May;78(5):308-315.
46. Yan X, Zhang M, Chen X, Wei W, Yang R, Yang Y, and colleagues Image-guided percutaneous renal cryoablation for stage 1 renal cell carcinoma with high surgical risk. *World J Surg Oncol* 2015 Jun 10;13:200-015-0610-x.
47. Georgiades CS, Rodriguez R. Efficacy and safety of percutaneous cryoablation for stage 1A/B renal cell carcinoma: results of a prospective, single-arm, 5-year study. *Cardiovasc Intervent Radiol* 2014 Dec;37(6):1494-1499.
48. Aron M, Kamoi K, Remer E, Berger A, Desai M, Gill I. Laparoscopic renal cryoablation: 8-year, single surgeon outcomes. *J Urol* 2010 Mar;183(3):889-895.
49. Haber GP, Lee MC, Crouzet S, Kamoi K, Gill IS. Tumour in solitary kidney: laparoscopic partial nephrectomy vs laparoscopic cryoablation. *BJU Int* 2012 Jan;109(1):118-124.
50. Blute ML, Jr, Okhunov Z, Moreira DM, George AK, Sunday S, Lobko II, and colleagues Image-guided percutaneous renal cryoablation: preoperative risk factors for recurrence and complications. *BJU Int* 2013 Apr;111(4 Pt B):E181-5.
51. Vricella GJ, Haaga JR, Adler BL, Dean N, Cherullo EE, Flick S, and colleagues Percutaneous cryoablation of renal masses: impact of patient selection and treatment parameters on outcomes. *Urology* 2011 Mar;77(3):649-654.
52. Breen DJ, Bryant TJ, Abbas A, Shepherd B, McGill N, Anderson JA, and colleagues Percutaneous cryoablation of renal tumours: outcomes from 171 tumours in 147 patients. *BJU Int* 2013 Oct;112(6):758-765.
53. Yoost TR, Clarke HS, Savage SJ. Laparoscopic cryoablation of renal masses: which lesions fail? *Urology* 2010 Feb;75(2):311-314.
54. Yamanaka T, Yamakado K, Yamada T, Fujimori M, Takaki H, Nakatsuka A, and colleagues CT-Guided Percutaneous Cryoablation in Renal Cell Carcinoma: Factors Affecting Local Tumor Control. *J Vasc Interv Radiol* 2015 Aug;26(8):1147-1153.
55. Emara AM, Kommu SS, Hindley RG, Barber NJ. Robot-assisted partial nephrectomy vs laparoscopic cryoablation for the small renal mass: redefining the minimally invasive 'gold standard'. *BJU Int* 2014 Jan;113(1):92-99.
56. Kim HK, Pyun JH, Kim JY, Kim SB, Cho S, Kang SG, and colleagues Renal cryoablation of small renal masses: a Korea University experience. *Korean J Urol* 2015 Feb;56(2):117-124.
57. Caputo PA, Ramirez D, Zargar H, Akca O, Andrade HS, O'Malley C, and colleagues Laparoscopic Cryoablation for Renal Cell Carcinoma: 100-Month Oncologic Outcomes. *J Urol* 2015 Oct;194(4):892-896.
58. Park SH, Kang SH, Ko YH, Kang SG, Park HS, Moon du G, and colleagues Cryoablation for endophytic renal cell carcinoma: intermediate-term oncologic efficacy and safety. *Korean J Urol* 2010 Aug;51(8):518-524.

59. Buy X, Lang H, Garnon J, Sauleau E, Roy C, Gangi A. Percutaneous renal cryoablation: prospective experience treating 120 consecutive tumors. *AJR Am J Roentgenol* 2013 Dec;201(6):1353-1361.
60. Atwell TD, Vlamincck JJ, Boorjian SA, Kurup AN, Callstrom MR, Weisbrod AJ, and colleagues Percutaneous cryoablation of stage T1b renal cell carcinoma: technique considerations, safety, and local tumor control. *J Vasc Interv Radiol* 2015 Jun;26(6):792-799.
61. Guazzoni G, Cestari A, Buffi N, Lughezzani G, Nava L, Cardone G, and colleagues Oncologic results of laparoscopic renal cryoablation for clinical T1a tumors: 8 years of experience in a single institution. *Urology* 2010 Sep;76(3):624-629.
62. Duffey B, Nguyen V, Lund E, Koopmeiners JS, Hulbert J, Anderson JK. Intermediate-term outcomes after renal cryoablation: results of a multi-institutional study. *J Endourol* 2012 Jan;26(1):15-20.
63. Johnson S, Pham KN, See W, Begun FP, Langenstroer P. Laparoscopic cryoablation for clinical stage T1 renal masses: long-term oncologic outcomes at the Medical College of Wisconsin. *Urology* 2014 Sep;84(3):613-618.
64. Larcher A, Fossati N, Mistretta F, Lughezzani G, Lista G, Dell'Oglio P, and colleagues Long-term oncologic outcomes of laparoscopic renal cryoablation as primary treatment for small renal masses. *Urol Oncol* 2015 Jan;33(1):22.e1-22.e9.
65. Guillotreau J, Haber GP, Autorino R, Miocinovic R, Hillyer S, Hernandez A, and colleagues Robotic partial nephrectomy versus laparoscopic cryoablation for the small renal mass. *Eur Urol* 2012 May;61(5):899-904.
66. Goldberg SN, Gazelle GS, Mueller PR. Thermal ablation therapy for focal malignancy: a unified approach to underlying principles, techniques, and diagnostic imaging guidance. *AJR Am J Roentgenol* 2000 Feb;174(2):323-331.
67. Castle SM, Salas N, Leveillee RJ. Initial experience using microwave ablation therapy for renal tumor treatment: 18-month follow-up. *Urology* 2011 Apr;77(4):792-797.
68. Li X, Liang P, Yu J, Yu XL, Liu FY, Cheng ZG, and colleagues Role of contrast-enhanced ultrasound in evaluating the efficiency of ultrasound guided percutaneous microwave ablation in patients with renal cell carcinoma. *Radiol Oncol* 2013 Oct 8;47(4):398-404.
69. Moreland AJ, Ziemlewicz TJ, Best SL, Hinshaw JL, Lubner MG, Alexander ML, and colleagues High-powered microwave ablation of t1a renal cell carcinoma: safety and initial clinical evaluation. *J Endourol* 2014 Sep;28(9):1046-1052.
70. Yu J, Zhang G, Liang P, Yu XL, Cheng ZG, Han ZY, and colleagues Midterm results of percutaneous microwave ablation under ultrasound guidance versus retroperitoneal laparoscopic radial nephrectomy for small renal cell carcinoma. *Abdom Imaging* 2015 Oct;40(8):3248-3256.
71. Wells SA, Wheeler KM, Mithqal A, Patel MS, Brace CL, Schenkman NS. Percutaneous microwave ablation of T1a and T1b renal cell carcinoma: short-term efficacy and complications with emphasis on tumor complexity and single session treatment. *Abdom Radiol (NY)* 2016 Jun;41(6):1203-1211.
72. Gao Y, Liang P, Yu X, Yu J, Cheng Z, Han Z, and colleagues Microwave treatment of renal cell carcinoma adjacent to renal sinus. *Eur J Radiol* 2016 Nov;85(11):2083-2089.
73. Dong X, Li X, Yu J, Yu MA, Yu X, Liang P. Complications of ultrasound-guided percutaneous microwave ablation of renal cell carcinoma. *Onco Targets Ther* 2016 Sep 26;9:5903-5909.

74. Chen CN, Liang P, Yu J, Yu XL, Cheng ZG, Han ZY, and colleagues Contrast-enhanced ultrasound-guided percutaneous microwave ablation of renal cell carcinoma that is inconspicuous on conventional ultrasound. *Int J Hyperthermia* 2016 Sep;32(6):607-613.
75. Muto G, Castelli E, Migliari R, D'Urso L, Coppola P, Collura D. Laparoscopic microwave ablation and enucleation of small renal masses: preliminary experience. *Eur Urol* 2011 Jul;60(1):173-176.
76. Guan W, Bai J, Liu J, Wang S, Zhuang Q, Ye Z, and colleagues Microwave ablation versus partial nephrectomy for small renal tumors: intermediate-term results. *J Surg Oncol* 2012 Sep 1;106(3):316-321.
77. Pham D, Thompson A, Kron T, Foroudi F, Kolsky MS, Devereux T, and colleagues Stereotactic ablative body radiation therapy for primary kidney cancer: a 3-dimensional conformal technique associated with low rates of early toxicity. *Int J Radiat Oncol Biol Phys* 2014 Dec 1;90(5):1061-1068.
78. Sun MR, Brook A, Powell MF, Kaliannan K, Wagner AA, Kaplan ID, and colleagues Effect of Stereotactic Body Radiotherapy on the Growth Kinetics and Enhancement Pattern of Primary Renal Tumors. *AJR Am J Roentgenol* 2016 Mar;206(3):544-553.
79. Chang JH, Cheung P, Erler D, Sonier M, Korol R, Chu W. Stereotactic Ablative Body Radiotherapy for Primary Renal Cell Carcinoma in Non-surgical Candidates: Initial Clinical Experience. *Clin Oncol (R Coll Radiol)*. 2016 Apr 27.
80. Yamamoto T, Kadoya N, Takeda K, Matsushita H, Umezawa R, Sato K, and colleagues Renal atrophy after stereotactic body radiotherapy for renal cell carcinoma. *Radiat Oncol* 2016 May 26;11(1):72-016-0651-5.
81. Staehler M, Bader M, Schlenker B, Casuscelli J, Karl A, Roosen A, and colleagues Single fraction radiosurgery for the treatment of renal tumors. *J Urol* 2015 2015/03;193(3):771-775.
82. Ponsky L, Lo SS, Zhang Y, Schluchter M, Liu Y, Patel R, and colleagues Phase I dose-escalation study of stereotactic body radiotherapy (SBRT) for poor surgical candidates with localized renal cell carcinoma. *Radiother Oncol* 2015 Sep 8.
83. CR Tracy, JD Raman, C Donnally, CK Trimmer, JA Cadeddu. Durable oncologic outcomes after radiofrequency ablation: experience from treating 243 small renal masses over 7.5 years. *Cancer* 2010;116:3135-3142.
84. M Pantelidou, B Challacombe, A McGrath, M Brown, S Ilyas, K Katsanos, and colleagues Percutaneous radiofrequency ablation versus robotic-assisted partial nephrectomy for the treatment of small renal cell carcinoma. *Cardiovasc Intervent Radiol* 2016;39:1595-1603.







# Superior target delineation for stereotactic body radiotherapy of bone metastases from renal cell carcinoma on MRI compared to CT

---

Fieke M. Prins  
Joanne M. van der Velden  
Anne S. Gerlich  
Alexis N.T.J. Kotte  
Wietse S.C. Eppinga  
Nicolien Kasperts  
Jorrit J. Verlaan  
Frank A. Pameijer  
Linda G.W. Kerkmeijer

## ABSTRACT

*Background.* In metastatic renal cell carcinoma (mRCC) there has been a treatment shift towards targeted therapy, which has resulted in improved overall survival. Therefore, there is a need for better local control of the tumor and its metastases. Image-guided stereotactic body radiotherapy (SBRT) in bone metastases provides improved symptom palliation and local control. With the use of SBRT there is a need for accurate target delineation. The hypothesis is that MRI allows for better visualization of the extend of bone metastases in mRCC and will optimize the accuracy of tumor delineation for stereotactic radiotherapy purposes, compared with CT only.

*Methods.* From 2013 to 2016, patients who underwent SBRT for RCC bone metastases were included. A planning CT and MRI were performed in radiotherapy treatment position. Gross tumor volumes (GTV) in both CT and MRI were delineated. Contouring was performed by a radiation oncologist specialized in bone metastases and verified by a radiologist, based on local consensus contouring guidelines. In both CT and MRI, the GTV volumes, conformity index (CI) and distance between the centers of mass (dCOM) were compared.

*Results.* Nine patients with 11 RCC bone metastases were included. The GTV volume as defined on MRI was in all cases larger or at least as large as the GTV volume on CT. The median GTV volume on MRI was 33.4 mL (range 0.2-247.6 mL), compared to 18.1 mL on CT (range 0.1 – 195.9) ( $p=0.013$ ).

*Conclusions.* Contouring of RCC bone metastases on MRI resulted in clinically relevant and statistically significant larger lesions (mean increase 41%) compared with CT. MRI seems to represent the extend of the GTV in RCC bone metastases more accurately. Contouring based on CT-only could result in an underestimation of the actual tumor volume, which may cause underdosage of the GTV in SBRT treatment plans.

## INTRODUCTION

Ninety percent of all tumors originating from the kidney are renal cell carcinomas (RCC) (1). The incidence of RCC is on the rise partially due to the increased use of diagnostic imaging(2). Of all patients with RCC, 20-35% will develop bone metastases during the course of their disease(3). In metastatic RCC (mRCC) there has been a treatment shift towards targeted therapy which has resulted in a 50% increase in overall survival (4). Due to the increasing overall survival in mRCC, there is a need for better local control of the tumor and its metastases. When used for curative intentions, conventional radiotherapy techniques have proven to be unable to manage kidney motion resulting in large radiation fields including large volumes of healthy kidney and surrounding abdominal organs(5). As a result, lower radiation doses compared to other tumor sites were applied and conventional radiotherapy was thought to lead to suboptimal tumor control rates. RCC was thus assumed to be radioresistant, however this misunderstanding was due to the low dose given in historic series (5).

In recent literature, RCC has been shown sensitive to high dose radiotherapy applied with stereotactic body radiotherapy (SBRT) techniques(6-8). SBRT assures a substantial higher biological effective dose to the tumor compared to conventional fractionation schemes. In RCC, a larger dose per fraction, in both curative and palliative setting(6), can lead to local control rates up to 90%(7). Recommendations have been made for fractionation schemes for optimal local control in primary tumors: 24 Gy in one fraction, 32 Gy in 2 fractions, 36 Gy in 3 fractions or 35 Gy in five fractions in the primary setting(6).

The radiosensitivity of RCC for treatment of localized RCC might be translated towards mRCC. Image-guided SBRT provides good symptom palliation and local control(7,9). Treatment with SBRT for RCC induced an increase in local control rates from 50% to up to 85%-100%(10-13). Currently the treatment planning of SBRT for mRCC is mainly CT-guided, including CT-based delineations(14-16). Furthermore in the delineation of spinal metastases, co-registration with MRI is recommended for the delineation of the spinal cord(16). However, SBRT is an emerging treatment option for non-spinal lesions, and in those treatment plans MRI is less frequently used(16). Recently, spine radiosurgery consortium consensus guidelines for target volume definition in spinal SBRT have been proposed. These recommendations included the use of MRI in target and organ at risk (OAR) delineation. The recommendations were assumed to be applicable to all types of spinal metastases, in which there was no special focus for bone metastases from RCC(17). However, we assume mRCC is a different subgroup within the bone metastases population, due to the different biological behavior of RCC tumor cells(6). In the non-metastatic setting of RCC there are recommendations to adjust the use of MRI in the diagnostic process, because the visibility of RCC is improved on

MRI(18). We hypothesize that MRI also plays an important role in the visibility of mRCC in the context of stereotactic treatment planning. In this paper we will emphasize the importance of the use of MRI in stereotactic treatment planning for RCC bone metastases.

## **MATERIALS AND METHODS**

From June 2013 to August 2016, all consecutive patients who underwent SBRT for RCC bone metastases were included. All patients are participating in a bone metastases cohort and signed informed consent for their clinical data to be used for research purposes (<https://clinicaltrials.gov/ct2/show/NCT02356497>). Within this cohort, patients are treated with standard radiotherapy of single fraction external beam radiotherapy of 8 Gy. The dose distribution usually consist of a single field in posteroanterior direction with the 100% isodoseline at 6 cm for a 6 MV photon beam and at 6 or 7 cm at a 10 MV photon beam.

### ***Image acquisition and patient positioning***

Prior to SBRT, patients CT and MRI images were acquired in radiotherapy position according to our clinical protocol. In plane resolution CT images were performed at 1 mm slice thickness on a large bore CT scanner (Philips Medical Systems, Best, The Netherlands). In addition, all patients underwent a 1.5T MRI scan (Achieva; Philips Medical System, Best, The Netherlands) with a 1.1 – 4 mm slice thickness. For every patient, T1-weighted images were acquired in transversal and sagittal direction, including a transversal multi echo DIXON scan, as well as T2-weighted images in transversal and sagittal direction, and diffusion weighted images (DWI). More details on MR sequences are listed in Table 1. During CT and MR imaging, patients were positioned in treatment position on a vacuum cushion (BlueBAG™, Elekta, Stockholm, Sweden), according to recommendation made by Dahele et al(16).

### ***Target volume delineation***

The transversal T1 TSE sequence was registered with the planning CT and all other MRI sequences were matched to this T1 sequence. Contouring was performed by a radiation oncologist specialized in bone metastases and verified by a radiologist on CT. Separately, the clinical contouring for MRI-based delineation was used, delineated by the responsible radiation oncologist, in adherence to local consensus contouring guidelines. Delineation was performed in an in house developed software system(19). The MR to CT registration was also executed in this software system according to clinical practice, using the mutual information registration algorithm within a rectangular box, containing the GTV.

**Table 1.** MR imaging parameters and MRI sequences

Name	tT1TSE	sT1TSE	tT2TSE	sT2TSE	DWI	tT1FFE
Sequence	Fast spin echo	Fast spin echo	Fast spin echo	Fast spin echo	Single shot spin-echo echo-planar imaging	3D spoiled gradient echo
Contrast	T1	T1	T2	T2	Diffusion	T1
Direction	Transverse	Sagittal	Transverse	Sagittal	Transverse	Transverse
Fat suppression	-	-	Multi echo Dixon	Multi echo Dixon	SPIR	Multi echo Dixon
TR/TE (ms)	623/16	658/8	2147/80	4105/80	4367/67	5.7/2.3
Echo train length	8	5	18	18	59	200
B-values (s/mm <sup>2</sup> )	-	-	-	-	0/200/800	-
Field of view (mm)	300 x 420	160x 352	300 x 201	350x 199	420 x 300	4530x 400
Acquisition matrix(mm <sup>2</sup> )	420 x 406	440 x 337	269 x 376	352 x 348	163 x 165	412 x 412
Slice thickness (mm)	4	4	4	4	4	1.1
Number of slices	25	25	25	50	25	273
Acceleration factor	2.9	1	1	1	2	3.4
Number of averages	2	2	4	2	3/5/7	2
Acquisition time (s)	127	181	360	378	179	304

tT1TSE: transverse T1 turbo spin echo, sT1TSE: sagittal T1 turbo spin echo, tT2TSE: transverse T2 turbo spin echo, sT2TSE: sagittal T2 turbo spin echo, DWI: diffusion weighted imaging, tT1FFE: transversal T1 fast field echo. TE : echo time, TR: repetition time.

In CT delineation, the focus was on delineation of tumor versus normal bone marrow and adjacent cortex. All scans were reviewed applying the same settings with window level at +300 hounsfield units (HU) and window width at 1000 HU. The standard setting of a window level at +40 HU and window width of 400 HU was also used. In MRI delineation, T1 images were used for target delineation aided by the information derived from the T2 and DWI sequences.

### Data analysis

A comparison was made of the gross tumor volume (GTV) as delineated on both CT and MRI, using the GTV volumes, the conformity index (CI) and distance between the centers of mass (dCOM). The CI is measured using the following formula: CI. A perfect agreement between the delineation on CT and MRI is indicated by a CI of 1. A CI of 0 means there is no overlap. The dCOM was defined as the distance between the centers of mass, which implies that the centers of the two delineations are the same if this value was 0.

Statistical differences in volumes between CT and MR were tested with Wilcoxon signed-rank test, with a significance level of  $\alpha=0.05$ . SPSS version 23.0 was used for the statistical analysis.

## RESULTS

### *Patient characteristics*

Nine patients with 11 bone metastases from RCC, treated with SBRT were included (Table 2), consisting of eight patients with a single lesion, and one patient with three lesions. The median age was 65 years (range 49-80 years). Most of the lesions were located in the thoracic or lumbar spine, and all lesions were osteolytic. All malignancies were pathologically proven RCC; eight lesions (72.7%) had a clearcell subtype, and three lesions (27.3%) a chromophobe subtype.

### *Tumor volume on CT and MRI*

The volumes of the lesions on MRI were larger in seven out of 11 cases compared to the CT, for the other four cases the volumes were comparable (Table 3). The mean size on MRI was 50.5 mL and the median 33.4 mL (range 0.2 – 247.6 mL), compared to a mean and median volume of 35.6 mL and 18.1 mL respectively on CT (range 0.1 – 195.9 mL). The difference in mean volume as delineated on CT and MRI was statistically significant ( $p=0.013$ ). The CI in the different lesions varied between 0.09 and 0.82. The dCOM varied between 0.7 and 13.2 mm. A visual example of the difference in delineation in a representative case is shown in Figure 1.

The seven lesions showing a larger volume on MRI do all have soft tissue involvement as well as bone marrow invasion. In all cases this was supported by the DWI sequence. In these lesions soft tissue involvement was not fully seen on the CT-scan. The median largest distance measured between the CT and MRI delineation was 26.7 (range 15.1 mm and 31.3 mm).

In the four lesions showing no difference in volume on MRI compared to CT, there was no bone marrow, nor soft tissue invasion. These findings were supported by the DWI image.

**Table 2.** Baseline characteristics

Characteristic	N
Patients	9
Lesions	11
Age (median, range)	65 (49-80)
Location (%)	
• Ilium	4 (36.4)
• Thoracic vertebrae	5 (45.5)
• Lumbar vertebrae	1 (9.1)
• Acetabulum	1 (9.1)
Histology (RCC) (%)	
• Clear cell	8 (72.7)
• Chromophobe	3 (27.3)

**Table 3.** Volumes, conformity index (CI), distance between the centers of mass (dCOM) in CT and MRI.

Lesions (n)	Location of mRCC	Volume in CT, mL	Volume in MRI, mL	Difference, mL	Increase, %	CI	dCOM, mm
1	Ilium left	47.9	50.1	2.1	4.4	0.82	1.8
2	Ilium left	39.8	72.1	32.3	81.2	0.47	10.4
3	Ilium right	195.9	247.6	51.7	26.4	0.68	5.8
4	Ilium right	46.1	75.5	25.9	56.2	0.52	5.7
5	Th 11	3.0	33.4	30.4	1013.3	0.09	13.2
6	Th 9	18.1	17.4	-0.6	-3.3	0.69	3.4
7	L2	30.1	42.2	12.1	40.2	0.39	10.2
8	Th 6	7.0	13.6	6.5	92.9	0.44	3.6
9	Th7	1.4	1.8	0.5	35.7	0.60	1.3
10	Th8	0.1	0.2	0.1	100	0.31	0.7
11	Acetabulum	1.7	1.6	-0.1	-5.9	0.68	1.9
Mean		35.6*	50.5*	14.6 (41%)	131.0	0.52	5.3
Median		18.1	33.40	6.5	40.2	0.52	3.6

\* p=0.013 (Wilcoxon signed-rank test). Th=thoracic vertebra, L=lumbar vertebra.

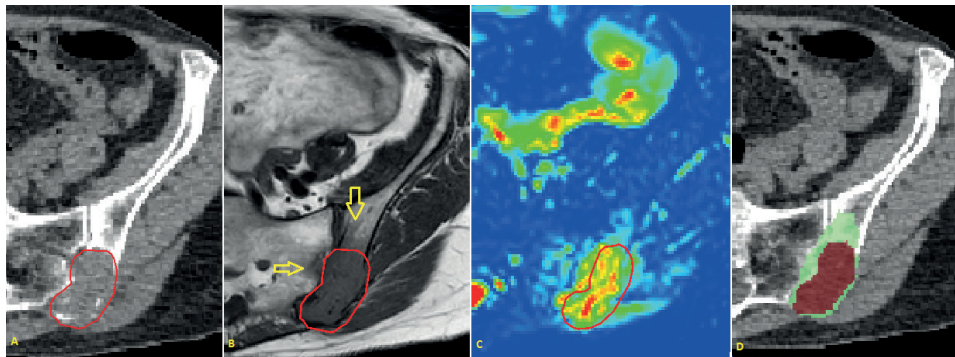


**Figure 1.** Visual example of a lytic iliac lesion showing the difference between CT and MRI. (A) Transversal reconstruction of computed tomography (CT) scan of the iliac bone showing a seemingly well-described lytic lesion; (B) T1 weighted MRI of the same lesion, the CT delineation is projected on this reconstruction showing a more extensive bone marrow infiltration medial and ventral of the lesion (yellow arrows); (C) diffusion weighted imaging of the same lesion, showing that the CT delineation is too narrow; (D) difference on MRI (green) and CT (red) GTV delineation.

## DISCUSSION

In this study, the use of CT and MRI for target volume delineation was prospectively compared in the stereotactic treatment of patients with bone metastases from RCC. The mean volume of the GTV on MRI was 41% larger (equaling almost 15 mL) compared to the mean volume of the GTV on CT, which was both clinically relevant and statistically significant. In seven out of 11 lesions the volumes of the lesions were larger on MRI comparing to the CT volume. This is probably due to superior visualization of soft tissue and bone marrow infiltration when using MR imaging compared with CT imaging(18). In four out of 11 lesions the volumes were comparable in size and, importantly, none of these lesions were smaller on MRI. Remarkably, three of those four lesions were chromophobe subtypes of RCC. However, it is more likely to conclude the lack of difference in those lesions is due to the absence of soft tissue or bone marrow infiltration, rather than a due to a different subtype of RCC.

The assumed radioresistance of RCC is questionable, as this was based on historic series prescribing radiation doses to primary RCC lesions which were too low to be effective(6). RCC may be more resistant than other tumors, but given high enough doses this may be overcome. However, results of this study suggest that part of the seemingly radioresistance of metastases from RCC might not be explained by inadequate dose regimen only, but also by suboptimal delineation due to CT-based contouring. It might be that part of the tumors received an underdosage if tumor delineation was based on CT information only. This would be the case especially in the peripheral parts of the bone lesions. In order to achieve optimal local control, an adequate dose on the entire GTV is relevant, which stresses the



importance of accurate tumor delineation and an adequate biological effective dose. In this study, we have shown that the use of MRI results in a mean increase of the GTV volume, which supports the hypothesis that parts of the GTV would not have been contoured in a CT-only approach.

Although it seems that visualization of mRCC lesions on MRI is superior to CT, in this study we did not perform a pathological validation of the size of the lesions. To the best of our knowledge, there is no pathological validation of MRI imaging of RCC bone metastases performed up to date. This leaves the possibility that for example edema instead of macroscopic tumor extension contributes to the difference in tumor volumes. Another limitation is the small sample size of the present study, which might influence the result. To our knowledge, a comparison in delineation between CT and MRI in mRCC has not been performed to date. Next step is to perform a study with a larger sample size to test our preliminary conclusions.

There is no specific literature available on the added value of the use of MRI in the planning of planning in mRCC bone metastases. In diagnostic and functional imaging of RCC, MRI is more frequently used. MRI is described as a feasible alternative to CT for imaging RCC(18). Recent evidence also shows that MRI might be better to differentiate between renal lesions, which remained inconclusive at first on CT imaging, leading to further utility of renal MRI(20). Diffusion-weighted and perfusion-weighted imaging is also more often used for the evaluation to diagnose renal masses(21). Metastases of RCC can occur anywhere in the body, but are most frequently found in lung, bone, brain and liver(14). Imaging of these metastases is mostly done by CT-imaging, although in the detection of small cerebral and bone lesions, MRI is more sensitive and therefore the image modality of preference for those localizations(22).

In a critical review, Sahgal et al. reported on SBRT in spinal metastases originating from different primary tumors, describing that the imaging technique for treatment planning varies between institutions using CT only, or a fusion technique with MRI(23). Nguyen et al. use MRI for delineation of the GTV, and discovered in certain occasions that extension of the size of the lesion in oligometastatic disease was revealed on MRI scan during work-up to SBRT treatment(15), so this also confirmed the adjusted value of MRI. Sikka et al. reported on the added value of MRI in pancreatic metastases from RCC. These are described as typically T1 hypointense and T2 hyperintense, and the authors suggest that DWI can be useful in the diagnosis of RCC metastases(24). Metastases of RCC show restricted diffusion on DWI and can increase the visibility, especially in small lesions. Furthermore, DWI may be useful when it is not possible to administer for example gadolinium contrast in certain patients. Our

results also show the usability of DWI in delineation. All lesions, in which invasions in bone marrow or soft tissue were shown, the DWI supports the suggestion that there is extension which is seen on the T1 MRI images.

In the primary setting, it may be safer to irradiate in a hypofractionated setting, as is used in most clinical studies to primary treatment of localized RCC(12,13) and which is also advised by DeMeerleer et al.(6). However, when more advanced image guided radiotherapy strategies show benefit of more precise targeting of the tumor, for example by MRI-guided linear accelerator radiotherapy with the MR-linac, it might be possible to increase the dose per fraction and treat patients with lesser fractions(25). Single fraction dose escalation up to 24 Gy in mRCC has been correlated with improved local control and progression free survival(14,26). In single fraction high dosages on spinal metastases the risk of vertebral compression fractures however increases(27). The cumulative incidence of compression fracture has been reported to be as high as 39% after single fraction spinal SBRT of 24 Gy. Considering the fact that the radioresistance of RCC is questionable, one could doubt whether it would be absolutely necessary to enhance this dosage to 24 Gy in a single fraction, instead of a slightly lower dose which is standard for bone metastases SBRT with different histology. For mRCC, single fraction SBRT is associated with better local control than multiple hypofractionated fractions(28), although the organ at risk constraints are leading in the decision to opt for a single or multiple fraction SBRT approach in individual cases.

An alternative approach, assuring a high dose within the GTV, would be to deliver SBRT using a simultaneous integrated boost (SIB-SBRT) strategy. In SIB-SBRT treatment plans, the GTV is boosted while the dose to the surrounding clinical tumor volume (CTV) possibly containing microscopic tumor extension, is reduced. By limiting the dose to the relatively healthy surrounding bone, the risk of vertebral compression fractures might be decreased. In order to be able to boost the GTV, it is necessary to be certain about the true extent of the GTV. It is therefore of critical importance to use accurate and precise imaging techniques for GTV delineation.

## CONCLUSION

Contouring of RCC bone metastases on MRI resulted in both clinically relevant and statistically significant larger volumes compared with contouring the same lesions with CT. It seems MRI represents the extent of the GTV in RCC bone metastases more accurately, possibly due to improved visualization of bone marrow infiltration and soft tissue expansion. Contouring based on CT-only could result in an underestimation of the actual tumor volume, which may cause an under dosage of the GTV in SBRT treatment plans, leading to lower local control rates.

## REFERENCES

1. Ljungberg B, Bensalah K, Bex A, et al. Guidelines on Renal Cell Carcinoma. European Association of Urology 2015.
2. Ferlay J, Steliarova-Foucher E, Lortet-Tieulent J, et al. Cancer incidence and mortality patterns in Europe: estimates for 40 countries in 2012. *Eur J Cancer* 2013 Apr;49(6):1374-1403.
3. Woodward E, Jagdev S, McParland L, et al. Skeletal complications and survival in renal cancer patients with bone metastases. *Bone* 2011 Jan;48(1):160-166.
4. Soerensen AV, Donskov F, Hermann GG, et al. Improved overall survival after implementation of targeted therapy for patients with metastatic renal cell carcinoma: results from the Danish Renal Cancer Group (DARENCA) study-2. *Eur J Cancer* 2014 Feb;50(3):553-562.
5. Ning S, Trisler K, Wessels BW, et al. Radiobiologic studies of radioimmunotherapy and external beam radiotherapy in vitro and in vivo in human renal cell carcinoma xenografts. *Cancer* 1997 Dec 15;80(12 Suppl):2519-2528.
6. De Meerleer G, Khoo V, Escudier B, et al. Radiotherapy for renal-cell carcinoma. *Lancet Oncol* 2014 Apr;15(4):e170-7.
7. Teh B, Bloch C, Galli-Guevara M, et al. The treatment of primary and metastatic renal cell carcinoma (RCC) with image-guided stereotactic body radiation therapy (SBRT). *Biomed Imaging Interv J* 2007 Jan;3(1):e6.
8. Svedman C, Karlsson K, Rutkowska E, et al. Stereotactic body radiotherapy of primary and metastatic renal lesions for patients with only one functioning kidney. *Acta Oncol* 2008;47(8):1578-1583.
9. Tree AC, Khoo VS, Eeles RA, et al. Stereotactic body radiotherapy for oligometastases. *Lancet Oncol* 2013 Jan;14(1):e28-37.
10. Staehler M, Bader M, Schlenker B, et al. Single fraction radiosurgery for the treatment of renal tumors. *J Urol* 2015 2015/03;193(3):771-775.
11. Ponsky L, Lo SS, Zhang Y, et al. Phase I dose-escalation study of stereotactic body radiotherapy (SBRT) for poor surgical candidates with localized renal cell carcinoma. *Radiother Oncol* 2015 Sep 8.
12. Sun MR, Brook A, Powell MF, et al. Effect of Stereotactic Body Radiotherapy on the Growth Kinetics and Enhancement Pattern of Primary Renal Tumors. *AJR Am J Roentgenol* 2016 Mar;206(3):544-553.
13. Chang JH, Cheung P, Erler D, et al. Stereotactic Ablative Body Radiotherapy for Primary Renal Cell Carcinoma in Non-surgical Candidates: Initial Clinical Experience. *Clin Oncol (R Coll Radiol)* 2016 Apr 27.
14. Zelefsky MJ, Greco C, Motzer R, et al. Tumor control outcomes after hypofractionated and single-dose stereotactic image-guided intensity-modulated radiotherapy for extracranial metastases from renal cell carcinoma. *Int J Radiat Oncol Biol Phys* 2012 Apr 1;82(5):1744-1748.
15. Nguyen QN, Shiu AS, Rhines LD, et al. Management of spinal metastases from renal cell carcinoma using stereotactic body radiotherapy. *Int J Radiat Oncol Biol Phys* 2010 Mar 15;76(4):1185-1192.
16. Dahele M, Zindler JD, Sanchez E, et al. Imaging for stereotactic spine radiotherapy: clinical considerations. *Int J Radiat Oncol Biol Phys* 2011 Oct 1;81(2):321-330.

17. Cox BW, Spratt DE, Lovelock M, et al. International Spine Radiosurgery Consortium consensus guidelines for target volume definition in spinal stereotactic radiosurgery. *Int J Radiat Oncol Biol Phys* 2012 Aug 1;83(5):e597-605.
18. Sankineni S, Brown A, Cieciera M, et al. Imaging of renal cell carcinoma. *Urol Oncol* 2016 Mar;34(3):147-155.
19. Bol GH, Kotte AN, van der Heide UA, et al. Simultaneous multi-modality ROI delineation in clinical practice. *Comput Methods Programs Biomed* 2009 Nov;96(2):133-140.
20. Willatt JM, Hussain HK, Chong S, et al. MR imaging in the characterization of small renal masses. *Abdom Imaging* 2014 Aug;39(4):761-769.
21. Capitanio U, Montorsi F. Renal cancer. *Lancet* 2016 Feb 27;387(10021):894-906.
22. Mueller-Lisse UG, Mueller-Lisse UL. Imaging of advanced renal cell carcinoma. *World J Urol* 2010 Jun;28(3):253-261.
23. Sahgal A, Larson DA, Chang EL. Stereotactic body radiosurgery for spinal metastases: a critical review. *Int J Radiat Oncol Biol Phys* 2008 Jul 1;71(3):652-665.
24. Sikka A, Adam SZ, Wood C, et al. Magnetic resonance imaging of pancreatic metastases from renal cell carcinoma. *Clin Imaging* 2015 Nov-Dec;39(6):945-953.
25. Raaymakers BW, Lagendijk JJ, Overweg J, et al. Integrating a 1.5 T MRI scanner with a 6 MV accelerator: proof of concept. *Phys Med Biol* 2009 Jun 21;54(12):N229-37.
26. Yamada Y, Bilsky MH, Lovelock DM, et al. High-dose, single-fraction image-guided intensity-modulated radiotherapy for metastatic spinal lesions. *Int J Radiat Oncol Biol Phys* 2008 Jun 1;71(2):484-490.
27. Sahgal A, Atenafu EG, Chao S, et al. Vertebral compression fracture after spine stereotactic body radiotherapy: a multi-institutional analysis with a focus on radiation dose and the spinal instability neoplastic score. *J Clin Oncol* 2013 Sep 20;31(27):3426-3431.
28. Ghia AJ, Chang EL, Bishop AJ, et al. Single-fraction versus multifraction spinal stereotactic radiosurgery for spinal metastases from renal cell carcinoma: secondary analysis of Phase I/II trials. *J Neurosurg Spine* 2016 May;24(5):829-836.





# Development and evaluation of a MRI based delineation guideline for renal cell carcinoma

---

Fieke M. Prins  
Linda G.W. Kerkmeijer  
Jochem R.N. van der Voort van Zyp  
Wietse S.C. Eppinga  
Hanne D. Heerkens  
Jan J. W. Lagendijk  
Rob H.N. Tijssen  
Evert-Jan P.A. Vonken  
Alexis N.T.J. Kotte  
Maurits M. Barendrecht  
William Chu  
Martijn P.W. Intven

*Submitted*

## ABSTRACT

*Purpose.* For renal cell carcinoma (RCC), surgery is standard of care. However, there is a need for non-invasive treatment alternatives like stereotactic body radiotherapy (SBRT). Nowadays, SBRT for RCC is mainly CT based with tumor delineation using CT and Cone-Beam CT (CBCT) guided dose delivery. SBRT for RCC could be optimized with the introduction of MR guided radiotherapy systems, like the MRI-Linac (MRL), in which real time MR imaging during dose delivery is possible. As a consequence of the introduction of MRI in the radiotherapy treatment of RCC, there is a need for guidelines on the delineation of RCC on MRI. In this study an RCC delineation guideline using MRI was developed and evaluated.

*Methods and materials.* Consecutive RCC patients underwent a contrast enhanced MRI scan. Five physicians received a MRI dataset (T2, pre- and post-contrast T1, DWI, and ADC), on which they contoured the tumor. On four datasets the tumor was delineated without instructions (development phase). With help of an expert radiologist new delineation guidelines were made based on these initial delineations. Next, another 10 new cases were delineated following these guidelines and subsequently evaluated (evaluation phase). The volumes, conformity index (CI) and distance between centers of the mass (dCOM) were calculated.

*Results.* Four RCC cases were delineated in the development phase and 10 RCC cases in the evaluation phase by 5 observers. The agreement between observers in the evaluation phase resulted in a mean CI of 0.77, ranging from 0.59-0.88. The mean dCOM was 0.55 mm.

*Conclusions.* A delineation guideline for RCC on MRI has been created, based on T2 weighted MR imaging with use of contrast enhanced T1 weighted imaging and DWI. Inter-observer delineation variations were limited. The recommendations for contouring and sequences used can be helpful in the introduction of MRI guided radiotherapy in the clinic.



## INTRODUCTION

The standard of care treatment for renal cell carcinoma (RCC) is surgery(1). However, due to the increasing incidence of RCC in mostly elderly patients there is also the need for less invasive treatments. Minimal invasive alternatives for surgery are radiofrequency ablation(RFA), cryoablation(CA) and microwave ablation(MWA). Radiotherapy is the only non-invasive curative treatment approach of RCC, provided that fiducial markers are not necessary to guide treatment(2).

From a historical point of view, RCC was thought to be radioresistant. Recent phase I/II studies seem to contradict this belief by showing local control rates of 80-90% with acceptable toxicity after a 3 year follow-up (3-6). Using modern radiotherapy techniques such as stereotactic body radiotherapy (SBRT), a curative dose can be delivered to the tumor without exceeding tolerance doses to critical structures as the small bowel or healthy kidney tissue. To make this possible, accurate target definition and precise dose delivery techniques are required (3).

Up to now, SBRT for RCC is mainly CT based with delineation of the tumor on CT and dose delivery based on Cone-Beam CT (CBCT)(7). With magnetic resonance imaging (MRI), SBRT for RCC could be optimized. Because of the better soft tissue contrast of MRI compared to CT, target definition potentially could be more accurate. Besides, with the clinical introduction of MR guided radiotherapy systems like the MRI-linac (MRL), real time MR imaging during dose delivery allows small or even no additional margin around the tumor for target position uncertainty during treatment(8,9). Both potential advantages of incorporation of MRI in the radiotherapy treatment of RCC lead to smaller irradiation fields allowing a higher dose to the tumor and lower doses to surrounding organs.

Because of the introduction of MRI in the radiotherapy treatment of RCC there is a need for standardization of tumor definition on MRI. In this study we aim to develop and evaluate a MRI based RCC delineation guideline.

## MATERIAL AND METHODS

### *Patient selection*

In 2016, 30 consecutive RCC patients were enrolled in the MRI-RCC study. The purpose of this study was to optimize scanning sequences for MRI-only radiotherapy in RCC on a 1.5T MRI scanner prior to treatment. The first 16 patients have been used for sequence optimization and the following 14 for development and evaluation of a MRI based RCC delineation guideline, with consistent sequences. The study was approved by the institutional review board and all patients signed informed consent for participation.

### ***Patient positioning and MR imaging***

Scanning was performed on a 1.5T Philips Ingenia scanner (Philips, Best, The Netherlands). Patients were scanned in head first supine position on a flat table top. Images were acquired using a 16-channel anterior and 12-channel posterior coil.

The imaging protocol consisted of the following sequences: a T2 weighted Turbo Spin Echo (T2-TSE), a pre- and post-contrast T1 weighted Turbo Field Echo (T1-TFE), and a Diffusion Weighted Image (DWI) with a Spin-Echo Echo-Planar Imaging (SE-EPI) readout. Contrast was administered via intravenous injection of Gadolinium (0.1 mL/kg), all patients were able to have contrast. The DWI data were processed on the scanner to produce an ADC map from the  $b = 0$  and  $b = 1000$  s/mm<sup>2</sup> images. For all acquisitions respiratory triggering was used to mitigate motion effects. The acquisition parameters are summarized in Table 1.

### ***Target volume delineation***

All MR images were transferred to an in house developed target volume delineation tool(10). Three experienced abdominal/urological radiation oncologists, one radiation oncologist in training and one researcher with over two years of experience in delineating renal cell tumors participated in this study. All observers received their own MRI dataset (T2, pre- and post-contrast T1, DWI and ADC). The gross tumor volume (GTV) was contoured on the T2 MRI; observers could additionally use the T1 and DWI sequences and the ADC map, which had been registered to the T2 MRI.

### ***Guideline development***

Without any instructions, four cases from the dataset were delineated independently by all five observers. The observers were only provided with clinical information like imaging reports and pathological findings. Afterwards a consensus meeting was held between the observers and an expert radiologist to develop GTV delineation instructions. With use of these GTV-delineation guidelines, all five observers independently delineated the GTV in 10 new cases of RCC.

### ***Data analyses***

The volumes, conformity index (CI) and distance between centers of the mass (dCOM) of the different delineations were calculated. To determine the inter-observer variation between the delineations, a generalized conformity index for overlap between observers was calculated according to the following formula: (11). A CI of 1 indicates a perfect agreement between observers, >0.8 very good, 0.7–0.8 good, 0.7–0.6 moderate, <0.6 low, and a CI of 0 mean there is no overlap in the delineations(12). The dCOM is expressed as the length of the 3 dimensional vector and is presented in mm. For dCOM a value of 0 means that the delineations are centered at the same position.

The GTV contours of all observers were used to create countmaps. In these countmaps the voxel value is the maximum number of observers and the corresponding image voxel as part of the GTV. The spread in volume over the percentile surfaces gives an indication of the GTV similarity over the observers. Visual countmaps that show the overlap, or differences in overlap between the five observers were created.

**Table 1.** Details on optimized MRI sequences used for delineation of RCC

Name	T2-TSE	T1-TFE	DWI
Sequence readout	Multi-slice TSE	3D TFE	Single-shot SE-EPI
Orientation	Transverse	Transverse	Transverse
Fat suppression	-	SPAIR	SPIR
TR/TE (ms)	1270/120	4.3/2.0	2167/83
b-values (s/mm <sup>2</sup> )	-	-	0, 1000
Field of view (mm)	350 x 350 x 210	375 x 375 x 176	450 x 350 x 212
Voxel size (mm)	1.4 x 1.4	2.0 x 2.0 x 2.0	2.5 x 3.1
Slice thickness (mm)	3.5	-	4
Flip angle (°)	90	10	90
Refocussing angle (°)	120	-	180
Acquisition matrix(mm)	252 x 249	192 x 190 x 88	180 x 110
Number of slices	60	-	53
SENSE acceleration factor	2.5	3	2
Number of averages (NSA)	2	1	$B_0 = 1, b_{1000} = 4$
Acquisition time (mm:ss)	2:00	00:22	2:15

T2-TSE: T2 turbo spin echo, T1-TFE: T1 turbo field echo, DWI: diffusion weighted imaging. TE : echo time, TR: repetition time.

## RESULTS

### *Patient characteristics*

Fourteen consecutive patients with primary RCC were included in the study. For four cases GTV's were delineated in the guideline development phase. Ten cases were delineated in the evaluation phase. The patient and tumor characteristics are described in table 2.

**Table 2.** Patient and tumor characteristics in development and evaluation phase

<b>Baseline characteristics</b>	<b>Development</b>	<b>Evaluation</b>
Patients (n)	4	10
Gender (%)		
- Male	3	5
- Female	1	5
Age (mean, range)	65,5 (56-74)	56,5 (43-68)
Side (%)		
- Left	2	8
- Right	2	2
Position		
- Upper pole	1	6
- Interpolar	0	2
- Lower pole	3	2
Histology		
- Clear cell	1	6
- Papillary	2	2
- Unknown	1	2
Tumor diameter in mm (median, range)	23 (19-42)	35 (9-90)

**Table 3.** volumes, conformity index (CI), distance between the centers of mass (dCOM) in 5 observers in development phase.

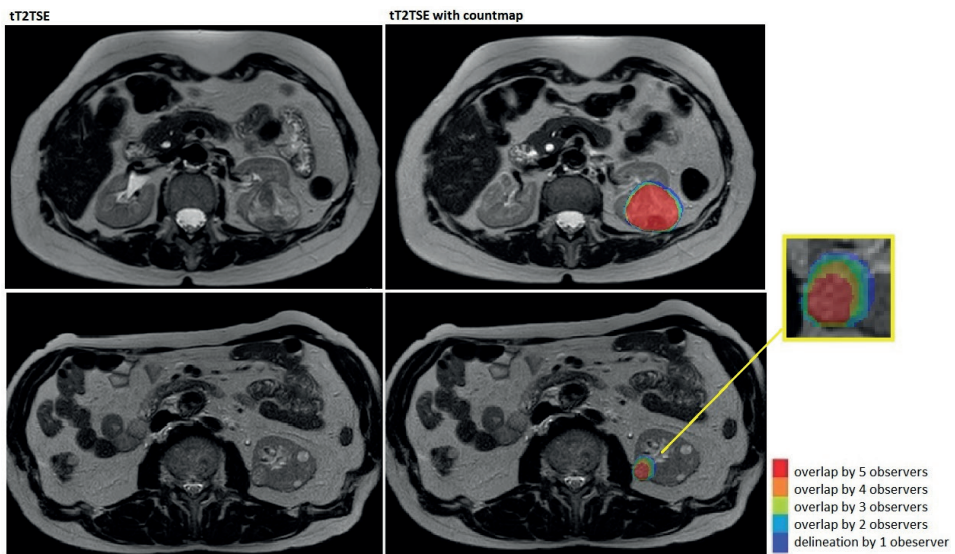
<b>Delineation</b>	<b>Observer 1 Volume (mL)</b>	<b>Observer 2 Volume (mL)</b>	<b>Observer 3 Volume (mL)</b>	<b>Observer 4 Volume (mL)</b>	<b>Observer 5 Volume (mL)</b>	<b>CI</b>	<b>dCOM (mm)</b>
1	4.5	6.1	9.1	4.1	4.0	0.59	1.59
2	11.4	11.5	15.2	10.5	8.3	0.63	2.89
3	46.2	45.3	57.0	44.5	46.6	0.83	1.20
4	3.9	3.3	6.4	3.0	2.6	0.48	3.13
Mean	16.5	16.6	21.9	15.5	15.4	0.63 (SD 0.15)	2.20 (SD 0.95)

### ***Volume, agreement and location of contours in evaluation phase***

Table 4 shows the volumes of the delineations per observer in the evaluation phase. The agreement between observers was good with a mean CI of 0.77. The CI varied between 0.59 and 0.88 for the 10 different cases. The mean dCOM was 0.55 mm. In Figure 2 an example of GTV delineations is presented in a count map. The delineation with the highest CI (delineation 4) and the lowest CI (delineation 7) are shown.

### ***Volume, agreement and location of contours in development phase***

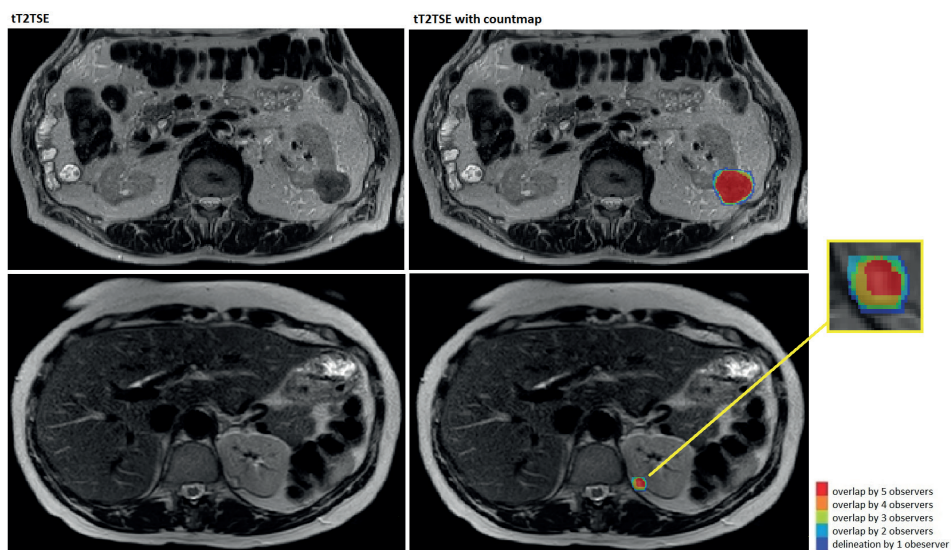
Table 3 shows the volumes of the delineations per observer in the development phase. The agreement between observers showed a CI of 0.59, 0.63, 0.83 and 0.48, with a mean CI of 0.63. The mean dCOM was 2.20 mm. In Figure 1 an example of GTV delineations is presented in a count map. The delineation with the highest CI (delineation 3) and the lowest CI (delineation 4) are shown.



**Figure 1.** Countmap (development phase) of case 3 (CI 0.83) and case 4 (CI 0.48), plain tT2TSE and tT2TSE with GTV countmap.

**Table 4.** volumes, conformity index (CI), distance between the centers of mass (dCOM) in 5 observers in evaluation phase.

Delineation	Observer 1 Volume (mL)	Observer 2 Volume (mL)	Observer 3 Volume (mL)	Observer 4 Volume (mL)	Observer 5 Volume (mL)	CI	dCOM (mm)
1	76.8	74.0	83.1	78.3	81.6	0.87	0.13
2	466.5	536.6	404.0	360.5	406.8	0.75	1.59
3	45.1	47.0	45.6	46.4	42.3	0.82	0.70
4	25.7	26.9	27.7	25.4	27.1	0.88	0.32
5	11.6	11.5	12.9	10.1	15.2	0.72	0.25
6	45.0	38.0	44.6	42.6	38.6	0.83	0.23
7	1.1	0.6	1.4	0.8	0.9	0.59	0.59
8	104.3	98.2	109.4	141.8	146.9	0.73	1.21
9	6.4	6.0	7.7	5.6	5.7	0.77	0.20
10	30.4	26.3	33.1	28.2	32.8	0.78	0.28
Mean	81.3	86.5	77.0	74.0	79.8	0.77 (SD 0.09)	0.55 (SD 0.49)

**Figure 2.** Countmap (evaluation phase) of case 4 (CI 0.88) and case 7 (CI 0.59), plain tT2TSE and tT2TSE with GTV countmap.

***Delineation guideline and evaluation***

Target definition of RCC on MRI is most accurate on T2 weighted sequences due to the clear differences in contrast between tumor and healthy kidney on the T2 sequence. Delineation of the GTV is therefore advised to be done on a T2-weighted image. In addition to the T2 weighted images, T1 weighted images with contrast can be used to differentiate tumor tissue from blood vessels. The b=1000 diffusion weighted image can be helpful to differentiate between tumorous tissue with high cellularity and healthy tissue with low cellularity in case of uncertainties on the T2 weighted image. As the ADC map contributes no extra information as compared to the b=1000 DWI, there is no additional value in using this for delineation purposes.

**DISCUSSION**

In this study we have developed and evaluated a MRI based RCC delineation guideline. After the development phase (and the consensus meeting with an expert radiologist) the mean CI improved from 0.63 to 0.77, and the mean dCOM improved from 2.20 mm to 0.55 mm. Based on T2 weighted imaging, with use of contrast enhanced T1 weighted and b=1000 diffusion weighted sequences, we have created recommendations for delineation of RCC on MRI.

To our knowledge, this is the first study to provide recommendations on GTV delineation for MRI-only treatment of RCC. Different delineation studies on MRI have been executed for other abdominal sites (13-15). Noel et al. used healthy subjects and delineated abdominal organs at risk on T2 weighted images instead of tumor. They reported the lowest precision of MRI in pancreas and duodenum and the highest in spleen and kidney(14). Heerkens et al. developed and evaluated a guideline for delineation of pancreatic tumors on MRI(13). They developed a contrast enhanced T1 weighted MRI based delineation guideline. This is in discordance with our T2 weighted MRI based guideline. This can be explained by the different anatomical location of the pancreas, in which a contrast enhanced T1 sequence is of higher importance than a T2 weighted sequence due to the highest contrast in T1 between tumor and healthy pancreas tissue. The use of T2 weighted MRI based delineation guidelines for RCC is also supported by a review by experts in diagnostic RCC imaging by Sankineni et al. (16). Although the DWI acquisitions in this study are effective to highlight the extent of the tumor, they should not be used to directly delineate on. DWI acquisitions typically employ single-shot EPI readouts, which are prone to geometrical distortions. This renders them not suitable for a direct match to the T2 images used for delineation. Although novel, distortion free, DWI sequences like DWI-SPLICE are on the horizon(17), these types of sequence are not yet standard available, and were therefore not included in this study.

In order to determine inter-observer variation in contouring, a large variety of contouring metrics exist. In this study, CI and dCOM were used(18). We showed an improvement of the CI and the dCOM after a consensus meeting with an expert radiologist. In the evaluation phase we demonstrated inter-observer agreement and contouring precision comparable to the studies by Noel and Heerkens. In the evaluation phase, one delineation showed a CI of 0.58, this difference could be explained due to the small size of the tumor. This is also visible in the development phase, in which the smallest lesion also showed the smallest CI. This effect of tumor size on the overlap index was previously described by Zou et al.(19). Following the guideline created in this study a mean CI of 0.77 was achieved, which we consider to be acceptable for use in clinic(12), although the clinical impact of variation in contouring is unknown(18).

The results of this study cannot be used in constructing a planning target volume (PTV) margin for radiotherapy in RCC. The PTV is a margin around the GTV compensating for several uncertainties in planning, patient positioning, tumor position and irradiation beam delivery(24,25). The PTV margin needed is calculated based on the expected size of the different uncertainties. Delineation uncertainties (as part of the PTV) cannot be taken into account, due to the larger amount of observers necessary to achieve this specific goal, which was outside the scope of this paper. To set a definitive PTV margin recommendation it is necessary in future research to look further into detail to one of the major components of the PTV margin like uncertainties due to tumor motion.

There were a few limitations in the conduction of the present study. The first is the relatively small number of patients. However, the number of observers was adequate, we do not expect our conclusions to be different when more cases would be used. Another limitation of this study is that no pathological validation was made on tumor size. In nine out of ten tumors RCC was pathological proven, but the actual tumor size was not correlated to the delineations on MRI. In other abdominal tumor sites, like pancreas, these comparisons with MRI and pathological specimen have been made, and show an underestimation of tumor size on MRI(20), but for kidney tumors this still needs to be sorted out.

A final limitation is that no comparison was made with delineation accuracy on CT imaging. With the clinical introduction of MRI guided radiotherapy the CT scan is expected to be omitted to plan and guide radiotherapy treatment (21-23).

In conclusion, we developed and evaluated a delineation guideline for RCC on MRI. Based on T2 weighted MR imaging with help of contrast enhanced T1 weighted imaging and DWI inter-observer delineation variations were limited. These recommendations can be used with the introduction of MRI guided radiotherapy in the clinic.



## REFERENCES

1. Ljungberg B, Bensalah K, Bex A, Canfield S, Dabestani S, Giles RH, et al. Guidelines on Renal Cell Carcinoma. European Association of Urology 2015.
2. Siva S, Pham D, Kron T, Bressel M, Lam J, Tan TH, et al. Stereotactic ablative body radiotherapy for inoperable primary kidney cancer: a prospective clinical trial. *BJU Int* 2017 Feb 10.
3. De Meerleer G, Khoo V, Escudier B, Joniau S, Bossi A, Ost P, et al. Radiotherapy for renal-cell carcinoma. *Lancet Oncol* 2014 Apr;15(4):e170-7.
4. Chang JH, Cheung P, Erler D, Sonier M, Korol R, Chu W. Stereotactic Ablative Body Radiotherapy for Primary Renal Cell Carcinoma in Non-surgical Candidates: Initial Clinical Experience. *Clin Oncol (R Coll Radiol)* 2016 Apr 27.
5. Staehler M, Bader M, Schlenker B, Casuscelli J, Karl A, Roosen A, et al. Single fraction radiosurgery for the treatment of renal tumors. *J Urol* 2015 2015/03;193(3):771-775.
6. Siva S, Kothari G, Muacevic A, Louie AV, Slotman BJ, Teh BS, et al. Radiotherapy for renal cell carcinoma: renaissance of an overlooked approach. *Nat Rev Urol* 2017 Sep;14(9):549-563.
7. Siva S, Pham D, Kron T, Bressel M, Lam J, Tan TH, et al. Stereotactic ablative body radiotherapy for inoperable primary kidney cancer: a prospective clinical trial. *BJU Int* 2017 Feb 10.
8. Crijns SP, Raaymakers BW, Lagendijk JJ. Proof of concept of MRI-guided tracked radiation delivery: tracking one-dimensional motion. *Phys Med Biol* 2012 Dec 7;57(23):7863-7872.
9. Lagendijk JJ, Raaymakers BW, Raaijmakers AJ, Overweg J, Brown KJ, Kerkhof EM, et al. MRI/linac integration. *Radiother Oncol* 2008 Jan;86(1):25-29.
10. Bol GH, Kotte AN, van der Heide UA, et al. Simultaneous multi-modality ROI delineation in clinical practice. *Comput Methods Programs Biomed* 2009 Nov;96(2):133-140.
11. Kouwenhoven E, Giezen M, Struikmans H. Measuring the similarity of target volume delineations independent of the number of observers. *Phys Med Biol* 2009 May 7;54(9):2863-2873.
12. Rucker G, Schimek-Jasch T, Nestle U. Measuring inter-observer agreement in contour delineation of medical imaging in a dummy run using Fleiss' kappa. *Methods Inf Med* 2012;51(6):489-494.
13. Heerkens HD, Hall WA, Li XA, Knechtges P, Dalah E, Paulson ES, et al. Recommendations for MRI-based contouring of gross tumor volume and organs at risk for radiation therapy of pancreatic cancer. *Pract Radiat Oncol* 2017 Mar - Apr;7(2):126-136.
14. Noel CE, Zhu F, Lee AY, Yanke H, Parikh PJ. Segmentation precision of abdominal anatomy for MRI-based radiotherapy. *Med Dosim* 2014 Autumn;39(3):212-217.
15. Vinod SK, Jameson MG, Min M, Holloway LC. Uncertainties in volume delineation in radiation oncology: A systematic review and recommendations for future studies. *Radiother Oncol* 2016 Nov;121(2):169-179.
16. Sankineni S, Brown A, Cieciera M, Choyke PL, Turkbey B. Imaging of renal cell carcinoma. *Urol Oncol* 2016 Mar;34(3):147-155.
17. Schakel T, Hoogduin JM, Terhaard CH, Philippens ME. Diffusion weighted MRI in head-and-neck cancer: geometrical accuracy. *Radiother Oncol* 2013 Dec;109(3):394-397.
18. Jameson MG, Holloway LC, Vial PJ, Vinod SK, Metcalfe PE. A review of methods of analysis in contouring studies for radiation oncology. *J Med Imaging Radiat Oncol* 2010 Oct;54(5):401-410.

19. Zou KH, Warfield SK, Bharatha A, Tempany CM, Kaus MR, Haker SJ, et al. Statistical validation of image segmentation quality based on a spatial overlap index. *Acad Radiol* 2004 Feb;11(2):178-189.
20. Hall WA, Mikell JL, Mittal P, Colbert L, Prabhu RS, Kooby DA, et al. Tumor size on abdominal MRI versus pathologic specimen in resected pancreatic adenocarcinoma: implications for radiation treatment planning. *Int J Radiat Oncol Biol Phys* 2013 May 1;86(1):102-107.
21. Raaymakers BW, Lagendijk JJ, Overweg J, Kok JG, Raaijmakers AJ, Kerkhof EM, et al. Integrating a 1.5 T MRI scanner with a 6 MV accelerator: proof of concept. *Phys Med Biol* 2009 Jun 21;54(12):N229-37.
22. Keall PJ, Barton M, Crozier S, Australian MRI-Linac Program, including contributors from Ingham Institute, Illawarra Cancer Care Centre, Liverpool Hospital, Stanford University, Universities of Newcastle, Queensland, Sydney, Western Sydney, and Wollongong. The Australian magnetic resonance imaging-linac program. *Semin Radiat Oncol* 2014 Jul;24(3):203-206.
23. Mutic S, Dempsey JF. The ViewRay system: magnetic resonance-guided and controlled radiotherapy. *Semin Radiat Oncol* 2014 Jul;24(3):196-199.
24. Burnet NG, Thomas SJ, Burton KE, Jefferies SJ. Defining the tumour and target volumes for radiotherapy. *Cancer Imaging* 2004 Oct 21;4(2):153-161.
25. van Herk M. Errors and margins in radiotherapy. *Semin Radiat Oncol* 2004 Jan;14(1):52-64.





# Intrafraction motion management of renal cell carcinoma with MRI guided stereotactic body radiotherapy

---

Fieke M. Prins  
Bjorn Stemkens  
Linda G.W. Kerkmeijer  
Maurits M. Barendrecht  
Hans J.C.J. de Boer  
Evert-Jan P.A. Vonken  
Jan J.W. Lagendijk  
Rob H.N. Tijssen

*Submitted*

## ABSTRACT

*Introduction.* One of the major challenges in stereotactic body radiotherapy (SBRT) of renal cell carcinoma (RCC) is internal motion during treatment. Previous literature has aimed on mitigating the effects of motion by expansion of treatment margins or respiratory tracking, using fluoroscopy of implanted fiducials. The arrival of online MR-guided radiotherapy has the potential to further improve the treatment of RCC as it will enable direct visualization of the tumor during treatment. The flexibility of online MR imaging allows for both tumor tracking as well as tumor trailing. However, the optimal strategy in RCC patients is unknown. In this paper we assess the efficacy of two motion management techniques: *tumor trailing* and *respiratory tracking*. Dedicated MRI scan sessions, which simulated single-fraction MRI-based SBRT treatments, were performed on patients suspected of RCC to quantify the different sources of intrafraction motion and assess the efficacy of the different motion management strategies.

*Methods.* Fifteen patients were included in this motion study. At the beginning and end of the scanning protocol two cine-MRI scans were acquired to assess cyclic respiratory motion. In addition to the cine scans, 3D spoiled gradient echo (SPGR) scans were acquired at four different time points to assess the slow drifts over a period of 25 minutes. The systematic and random errors due to intrafraction drift ( $\Sigma_{\text{DRIFT}}$  and  $\sigma_{\text{DRIFT}}$ , respectively) were calculated as well as the random error induced by respiratory motion ( $\sigma_{\text{RESP}}$ ). Motion margins were calculated for tumor trailing and respiratory tracking and compared to the margin when no motion compensation would be performed to assess the relative efficacy of each technique.

*Results.* The largest respiratory tumor motion was observed along the caudo-cranial (CC) direction with a median 95% maximum amplitude of approximately 12 mm.  $\Sigma_{\text{DRIFT}}$ ,  $\sigma_{\text{DRIFT}}$  and  $\sigma_{\text{RESP}}$  were determined to be 1.0 mm, 1.8 mm and 3.8 mm. Without mechanical immobilization intrafraction drift accounted for 75% of the total intrafraction motion margin for online mid-position based SBRT treatments.

*Conclusion.* Due to the systematic nature of intrafraction drift the contribution to the total internal motion margin is much larger than periodic respiratory motion in the patient group investigated. This makes tumor trailing a viable option to consider on the MR-linac as it would allow 3D MRI acquisitions during beam delivery, which simplifies the introduction of new techniques like dose accumulation and online intrafraction replanning.

## INTRODUCTION

Although surgery has been considered the gold standard for the treatment of primary renal cell carcinoma (RCC)(1), the demand for non-invasive treatment options of RCC has increased(2). The feasibility of stereotactic body radiotherapy (SBRT) for primary RCC has been investigated in several clinical trials(3,4). Recently, a consensus statement by the international radiosurgery oncology consortium for RCC has been published that covers aspects of patient selection and follow-up(5). However, detailed guidelines on motion management strategies are still lacking. Previously reported strategies included expansion of the treatment margins, mechanical immobilization and robotic tracking with fiducials, but MR-guidance has not yet been explored. Online MR-guided radiotherapy has the potential to further improve the quality of RCC SBRT as it will enable direct visualization of the tumor during treatment.

Once an online plan based on the daily anatomy is generated, the internal motion of the tumor can be monitored by continuous MR acquisition during beam delivery. The flexibility of online MR imaging allows for both tumor tracking as well as tumor trailing. In tumor trailing the beam delivery only tracks the slow systematic trends, whereas the “fast” cyclic motion is accounted for by motion-robust treatment planning(6). The choice of motion management strategy is directly linked to the type of imaging that is performed during the treatment. Whereas respiratory tracking requires the acquisition of a fast 2D imaging slice covering the tumor, the reduced demands in terms of temporal resolution can be used to extent the spatial coverage allowing one to not only visualize the tumor, but also nearby organs at risk. It is therefore important to determine whether tumor trailing is feasible for SBRT of RCC on the MR-linac.

In the past, various studies have investigated kidney motion, but the quantification of the intrafraction motion has primarily focused on periodic respiratory motion. Intrafraction drift has largely been neglected(7-9). Stemkens et al. demonstrated when simulating the dose deposition during free breathing, slow intrafraction drift can result in local dose differences of up to 40% in some patients(10), but included only five patients. Sonier et al.(11) included an assessment on the intrafraction drift over all fractions in 15 patients based on pre-, and post-treatment cone-beam CT (CBCT), but their findings are specific for a setup with belly press and vacuum cushion immobilization and are not applicable to a free-breathing setup that is envisioned for a MRI-linac.

In this paper a MRI-guided single-fraction SBRT treatment was simulated in 15 patients. Over a period of 25 minutes several dedicated motion assessment scans were acquired, which allowed decoupling of the systematic trends due to intrafraction drifts and periodic respiratory motion. The relative contribution to the total motion margin of both components of motion were determined to assess the maximum achievable margin reduction when using either tumor trailing or respiratory tracking.

## METHODS

### *Patient inclusion*

The patients signed informed consent and were included in the MRI-RCC study, which was approved by our local institutional review board. All patients with a solid tumor suspected of RCC or a cystic tumor with a Bosniak classification of III or IV were selected for this study. Patients underwent a single free-breathing MRI exam, positioned on a flat table top, with arms down, without the use of any immobilization devices (only a knee-cushion was used). The MRI scan was performed prior to their treatment, i.e. surgery, radiofrequency ablation (RFA) or active surveillance (AS). Patient characteristics are shown in Table 1.

**Table 1.** Patient characteristics

<b>Characteristic</b>	<b>N</b>
Patients	15
Age (median, range)	60 (38-83)
Gender male/female (%)	60/40
Diameter of tumor in mm (median, range)	36 (19-90)
Treatment	
- Surgery	11
- RFA	1
- AS	3
Pathology	
- RCC	9
- Benign	3
- Unknown	3
Metastases	0

### *Image acquisition protocol*

MRI scanning was performed on a 1.5T MRI-RT scanner (Ingenia, Philips, Best, the Netherlands), using a 16-channel anterior and 12-channel posterior coil array. An end-expiration respiratory gated T2-weighted Turbo Spin Echo (T2-TSE) scan was performed at the start, which served as a reference scan at T=0. 2D coronal and sagittal balanced steady-state free precession (bSSFP) cine-MRI time series were acquired sequentially at the beginning ( $t_{acq} = 150$  sec) and end of the MRI exam ( $t_{acq} = 50$  sec) to assess respiratory-induced periodic motion. The sagittal and coronal imaging planes were positioned through the center of the tumor. The coronal slice was angulated along the principal axis of kidney motion, following the anatomic contour. The imaging parameters are listed in Table 2. In addition to the 2D



time series acquisition, end-expiration respiratory gated transversal 3D spoiled gradient echo (SPGR) scans were acquired at four different time points ( $t=200$ ,  $t=500$ ,  $t=700$  and  $t=1400$  seconds) in order to assess intrafraction drifts within the time estimated for a single-fraction MRI-guided treatment. The estimated time was approximately 25 minutes, based on an IMRT approach with a dosage of 5x7 Gy. The timing of the various scans within the protocol is shown graphically in Figure 1.

**Table 2.** MR imaging parameters and MRI sequences.

Name	T2	bSSFP-cine	Gated SPGR
Sequence type	Multi-slice T2-TSE	2D bSSFP	3D SPGR
Orientation	Transversal	Sagittal/Coronal	Transversal
Contrast	T2	T2/T1	T1
TR/TE (ms)	1500*/80	3.0/1.5	4.3/2.0
Field of view (mm)	400 x 311 x 151	450 x 394	375 x 375 x 176
Slice thickness (mm)	3	8	-
Voxel size (mm)	1.5 x 1.5	2.34 x 2.34	1.97 x 1.97 x 2.0
Flip angle (°)	90	50	10
Acquisition matrix	268 x 208	192 x 168	192 x 190
Number of slices	46	1	88
SENSE acceleration factor	2	1	3
Acquisition time (s)	138	150/50	22.2
Tdyn (ms)	5:00	504	-

TR=repetition time, TE= echo time, Tdyn = time to acquire one dynamic (i.e., a single slice in the time-series). In all 15 patients, the imaging parameters were the same, except in one patient, where a field-of-view (FOV) of 375x375x150 mm<sup>3</sup> was used in the gated 3D scans. \*The TR listed for the T2-TSE specifies the minimum TR. The actual TR is dependent on the respiration rate.

### **Respiratory motion analysis**

Respiratory-induced tumor motion was assessed on all four (two time points and two orientations) cine-MRI time series. To quantify the motion, a 2D optical flow algorithm was used, which registered all MR images to a reference dynamic for each time series(12). The reference dynamic was set to the 10<sup>th</sup> dynamic. The first four time points were excluded from analysis to ensure steady-state in all analyzed cine-MR images. Right-left (RL) and caudo-cranial (CC) motion was extracted from the coronal images, while anterior-posterior (AP) and CC motion was calculated on the sagittal images. After a detrend of the motion signal, both the maximum and 95<sup>th</sup> percentile amplitude were calculated for all directions. The

random error, introduced by the respiratory-induced periodic motion ( $\sigma_{RESP}$ ), was calculated by the root mean square of the standard deviation (SD) of the respiratory displacements over all patients.

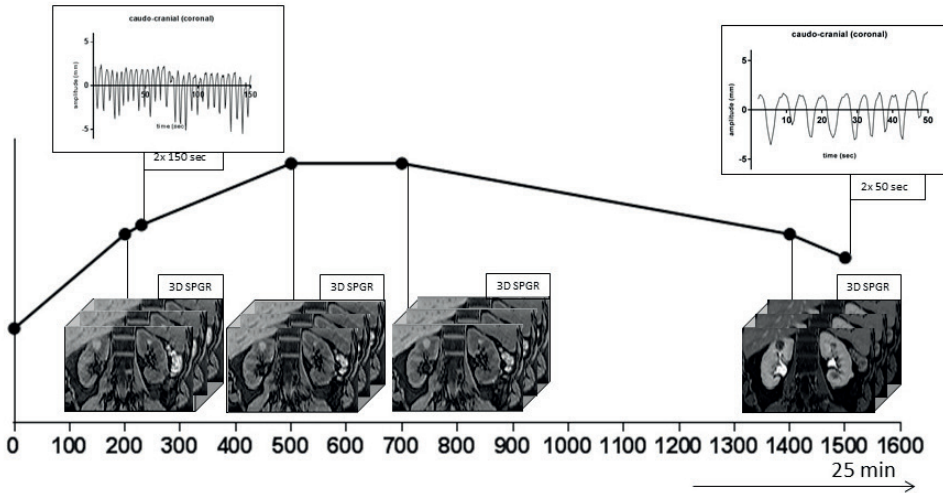


**Figure 1.** visualization of the scan protocol, with a cine-MRI at 230 sec and 1500 sec shown by the respiratory amplitude in the two images above the curve. At 4 time-points a 3D-SPGR scan was acquired: 200 sec, 500 sec, 700 sec, and 1400 sec, shown by the images below the curve.

### ***Intrafraction drift analysis***

The 3D SPGR acquisitions, acquired at four time-points throughout the scan session, were used to analyze slow varying motion, such as drifts, over a longer time-period. Each 3D volume was registered to the T2-TSE reference scan. A local rigid tumor registration (translations only), based on mutual information, was performed within a region-of-interest (ROI) that was placed around the ipsilateral kidney. The translations found at these four time-points were used as a measure for motion drifts over an entire MRI-linac SBRT treatment. In between the sampled time-points the intrafraction drift was assumed to change linearly over time(13,14). The systematic error, due to intrafraction drift ( $\Sigma_{DRIFT}$ ) was calculated by taking the SD over the temporal mean of each drift time-course, whereas the random error due to drift ( $\sigma_{DRIFT}$ ) was calculated by the root mean square of the standard deviations of the time-courses.

### **Motion margins**

To assess the effect of the various motion management strategies, the intrafraction motion margins ( $M$ ) were calculated by the nonlinear margin recipe by van Herk et al. for the 80% dose level(15):

$$M = 2.5 \Sigma + 0.84 \left( \sqrt{\sigma^2 + \sigma_p^2} - \sigma_p \right) \quad (1)$$

Where  $\Sigma$  and  $\sigma$  denote the quadratic sum of the SD of the systematic and random errors and  $\sigma_p$  (3.2 mm) the SD that describes the width of the penumbra in water. It is worth noting that systematic and random errors are calculated differently for the online daily adaptive treatment strategy of a MRI-linac compared to conventional radiotherapy. In conventional, fractionated radiotherapy the systematic errors are thought of as localization errors in planning imaging, whereas random errors are thought of as localization errors during treatment delivery(16). However, on a MRI-linac the treatment will be based on a daily mid-position scan. All simulations assume that setup is performed on the mid-position(16). Hence, uncertainty due to baseline variation is reduced to zero and the periodic respiratory motion only contributes to the random error. The intrafraction drift, on the other hand, contributes to both the random as well as the systematic error. Following this reasoning,  $\Sigma$  and  $\sigma$  were calculated as  $\Sigma = \Sigma_{\text{DRIFT}}$  and  $\sigma = \sqrt{[\sigma_{\text{DRIFT}}^2 + \sigma_{\text{RESP}}^2]}$ , where the subscript DRIFT refers to slow interfraction drift measured by the 3D SPGR acquisitions and RESP refers to the periodic respiratory motion measured by the 2D time series measurements. Based on these standard deviations, the motion margin required for three scenarios are calculated: *static* simulates an online planned treatment without active motion compensation; *trailing* involves slow moving aperture updates during treatment delivery to follow the mid-position of the tumor; *respiratory tracking* simulates tracked delivery in which the aperture perfectly follows the entire respiratory motion, including the (slower) tumor drift. To restrict our simulation to motion uncertainties only, delineation uncertainty and setup uncertainties (i.e., machine alignment) were not included.

## **RESULTS**

### **Respiratory motion analysis**

The respiratory movement along RL, AP, and CC direction was measured in both sagittal and coronal imaging at two different time points for each patient. The largest motion was observed along the CC direction showing a median 95% maximum amplitude of

approximately 12 mm. The median 95% maximum amplitude represents 95% of the bandwidth of all data points, and is therefore a more robust measure. The amplitudes along RL and AP were 1.9 mm and 4.7 mm, respectively (Table 3). The measurements on the amplitude of the tumor motion show no significant difference in all directions. The other directions did not show a significant difference between the different time-points ( $T_{start}$  and  $T_{end}$ ). A visual example of the motion of one patient in three different directions at  $T_{start}$  is displayed in Figure 2.

**Table 3.** respiratory movement along RP, AP and CC direction

		$T_{start}$	$T_{end}$	$p$
Median 95% (SD) in mm	RLc	1.8 (0.48)	2.0 (0.82)	0.05
	APs	4.7 (2.68)	4.7 (2.70)	0.50
	CCc	12.3 (5.45)	11.5 (3.83)	0.73
	CCs	11.6 (5.14)	12.0 (4.03)	0.53

$p < 0.05$ , Wilcoxon signed rank test. RLc: left-right coronal, APs: anterior-posterior sagittal, CCc: caudo-cranial coronal, CCs: caudo-cranial sagittal.

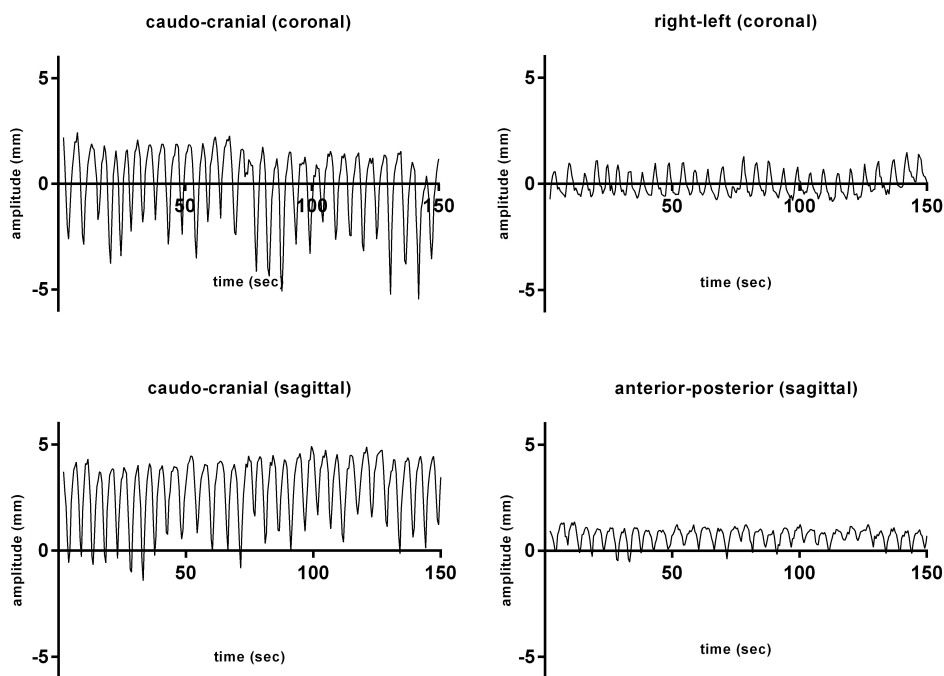


**Figure 2.** Raw unprocessed data sets of the motion of one patient (without detrend performed) in CCc (caudo-cranial coronal), RLc (right-left coronal), CCs (caudo-cranial sagittal), and APs (anterior-posterior sagittal), direction at  $T_{start}$ .

**Intrafraction drift analysis**

Figure 3 shows the rigid body translations along RL, AP, and CC direction over a 25 min period for each patient. Figure 3 shows that the drift is not linear like usually is assumed. Some patients demonstrate a considerable drift during the first three minutes after which the position stabilizes (e.g., Fig 3c, P11) whereas others even return to baseline (Fig 3c, P3). These plots also demonstrate that quite often the drift is not unidirectional over a period of 25 minutes. Finally, P8 shows an extreme amount of drift of up to 24 mm along CC. This patient was therefore considered as an outlier and was excluded from further group statistics. The mean systematic drift (i.e., mean of the means) of all patients was 0.6 mm along RL, 0.8 mm along AP, and 1.2 mm along CC.

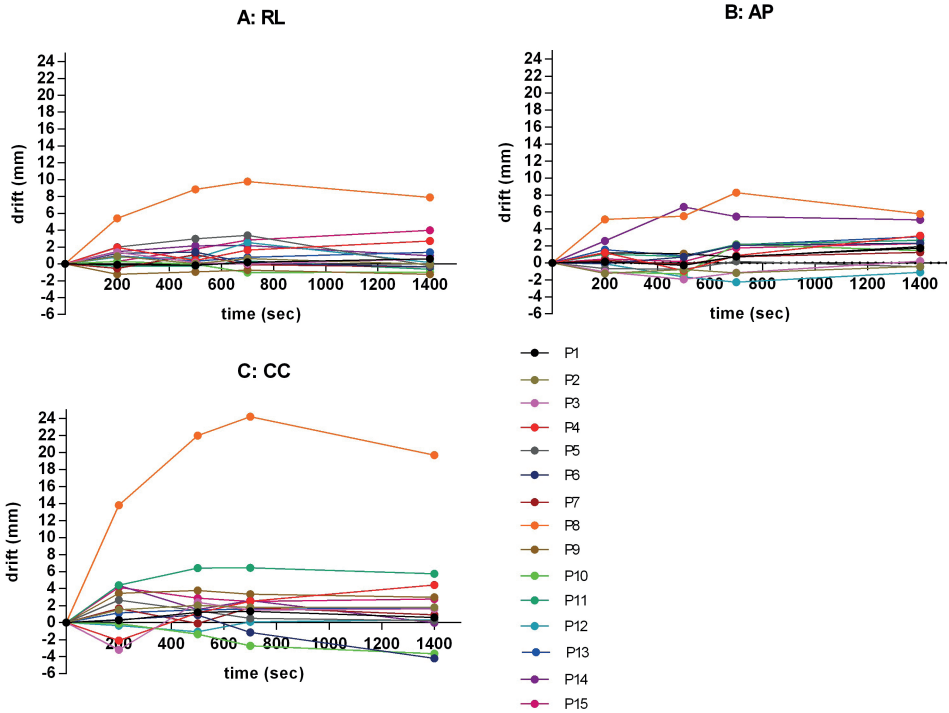


**Figure 3.** motion related to drift in right-left (RL), anterior-posterior (AP) and caudo-cranial (CC) direction of all 15 patients.

### Intrafraction motion margins

Table 4 shows the contributions of the systematic and random errors in each of the three scenarios: *static*, *tumor trailing*, and *respiratory tracking* for online mid-position SBRT treatments. Without active motion compensation (i.e., *static*) contributions from  $\Sigma_{\text{DRIFT}}$ ,  $\sigma_{\text{DRIFT}}$ , and  $\sigma_{\text{RESP}}$  all need to be accounted for by the motion margin. When tumor trailing is applied only  $\sigma_{\text{RESP}}$  contributes to the required motion margin (Table 4; column 2) as  $\Sigma_{\text{DRIFT}}$  and  $\sigma_{\text{DRIFT}}$  are actively compensated for. Respiratory tracking compensates for both intrafraction drift and respiratory motion (Table 4; column 3). Using Eq. 1 we find that a motion margin of 6.1 mm would be required for the static scenario. Tumor trailing greatly reduces this margin to 1.5 mm (assuming perfect tumor trailing). Tumor tracking only mitigates the 1.5 mm motion margin introduced by  $\sigma_{\text{RESP}}$ .

**Table 4.** Contributions of respiratory motion and intrafraction drift to the motion margin for three simulated motion management strategies on the MR-Linac: 1) static (i.e., without any active motion compensation), 2) tumor trailing, and 3) tumor tracking. Only caudo-cranial motion statistics and margins are given. Note that perfect tumor trailing and respiratory tracking is assumed and the table is confined to motion margins only. Delineation, setup, and registration errors are not included here.

	Static		Tumor trailing		Respiratory tracking	
	$\Sigma$	$\sigma$	$\Sigma$	$\sigma$	$\Sigma$	$\sigma$
Respiratory (periodic) motion (mm)	-	3.8	-	3.8	-	-
Intrafraction drift (mm)	1.8	1.0	-	-	-	-

## DISCUSSION

In the present study a single-fraction MRI-guided SBRT treatment was simulated in 15 patients to decouple and quantify the different components of intrafraction motion and their relative contribution to the total motion margin that is required for various motion management strategies. The goal was to assess the efficacy of tumor trailing and respiratory tracking, as this choice directly influences the type of imaging that is required during beam delivery.

Although RCC motion has been assessed before(7-9,11), most of the existing work has focused either on periodic respiratory motion only, or included specific immobilization techniques that are not representative for future use on a MRI-linac. One of the strengths of hybrid MRI-linac systems is the ability to continuously perform imaging and visualize the tumor during the treatment, which allows treatment under free-breathing conditions. MRI-guided motion compensation discards the need for immobilization devices like abdominal

compression or implantation of fiducials, which considerably increases patient comfort. To mimic the intended treatment setup on a MRI-linac, the experiments in this study were performed on patients without the use of mechanical immobilization devices. Consequently, the results described in the present paper are only generalizable to treatment strategies that also employ similar patient positioning strategies or that use minimal immobilization. The intrafraction motion was carefully assessed over a period of 25 minutes, which is representative of a single-fraction MRI-guided SBRT treatment. We found that the systematic nature of intrafraction drift results in a much larger effect on the motion margin than periodic respiratory motion, which confirms preliminary findings by Stemkens et al.(11). Following this, drift compensation (*tumor trailing*) would be able to reduce the motion margin by up to 75%, (6.1 mm to 1.5 mm assuming perfect tumor trailing). Additional compensation of the periodic motion by means of respiratory tracking further mitigates this margin, but is technically more demanding and requires the acquisition of fast 2D imaging with minimal latency during beam delivery(17). Tumor trailing allows one to trade-off temporal resolution for spatial extent enabling the acquisition of 3D volumetric data during beam delivery. This allows simultaneous visualization of both the tumor and organs at risk and facilitates the introduction of online intrafraction re-planning (18) and online 3D dose accumulation method(19,20).

## CONCLUSION

Periodic respiratory motion and intrafraction drift were assessed by MR imaging in 15 patients suspected of having RCC, using realistic single-fraction SBRT treatment times. It was found that

intrafraction drift is considerable and not linear over time when no mechanical immobilization is used. Due to the systematic nature of intrafraction drift, the contribution to the motion margin is large and makes up 75% of the total motion margin for online mid-position based SBRT treatments. This makes tumor trailing an interesting option to consider on the MR-linac as it would allow 3D volumetric MR imaging during beam delivery enabling the option to visualize both the tumor as well as the surrounding organs at risk.

## REFERENCES

1. Ljungberg B, Bensalah K, Bex A, Canfield S, Dabestani S, Giles RH, et al. Guidelines on Renal Cell Carcinoma. European Association of Urology 2015.
2. De Meerleer G, Khoo V, Escudier B, Joniau S, Bossi A, Ost P, et al. Radiotherapy for renal-cell carcinoma. *Lancet Oncol* 2014 Apr;15(4):e170-7.
3. Siva S, Pham D, Kron T, Bressel M, Lam J, Tan TH, et al. Stereotactic ablative body radiotherapy for inoperable primary kidney cancer: a prospective clinical trial. *BJU Int* 2017 Feb 10.
4. Siva S, Kothari G, Muacevic A, Louie AV, Slotman BJ, Teh BS, et al. Radiotherapy for renal cell carcinoma: renaissance of an overlooked approach. *Nat Rev Urol* 2017 Sep;14(9):549-563.
5. Siva S, Ellis RJ, Ponsky L, Teh BS, Mahadevan A, Muacevic A, et al. Consensus statement from the International Radiosurgery Oncology Consortium for Kidney for primary renal cell carcinoma. *Future Oncol* 2016 Mar;12(5):637-645.
6. Trofimov A, Vrancic C, Chan TC, Sharp GC, Bortfeld T. Tumor trailing strategy for intensity-modulated radiation therapy of moving targets. *Med Phys* 2008 May;35(5):1718-1733.
7. Siva S, Pham D, Gill S, Bressel M, Dang K, Devereux T, et al. An analysis of respiratory induced kidney motion on four-dimensional computed tomography and its implications for stereotactic kidney radiotherapy. *Radiat Oncol* 2013 Oct 26;8:248-717X-8-248.
8. Pham D, Kron T, Foroudi F, Schneider M, Siva S. A review of kidney motion under free, deep and forced-shallow breathing conditions: implications for stereotactic ablative body radiotherapy treatment. *Technol Cancer Res Treat* 2014 Aug;13(4):315-323.
9. Stam MK, van Vulpen M, Barendrecht MM, Zonnenberg BA, Intven M, Crijns SP, et al. Kidney motion during free breathing and breath hold for MR-guided radiotherapy. *Phys Med Biol* 2013 Apr 7;58(7):2235-2245.
10. Stemkens B, Tijssen RH, de Senneville BD, Lagendijk JJ, van den Berg CA. Image-driven, model-based 3D abdominal motion estimation for MR-guided radiotherapy. *Phys Med Biol* 2016 Jul 21;61(14):5335-5355.
11. Sonier M, Chu W, Lalani N, Erler D, Cheung P, Korol R. Evaluation of kidney motion and target localization in abdominal SBRT patients. *J Appl Clin Med Phys* 2016 Nov 8;17(6):6406.
12. Zachiu C, Papadakis N, Ries M, Moonen C, Denis de Senneville B. An improved optical flow tracking technique for real-time MR-guided beam therapies in moving organs. *Phys Med Biol* 2015 Dec 7;60(23):9003-9029.
13. Rossi MM, Peulen HM, Belderbos JS, Sonke JJ. Intrafraction Motion in Stereotactic Body Radiation Therapy for Non-Small Cell Lung Cancer: Intensity Modulated Radiation Therapy Versus Volumetric Modulated Arc Therapy. *Int J Radiat Oncol Biol Phys* 2016 Jun 1;95(2):835-843.
14. Sonke JJ, Rossi M, Wolthaus J, van Herk M, Damen E, Belderbos J. Frameless stereotactic body radiotherapy for lung cancer using four-dimensional cone beam CT guidance. *Int J Radiat Oncol Biol Phys* 2009 Jun 1;74(2):567-574.
15. van Herk M, Remeijer P, Rasch C, Lebesque JV. The probability of correct target dosage: dose-population histograms for deriving treatment margins in radiotherapy. *Int J Radiat Oncol Biol Phys* 2000 Jul 1;47(4):1121-1135.



16. Wolthaus JW, Sonke JJ, van Herk M, Damen EM. Reconstruction of a time-averaged midposition CT scan for radiotherapy planning of lung cancer patients using deformable registration. *Med Phys* 2008 Sep;35(9):3998-4011.
17. Glitzner M, Fast MF, de Senneville BD, Nill S, Oelfke U, Lagendijk JJ, et al. Real-time auto-adaptive margin generation for MLC-tracked radiotherapy. *Phys Med Biol* 2017 Jan 7;62(1):186-201.
18. Kontaxis C, Bol GH, Stemkens B, Glitzner M, Prins FM, Kerkmeijer LGW, et al. Towards fast online intrafraction replanning for free-breathing stereotactic body radiation therapy with the MR-linac. *Phys Med Biol* 2017 Aug 21;62(18):7233-7248.
19. Glitzner M, Crijns SP, de Senneville BD, Kontaxis C, Prins FM, Lagendijk JJ, et al. On-line MR imaging for dose validation of abdominal radiotherapy. *Phys Med Biol* 2015 Nov 21;60(22):8869-8883.
20. Glitzner M, de Senneville BD, Lagendijk JJ, Raaymakers BW, Crijns SP. On-line 3D motion estimation using low resolution MRI. *Phys Med Biol* 2015 Aug 21;60(16):N301-10.



# **A dual-purpose MRI acquisition to combine 4D-MRI and Dynamic Contrast-Enhanced imaging for abdominal stereotactic body radiotherapy planning**

---

Bjorn Stemkens  
Fieke M. Prins  
Tom Bruijnen  
Linda G.W. Kerkmeijer  
Jan J.W. Lagendijk  
Cornelis A.T. van den Berg  
Rob H.N. Tijssen

*Submitted*

**ABSTRACT**

For successful abdominal stereotactic body radiotherapy (SBRT) it is crucial to have both a clear tumor definition and an accurate characterization of the motion. While dynamic contrast-enhanced (DCE) MRI aids tumor visualization, it is often hampered by motion artifacts. 4D-MRI, on the other hand, characterizes this motion, but often lacks the contrast to clearly visualize the tumor. Unfortunately, both acquisitions are lengthy leading to patient discomfort and possibly increased motion artifacts. The aim of this work is to combine DCE- and 4D-MRI into a single continuous free-breathing acquisition to extract the necessary information for planning. A 5-minute T1-weighted DCE acquisition was collected in five renal cell carcinoma (RCC) patients. Data were acquired continuously using a 3D golden angle radial stack-of-stars acquisition. This enabled three types of reconstruction; 1) a high spatio-temporal resolution DCE time series for improved tumor visualization, 2) a 5D reconstruction that characterizes both contrast enhancement and motion, and 3) a contrast-enhanced 4D-MRI of the last 170 seconds of acquisition for motion characterization. Motion extracted from the 4D- and 5D-MRI was compared with a previously validated, separately acquired 4D-MRI and additional 2D cine MR imaging.

Reconstructions demonstrated clear tumor visualization and contrast enhancement throughout the entire field-of-view. Motion in the CE-4D-MRI was similar to the motion in the separately acquired 4D-MRI and approximately 10% smaller than the motion in the 2D cine MRI (5.8mm vs 5.9mm and 6.5mm). 5D reconstructions underestimated the motion by more than 30%, but minimized respiratory-induced blurring in the contrast enhanced images.

DCE- and 4D-MRI can be integrated into a single acquisition that enables different reconstructions with complementary information for abdominal SBRT planning and, in an MRI-guided treatment, precise motion information, input for motion models, and rapid feedback on the contrast enhancement characteristics.

## INTRODUCTION

Stereotactic body radiation therapy (SBRT) is increasingly used in abdominal tumors to increase local control probabilities(1-4). Characterized by tight margins, steep dose gradients and a few high dose fractions(5), successful abdominal SBRT treatments require 1) accurate imaging in order to precisely depict the tumor and organs-at-risk (OARs) and 2) characterization of the respiratory-induced motion. Both functional imaging, such as dynamic contrast-enhanced (DCE), and anatomical scans can be used to define the tumor, while 4D-MRI can be used to characterize the motion.

DCE-MRI is a functional imaging technique that is used to enhance contrast between tumor and OARs, determine micro-vascular parameters, such as the transfer constant  $K_{trans}$  through pharmino-kinetic modeling(6), and characterize tumor-specific contrast uptake values that may provide important information for therapy response. In the abdomen, DCE-MRI mostly refers to acquiring a small series of contrast-enhanced (CE) volumes to capture the different enhancement phases (e.g. arterial, venous and late enhancement). These volumes are generally acquired in multiple (up to ten) breath-holds to minimize respiratory-induced artifacts. This is not only demanding for the patients, but it also limits scan time and thus compromises have to be made on resolution, coverage and/or signal-to-noise ratio (SNR). Moreover, breath-holds vary and patients are often unable to suspend respiration sufficiently multiple consecutive times(7). To relieve patients, no (breath- hold) data is acquired between 3.5 and 5 minutes after contrast injection at our institute, resulting in an inefficient DCE protocol. Furthermore, these breath-holds are not representative for the position of the tumor during radiation. Mid-ventilation(8) or mid-position volumes(9) that approximate or represent the time-weighted average anatomical position, can be calculated using an additional 4D-MRI acquisition(10-12). Unfortunately, both DCE-MRI and 4D-MRI are lengthy acquisitions. Moreover, warping the DCE breath-hold volumes to the mid-position introduces uncertainties, as it is an additional registration step.

To accelerate MR imaging, compressed sensing (CS) has been proposed for many applications in the past few years(33). A recent published review gives a comprehensive overview of CS techniques for body MRI(13). Unfortunately, DCE-MRI time-series require a fixed acquisition time (typically between 2.5 and 5 minutes) in order to characterize the pre-contrast, arterial-, venous-, and late-enhancement of both tumor and OARs. DCE acquisitions are therefore difficult to accelerate, although the acquisition time of individual volumes can be reduced using CS. Consequently, an increased number of contrast-enhanced volumes can be acquired in the same imaging time(14), thereby enabling pharmino-kinetic modeling, which requires high temporal resolution (e.g. at least four seconds for renal perfusion measurements)(15).

Here we propose a dual-purpose, free-breathing MRI acquisition that combines DCE- and 4D-MRI. This obviates the need for a separate 4D-MRI acquisition and gives superior tumor contrast in the phase-resolved 4D-MRI reconstruction. To achieve this, continuous 3D golden angle(16) radial stack-of-stars sampling is used in combination with a previously published CS reconstruction, called (XD-)GRASP(14,17). This CS algorithm has been proposed in combination with the golden angle acquisition for radiological exams to minimize motion artifacts and improve spatial and/or temporal resolution of DCE time series and has been used previously to generate a 4D-MRI within a few minutes(18). However, the combination of both is unique and valuable in the context of abdominal radiotherapy, since abdominal scan protocols are usually very long and contrast between pathologies can be limited. In this study we examine the benefits of combining these reconstructions and the value of an additional 5D reconstruction, for characterizing the motion and defining the GTV for abdominal MRI- guided radiotherapy. The reconstructions are compared to self-navigated golden angle 3D stack-of-stars 4D-MRI method(11,18) and 2D cine imaging to quantify the accurateness of the estimated motion. Moreover, mid-pos volumes are generated from these data for mid-position radiotherapy planning. The goal is to determine the value and accuracy of the different reconstructions for MR-aided abdominal radiotherapy. It is shown that the reconstructions from this dual-purpose acquisition provide complementary information for tumor characterization, precise delineations, and mid-pos volume generation, and enhance image quality.

## METHODS

### 2.1 Theory

The proposed dual-purpose continuous DCE acquisition employs 3D golden angle radial stack-of-stars sampling, which uses Cartesian sampling along the  $k_z$  dimension (partitions), while radial encoding is used in the  $k_x$ - $k_y$  plane (see Figure 1a). All  $k_z$  lines are acquired for one azimuthal angle, before the next radial projection is acquired in a similar fashion. The increased robustness against motion artifacts of radial sampling(19) enables free-breathing acquisitions, thus eliminating the need for breath-holds, while the continuous golden angle sampling allows for reconstructions with flexible temporal resolutions(16). This flexibility opens up the possibility to reconstruct an additional 4D-MRI, facilitating a time-efficient DCE-4D-MRI acquisition for both high spatio-temporal resolution DCE- and 4D-MRI generation. Since undersampled data is used for reconstruction, a CS algorithm in the form of (XD-)GRASP is used to eliminate undersampling artifacts. However, the (XD-)GRASP CS algorithm exploits temporal sparsity in one (contrast enhancement or respiratory for GRASP) or two (contrast enhancement and respiratory for XD-GRASP) dimensions using first-order, temporal total-variation sparsity constraints(14,17). Using

one or two controllable regularization parameters ( $\lambda$ ) the amount of regularization along the sparse dimension(s) is specified. Increasing the regularization results in smoother images with reduced artifacts, but may also yield underestimations of the motion in the phase-resolved 4D-MRI as was shown by Mickevicius and Paulson(18). The combination of CS and golden angle sampling enables us to reconstruct the data set in three different ways where the 4th (and 5th) dimension are selected to represent aspects important for abdominal SBRT treatment planning: 1) a heavily undersampled DCE time-series where the 4th dimension represent time that is used to visualize the contrast uptake in the tumor and OARs (see Figure 1b). It is hypothesized that this time series represents time-averaged anatomy, thus mid-position, since the underlying anatomy contributes equally to the reconstructed volumes. Consequently, respiratory-induced blurring may be present in the images. 2) a 5D reconstruction, where the 4th dimension represents time (or contrast enhancement), while the 5th dimension depicts the respiratory phase (see Figure 1c). 3) a contrast-enhanced (CE)-4D-MRI of the last 2:40 minutes of DCE data where the 4th dimension is the respiratory phase (see Figure 1d). This respiratory-resolved reconstruction is compared to a separately acquired 4D-MRI method and 2D cine imaging to quantify the accuracy of the estimated motion. Additionally, it can be used to calculate the mid-position or internal target volume (ITV) (International Commission on Radiation Units and Measurements 2010). Moreover, the motion in this CE-4D-MRI is compared with the motion in the 5D reconstructions.

## 2.2 MR image acquisition

Five patients suspected of renal-cell carcinoma (RCC) were included in this institutional review board approved study. After informed consent all patients were scanned on a 1.5T MRI-RT scanner (Ingenia, Philips, Best, the Netherlands) using a 28-element receive body array. Three different acquisitions were performed for each patient to compare the motion quantification. The DCE acquisition for one patient was, unfortunately, mis-positioned and this patient was therefore excluded from further analyses.

First, a respiratory-correlated (phase-resolved) 4D-MRI was acquired that serves as comparison to the CE-4D-MRI. This 4D-MRI implementation acquires 3D data continuously using a balanced steady-state free-precession (bSSFP) sequence with a golden angle radial stack-of-stars trajectory (TR/TE = 3.0/1.45 ms, voxel size =  $1.9 \times 1.9 \times 4.0 \text{ mm}^3$ ,  $\alpha = 30^\circ$ , partial fourier = 0.75, bandwidth = 867 Hz/px). Instead of acquiring a separate 1D-MR navigator as was done in the original implementation, a self-gating signal was extracted from the center of k-space(17,18,20). Phase binning was used to sort the radial projections into ten respiratory phases. The field-of-view (FOV) was set to include both kidneys and ranged between  $300 \times 300 \times 132 \text{ mm}^3$  to  $350 \times 350 \times 200 \text{ mm}^3$ . Acquisition times ranged between 230 and 301 seconds.

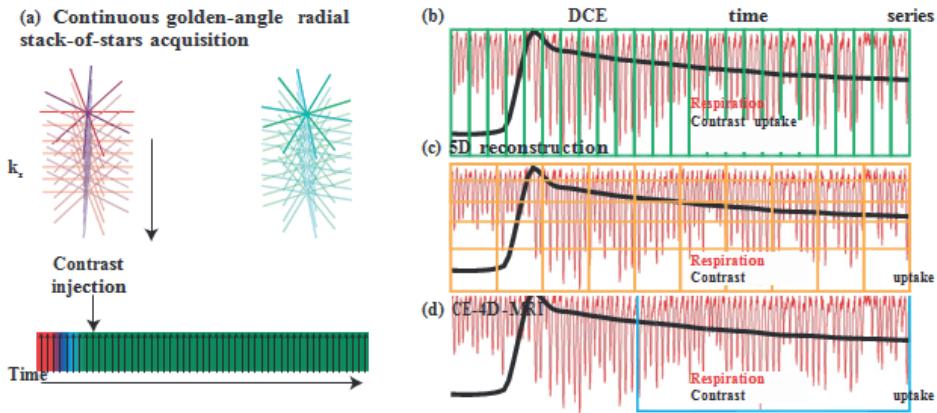


**Figure 1.** (a) The golden angle radial stack-of-stars acquisition continuously acquires data before, during and after contrast injection. In this stack-of-stars read-out all  $k_z$  lines are acquired per azimuthal angle, before moving on to the next. (b-d) Three different reconstructions are performed from a single continuous DCE acquisition. During the acquisition there is both contrast uptake (black) and respiratory motion (red). (a) For the DCE time-series, the data is reconstructed into 96 3D volumes, each consisting of 3.6 seconds of data. (b) For the CE-4D-MRI, the last 170 seconds of data are sorted into ten respiratory phases. (c) The 5D data set is reconstructed by dividing the data into 25 3D volumes, each consisting of five respiratory phases.

Second, two (sagittal and coronal) 2D cine images were acquired in an interleaved fashion for 306 seconds using a bSSFP sequence ( $TR/TE = 3.0/1.5$  ms,  $\alpha = 30^\circ$ ,  $FOV = 450 \times 345$  mm<sup>2</sup>,  $voxelsize = 1.8 \times 1.8$  mm<sup>2</sup>, slice thickness = 8 mm, SENSE = 2, partial Fourier = 0.75, bandwidth = 2034 Hz/px,  $tacq = 360$  ms). These fast cine images serve as reference for the tumor motion estimations.

Third, for the dual-purpose DCE acquisition a fat-suppressed, an RF and gradient spoiled gradient echo (SPGR) 3D radial stack-of-stars acquisition was used ( $TR/TE = 3.5/1.5$  ms,  $FOV = 300 \times 300 \times 132$  mm<sup>3</sup>,  $\alpha = 15^\circ$ ,  $voxelsize = 1.9 \times 1.9 \times 4.0$  mm<sup>3</sup>, partial fourier = 0.75, bandwidth = 656 Hz/px). To include both kidneys, the FOV of one patient was increased to  $300 \times 300 \times 200$  mm<sup>3</sup>. Data were acquired for 350 seconds and 30 seconds after the start of the acquisition contrast (Gadovist, Bayer AG, Leverkusen, Germany) was intravenously injected.

### 2.3. Reconstruction

The DCE acquisition was reconstructed offline into three different data sets (see Figure 1b-d).

First, the DCE acquisition was used to reconstruct a DCE time-series with a temporal resolution of  $\approx 3.6$  seconds (21 projections per volume, acceleration factor  $R \approx 10.5$ ), yielding 96 volumes to identify the dynamic uptake of the contrast agent in both the tumor and OARs.



Second, the DCE acquisition was reconstructed into a 5D-DCE time series of 25 volumes, corresponding to a temporal resolution of 13.8 seconds, where each time-point consists of five respiratory phases ( $R \approx 13.8$ ). Amplitude binning with variable bin width was used to sort the data per volume into the different respiratory phases, since insufficient data was available per CE time-point to perform phase binning.

Lastly, for the 4D-MRI as well as the CE-4D-MRI reconstructed from the DCE acquisition, the last 170 seconds of data were used to generate a phase-resolved 4D-MRI. Using phase binning data were sorted into ten respiratory phases. To minimize temporal regularization in the GRASP reconstruction, which may underestimate motion in the 4D reconstruction, but at the same time remove undersampling artifacts sufficiently, the regularization parameter  $\lambda$  was determined as an initial processing step for one patient. Normalized regularization weights between 0.001 and 1 were tested by comparing the resulting tumor motion with the tumor motion in the 2D cine images. We hypothesize that a moderate value for  $\lambda$  yielded the best results in terms of correct motion estimations and minimization of artifacts. Moreover, besides the GRASP reconstruction, the (non contrast-enhanced) 4D data was also reconstructed in a linear fashion using regular gridding followed by an inverse FFT(34) to investigate the influence of the regularization.

The different acquisitions (bSSFP and SPGR), will exhibit different contrast characteristics for the tumor and OARs, though a similar reconstruction is performed. The bSSFP was chosen for the non-CE scan for its high SNR and contrast between organs, while the fat-suppressed SPGR is generally used in DCE scans to pinpoint the contrast enhancements. All processing steps were performed in Matlab (The Mathworks, Natick, MA). The tumor was delineated on the exhale volume of the bSSFP 4D-MRI and used for all analyses.

#### **2.4. Motion analysis**

Motion in the all 4D-MRI reconstructions, the 5D reconstructions, and in the 2D cine images were extracted using an optical flow algorithm from the realTITracker toolbox (bsenneville.free.fr) (21). This algorithm was previously validated on phantom and in-vivo data and calculates a voxel-by-voxel deformable vector field (DVF)(22-24).

Additionally, a mid-pos volume was constructed from the CE-4D-MRI by warping the reference phase with the inverse of the average DVF(25). To test the hypothesis that the DCE time series represent anatomy in mid-position, the last 170 seconds of the DCE time series (similar time span as was used to generate the CE-4D-MRI) were non rigidly registered to the mid-pos volume. The tumor position over time was compared to the tumor mid-position. Moreover, the tumor motion in the separately acquired 4D-MRI and in the CE-4D-MRI reconstruction was compared with the tumor motion in the 2D cine images, as well as the tumor motion in the last 170 seconds of the 5D reconstruction. Furthermore, the motion in the GRASP-reconstructed 4D-MRI was compared with the

motion in the gridded 4D-MRI to analyze the influence of the temporal regularization. This serves both as a validation of the 4D reconstruction and to examine the differences between the 4D- and CE-4D-MRI.

## RESULTS

### 3.1. Influence of regularization

Initial experiments showed that a normalized regularization weight of  $\lambda = 0.01$  yielded motion estimations that were close to the motion in the 2D cine images. This moderate  $\lambda$  removes undersampling (i.e. streaking) artifacts to a large extent, but minimizes temporal smoothing and was used for all patient data sets. Using this  $\lambda$ , tumor motion in the GRASP-reconstructed 4D-MRI was on average 0.1 mm smaller over all patients, compared to the linearly reconstructed 4D-MRIs.

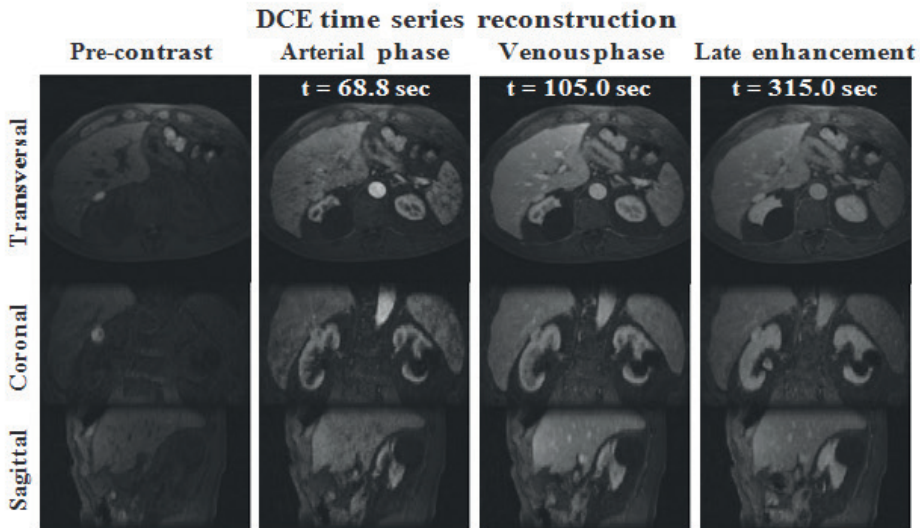
### 3.2. DCE time series

Figure 2 displays the pre-contrast, arterial, venous and late enhancement phase in transversal, coronal and sagittal orientation. All phases show distinct uptake rates in both the tumor and other structures, such as the kidney and liver and no uptake in the cysts in the medial posterior part of the right kidney. Some respiratory blurring can be observed in the superior-inferior (SI) direction. This particular tumor (a cystic tumor) is clearly visible on all phases, even before contrast enhancement.

Motion analysis showed that the difference in absolute tumor position between the DCE time series and the CE mid-pos volume was small with mean differences over all subject of  $-0.14 \text{ mm} \pm 0.40 \text{ mm}$ ,  $0.09 \text{ mm} \pm 0.62 \text{ mm}$ , and  $0.25 \text{ mm} \pm 0.85 \text{ mm}$  in left-right (LR), antero-posterior (AP) and cranio-caudal (CC) direction, respectively. This confirms our hypothesis that the anatomical position of the reconstructed DCE time series resembles the mid-position very well. However, residual respiratory blurring is observed in the SI direction.

### 3.3. 5D-MRI

Figure 3 demonstrates an example of the 5D reconstruction where end-exhale and end-inhale are shown for the arterial and late enhancement phase, alongside the registered image where all five respiratory phases are registered to the exhale phase. Compared to the DCE time series (Figure 2) less blurring is observed, especially in the end-exhale and registered reconstruction, which may aid delineation. Note that each volume is reconstructed using solely 16 projections.



**Figure 2.** Example of the DCE time series reconstruction of the same patient for the pre-contrast, arterial, venous, and late enhancement phase in the transversal, coronal and sagittal plane. Temporal resolution is 3.6 seconds/volume, corresponding to an acceleration factor of 10.5.

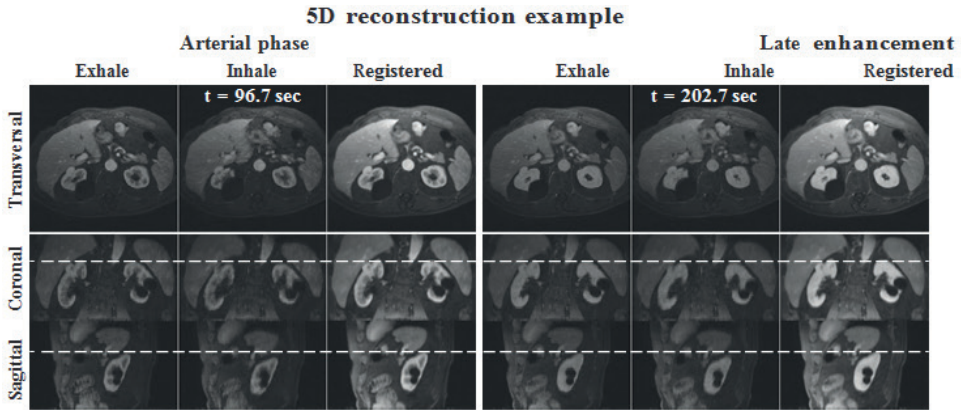
### 3.4 CE-4D-MRI

Figure 4a shows an example of the 4D-MRI reconstruction from the continuous DCE acquisition, alongside the separately acquired bSSFP 4D-MRI reconstruction in panel b. The end-exhale and -inhale are shown as well as the mid-position reconstruction. Although the contrast is different, the relatively small motion is captured in both reconstructions. The tumor (black arrow) has hyper-intense contrast in both reconstructions, while the renal cyst (white arrow) displays a hypo-intense signal in the CE-4D-MRI reconstruction and a hyper-intense signal in the bSSFP 4D-MRI encumbering the distinction between both structures.

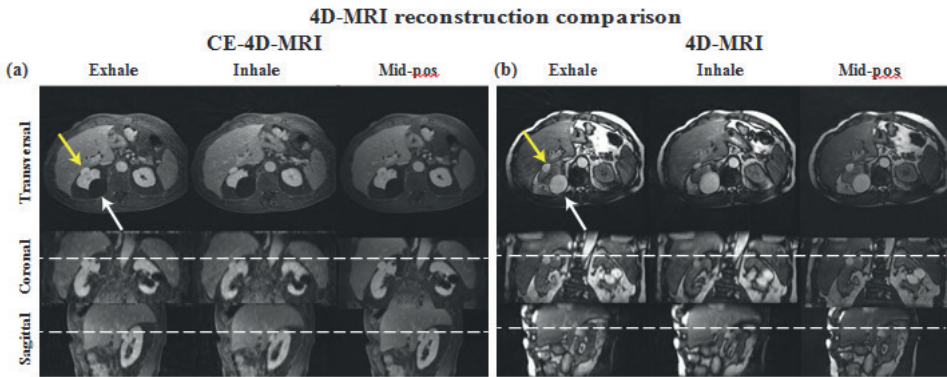
### 3.5. Motion analysis

Figure 5 displays the cranio-caudal GTV motion extracted from the 5D-MRI, CE-4D-MRI (both reconstructed from the DCE acquisition), 4D-MRI, and 2D cine images for all patients. The 5D reconstruction consists of only 5 respiratory phases, since a limited amount of data was available for respiratory sorting. Moreover, amplitude binning was used, while for the other reconstructions phase binning was used. Motion in the 5D reconstruction was smaller than the motion in the CE-4D-MRI (0.3, 0.6, and 1.8 mm in LR, AP and CC, respectively), despite the fact that they were reconstructed from the same

acquisition. CE-4D-MRI showed similar GTV motion as the bSSFP 4D-MRI ( $5.8 \pm 1.1$  mm vs  $5.9 \pm 0.8$  mm), which was approximately 10% smaller than the motion in the 2D cine images ( $6.5 \pm 0.9$  mm).



**Figure 3.** Example of the 5D-DCE reconstruction. The exhale and inhale phase are shown for all planes in the arterial and late enhancement phase. The third and sixth column display the registered volumes for both arterial and late-enhanced phase, showing sharp and clear contrast-enhanced volumes. For each volume 16 projections are used, corresponding to an acceleration factor of 13.75.



**Figure 4.** 4D-MRI reconstructed from a) the proposed dual-purpose acquisition (T1 - weighted) and b) from the separately acquired 4D-MRI (T2 /T1 contrast weighting). The exhale, inhale and mid-pos volumes are shown in the transversal, coronal and sagittal orientation. The yellow arrow pinpoints the tumor, while the white arrow shows a renal cysts. The white dotted line is plotted as visual aid.

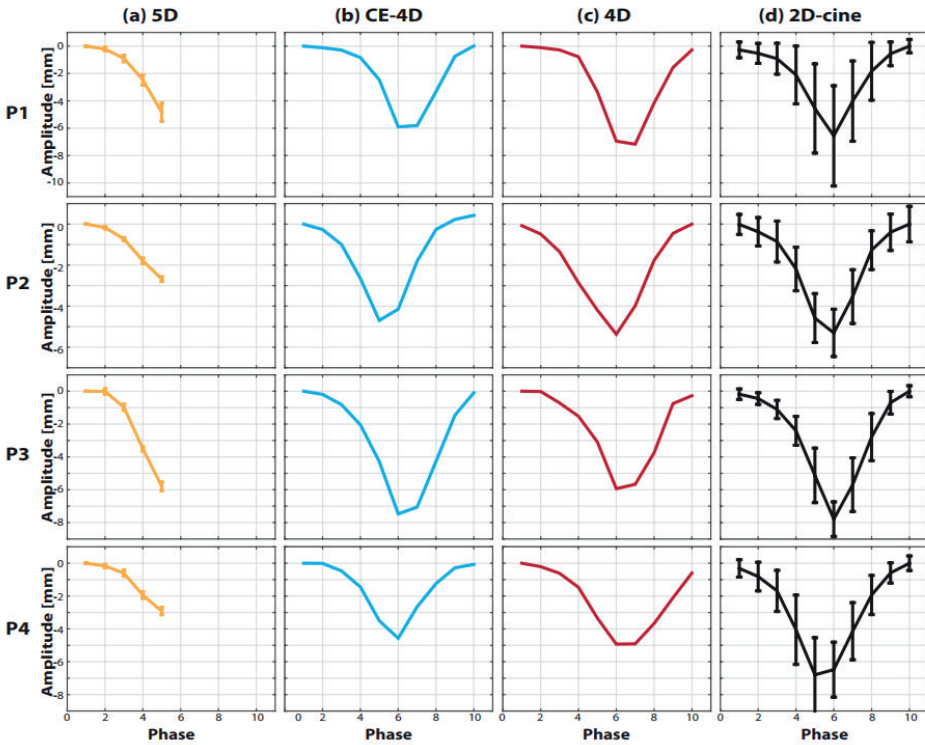


**Figure 5.** GTV motion for all patients (P1-P4) calculated from the (a) 5D reconstruction, (b) CE-4D-MRI reconstruction, (c) separately acquired bSSFP 4D-MRI, and (d) 2D cine imaging. The errorbars represent  $\pm 1$  standard deviation, which are not present for (b) and (c), since this motion was calculated from a single (CE)-4D-MRI reconstruction.

## DISCUSSION

In this study, a single free-breathing, dual purpose DCE acquisition was evaluated to determine its value for SBRT treatment planning by obviating the need for two separate acquisitions. The proposed acquisition is able to generate high spatio-temporal DCE volumes for contrast enhancement characterization and tumor delineation, and, at the same time, characterizes motion precisely using an additional 4D-MRI reconstruction. This latter reconstruction can be used to calculate a mid-pos volume or ITV margin without the need for a separate 4D acquisition, thus reducing overall scan time with several minutes. Additionally, SNR and contrast-to-noise ratio in these reconstructions can be higher, expediting non-rigid registration. Since no breath-holds are required, the reproducibility of DCE imaging is increased, while simultaneously patient comfort is

improved. Furthermore, the high temporal resolution enables pharMO-kinetic modeling without the need for registration, since the same anatomical position is reconstructed. An extra 5D reconstruction can provide DCE volumes with reduced respiratory-induced blurring, but does not provide accurate motion estimation. However, as demonstrated in this paper, the contrast enhanced part of the acquisition can be used to successfully reconstruct a CE-4D-MRI.

The CS algorithm used in this study has been used previously for different purposes, but its combined use for GTV delineation and motion quantification is novel and valuable in the context of MRI-guided SBRT. For a regular linac treatment, these reconstructions can provide necessary information for tumor characterization, delineation, and motion characterization. In the setting of a hybrid MRL(26-30), this technique can be acquired both in the pre-treatment phase and immediately after a treatment fraction. For SBRT this can, for example, be once a week. The DCE acquisition may be able to pinpoint differences in contrast enhancement that represent changes in perfusion related to hypoxic sub-regions of the tumor. Based on this information, the treatment can be adapted to increase dose for radioresistant parts of the tumor.

It was shown previously by Mickevicius and Paulson(18) that the GRASP algorithm may underestimate motion, as a result of temporal smoothing. For this reason, the regularization parameter  $\lambda$  was set conservatively low. Comparing tumor motion estimated from the GRASP-reconstructed images and linearly reconstructed (gridded) volumes showed an underestimation of 0.1 mm. This contributes towards 2% of the 10% underestimation that was observed when compared with tumor motion estimated on the 2D cine slices. Another source is the fact that the absolute inhale peaks are averaged out in a respiratory-resolved 4D-MRI, as a result of phase binning that sorts data in equal-time bins(35). Finally, motion can vary between the different acquisitions. While the same  $\lambda$  was used for the respiratory dimension in the 5D reconstruction, the motion was approximately 30% smaller than the CE-4D-MRI, though the same acquisition was used. This may be a result of the employed amplitude binning with variable width bin, the additional temporal regularization using a second  $\lambda$ , or the fact that less data was available per individual phase volumes.

Although blurring in the respiratory dimension was minimized in this study to obtain accurate motion estimations, blurring in the contrast enhancement dimension was not investigated. Too much blurring can be problematic for quantitative DCE analyses. However, Wang et al.(31) recently showed that a total variation regularization, similar to the one used in this study, produced the most accurate pharmacokinetic parameters in DCE-MRI in the breast.

The iterative CS reconstructions in this study is computationally intensive and reconstruction times ranged between 45 mins for the 4D-MRI to 10 hours for the 5D reconstruction using Matlab code on a 32Gb RAM, 8-core CPU desktop PC. While this may not be an issue for pre-treatment exams, an accelerated algorithm is beneficial for clinical usage. In future research this can be achieved using parallelization of the code, conversion and optimization of the code into C++, and reconstructing the data automatically after acquisition using a reconstruction server(18,36).

The three different reconstructions that were presented in this study provide complementary information. If an ITV concept is used, the DCE time series supports an ITV delineation, as respiratory motion is inherently included in the reconstruction. The CE-4D-MRI can additionally be used to warp other (respiratory-gated or -triggered) acquisitions to the same anatomical position (e.g. mid-pos or end-exhale), although this may introduce registration errors. Moreover, it can be used as input for a motion model for MRI-guided radiotherapy(24,32). If a mid-pos treatment is planned, on the other hand, the registered 5D reconstruction can yield the necessary imaging for GTV delineation, while the CE-4D-MRI can be used to warp the delineations to the mid-position. Moreover, the 5D reconstruction can be useful to minimize respiratory-induced blurring, when large and/or irregular respiratory motion is present.

## CONCLUSION

In this study a continuous, free-breathing DCE acquisition was presented that supports multiple, complementary reconstructions. These reconstructions visualize contrast uptake for delineation purposes, characterize motion throughout a large field-of-view, and minimize respiratory-induced blurring for both tumor and all OARs. The combination of the DCE time series and the CE-4D-MRI is valuable for abdominal SBRT, while the 5D-MRI reconstructions proved to be mainly useful for minimizing respiratory-induced blurring.

## ACKNOWLEDGMENTS

This work is part of the research program HTSM with project number 15354, which is (partly) financed by the Netherlands Organization for Scientific Research(NWO). The authors would like to thank Li Feng for the (XD-)GRASP Matlab code.

## REFERENCES

1. Feng M, Ben-Josef E. Radiation therapy for hepatocellular carcinoma. *Semin Radiat Oncol* 2011 Oct;21(4):271-277.
2. Chuong MD, Springett GM, Freilich JM, Park CK, Weber JM, Mellon EA, et al. Stereotactic body radiation therapy for locally advanced and borderline resectable pancreatic cancer is effective and well tolerated. *Int J Radiat Oncol Biol Phys* 2013 Jul 1;86(3):516-522.
3. De Meerleer G, Khoo V, Escudier B, Joniau S, Bossi A, Ost P, et al. Radiotherapy for renal-cell carcinoma. *Lancet Oncol* 2014 Apr;15(4):e170-7.
4. Siva S, Pham D, Kron T, Bressel M, Lam J, Tan TH, et al. Stereotactic ablative body radiotherapy for inoperable primary kidney cancer: a prospective clinical trial. *BJU Int* 2017 Nov;120(5):623-630.
5. Potters L, Steinberg M, Rose C, Timmerman R, Ryu S, Hevezi JM, et al. American Society for Therapeutic Radiology and Oncology and American College of Radiology practice guideline for the performance of stereotactic body radiation therapy. *Int J Radiat Oncol Biol Phys* 2004 Nov 15;60(4):1026-1032.
6. Tofts PS, Brix G, Buckley DL, Evelhoch JL, Henderson E, Knopp MV, et al. Estimating kinetic parameters from dynamic contrast-enhanced T(1)-weighted MRI of a diffusable tracer: standardized quantities and symbols. *J Magn Reson Imaging* 1999 Sep;10(3):223-232.
7. Chandarana H, Block TK, Rosenkrantz AB, Lim RP, Kim D, Mossa DJ, et al. Free-breathing radial 3D fat-suppressed T1-weighted gradient echo sequence: a viable alternative for contrast-enhanced liver imaging in patients unable to suspend respiration. *Invest Radiol* 2011 Oct;46(10):648-653.
8. Wolthaus JW, Schneider C, Sonke JJ, van Herk M, Belderbos JS, Rossi MM, et al. Mid-ventilation CT scan construction from four-dimensional respiration-correlated CT scans for radiotherapy planning of lung cancer patients. *Int J Radiat Oncol Biol Phys* 2006 Aug 1;65(5):1560-1571.
9. Wolthaus JW, Sonke JJ, van Herk M, Belderbos JS, Rossi MM, Lebesque JV, et al. Comparison of different strategies to use four-dimensional computed tomography in treatment planning for lung cancer patients. *Int J Radiat Oncol Biol Phys* 2008 Mar 15;70(4):1229-1238.
10. von Siebenthal M, Szekeley G, Gamper U, Boesiger P, Lomax A, Cattin P. 4D MR imaging of respiratory organ motion and its variability. *Phys Med Biol* 2007 Mar 21;52(6):1547-1564.
11. Stemkens B, Tijssen RH, de Senneville BD, Heerkens HD, van Vulpen M, Lagendijk JJ, et al. Optimizing 4-dimensional magnetic resonance imaging data sampling for respiratory motion analysis of pancreatic tumors. *Int J Radiat Oncol Biol Phys* 2015 Mar 1;91(3):571-578.
12. Deng Z, Pang J, Yang W, Yue Y, Sharif B, Tuli R, et al. Four-dimensional MRI using three-dimensional radial sampling with respiratory self-gating to characterize temporal phase-resolved respiratory motion in the abdomen. *Magn Reson Med* 2016 Apr;75(4):1574-1585.
13. Feng L, Benkert T, Block KT, Sodickson DK, Otazo R, Chandarana H. Compressed sensing for body MRI. *J Magn Reson Imaging* 2017 Apr;45(4):966-987.
14. Feng L, Grimm R, Block KT, Chandarana H, Kim S, Xu J, et al. Golden-angle radial sparse parallel MRI: combination of compressed sensing, parallel imaging, and golden-angle radial sampling for fast and flexible dynamic volumetric MRI. *Magn Reson Med* 2014 Sep;72(3):707-717.



15. Michaely HJ, Sourbron SP, Buettner C, Lodemann KP, Reiser MF, Schoenberg SO. Temporal constraints in renal perfusion imaging with a 2-compartment model. *Invest Radiol* 2008 Feb;43(2):120-128.
16. Winkelmann S, Schaeffter T, Koehler T, Eggers H, Doessel O. An optimal radial profile order based on the Golden Ratio for time-resolved MRI. *IEEE Trans Med Imaging* 2007 Jan;26(1):68-76.
17. Feng L, Axel L, Chandarana H, Block KT, Sodickson DK, Otazo R. XD-GRASP: Golden-angle radial MRI with reconstruction of extra motion-state dimensions using compressed sensing. *Magn Reson Med* 2016 Feb;75(2):775-788.
18. Mickevicius NJ, Paulson ES. Investigation of undersampling and reconstruction algorithm dependence on respiratory correlated 4D-MRI for online MR-guided radiation therapy. *Phys Med Biol* 2017 Apr 21;62(8):2910-2921.
19. Glover GH, Pauly JM. Projection reconstruction techniques for reduction of motion effects in MRI. *Magn Reson Med* 1992 Dec;28(2):275-289.
20. Zhang T, Cheng JY, Chen Y, Nishimura DG, Pauly JM, Vasanawala SS. Robust self-navigated body MRI using dense coil arrays. *Magn Reson Med* 2016 Jul;76(1):197-205.
21. Zachiu C, Papadakis N, Ries M, Moonen C, Denis de Senneville B. An improved optical flow tracking technique for real-time MR-guided beam therapies in moving organs. *Phys Med Biol* 2015 Dec 7;60(23):9003-9029.
22. Roujol S, Benois-Pineau J, de Senneville BD, Ries M, Quesson B, Moonen CT. Robust real-time-constrained estimation of respiratory motion for interventional MRI on mobile organs. *IEEE Trans Inf Technol Biomed* 2012 May;16(3):365-374.
23. Ostergaard Noe K, De Senneville BD, Elstrom UV, Tanderup K, Sorensen TS. Acceleration and validation of optical flow based deformable registration for image-guided radiotherapy. *Acta Oncol* 2008;47(7):1286-1293.
24. Stemkens B, Tijssen RH, de Senneville BD, Lagendijk JJ, van den Berg CA. Image-driven, model-based 3D abdominal motion estimation for MR-guided radiotherapy. *Phys Med Biol* 2016 Jul 21;61(14):5335-5355.
25. Stemkens B, Glitzner M, Kontaxis C, de Senneville BD, Prins FM, Crijns SPM, et al. Effect of intra-fraction motion on the accumulated dose for free-breathing MR-guided stereotactic body radiation therapy of renal-cell carcinoma. *Phys Med Biol* 2017 Sep 1;62(18):7407-7424.
26. Raaymakers BW, Lagendijk JJ, Overweg J, Kok JG, Raaijmakers AJ, Kerkhof EM, et al. Integrating a 1.5 T MRI scanner with a 6 MV accelerator: proof of concept. *Phys Med Biol* 2009 Jun 21;54(12):N229-37.
27. Mutic S, Dempsey JF. The ViewRay system: magnetic resonance-guided and controlled radiotherapy. *Semin Radiat Oncol* 2014 Jul;24(3):196-199.
28. Keall PJ, Barton M, Crozier S, Australian MRI-Linac Program, including contributors from Ingham Institute, Illawarra Cancer Care Centre, Liverpool Hospital, Stanford University, Universities of Newcastle, Queensland, Sydney, Western Sydney, and Wollongong. The Australian magnetic resonance imaging-linac program. *Semin Radiat Oncol* 2014 Jul;24(3):203-206.
29. Fallone BG. The rotating biplanar linac-magnetic resonance imaging system. *Semin Radiat Oncol* 2014 Jul;24(3):200-202.

30. Legendijk JJ, Raaymakers BW, Van den Berg CA, Moerland MA, Philippens ME, van Vulpen M. MR guidance in radiotherapy. *Phys Med Biol* 2014 Nov 7;59(21):R349-69.
31. Wang D, Arlinghaus LR, Yankeelov TE, Yang X, Smith DS. Quantitative Evaluation of Temporal Regularizers in Compressed Sensing Dynamic Contrast Enhanced MRI of the Breast. *Int J Biomed Imaging* 2017;2017:7835749.
32. Harris W, Ren L, Cai J, Zhang Y, Chang Z, Yin FF. A Technique for Generating Volumetric Cine-Magnetic Resonance Imaging. *Int J Radiat Oncol Biol Phys* 2016 Jun 1;95(2):844-853.
33. Lustig M, Donoho D, Santos JM, Pauly JM. Compressed Sensing MRI Technical Report 2006.
34. Fessler JA, Member S, Sutton BP. Nonuniform Fast Fourier Transforms Using Min-Max Interpolation. *IEEE Trans. Signal Process.* 51(2), 560-574.
35. Heerkens HD, Reerink O, Intven MPW, Hiensch RR, van den Berg CAT, Crijns SPM, van Vulpen M, Meijer GJ. Pancreatic tumor motion reduction by use of a custom abdominal corset. *Phys. Imaging Radiot.* 2, 7-10.
36. Block KT, Chandarana H, Milla S, Bruno M, Mulholland T, Fatterpekar G, Hagiwara M, Grimm R, Geppert C, Kiefer B, Sodickson DK. Towards routine clinical use of radial stack-of-stars 3D gradient-echo sequences for reducing motion sensitivity. *J. Korean Soc. Magn. Reson. Med.* 18(2), 87-106.





# **Ablative tReatment of inoperable REnal cell carcinoma using STereotactic body radiotherapy (ARREST-study): study protocol and first clinical experience**

---

Fieke M. Prins  
Maurits M. Barendrecht  
Jan J.W. Lagendijk  
Chris H.J. Terhaard  
Jochem Hes  
Hans J.C.J. de Boer  
Evert-Jan P.A. Vonken  
Linda G.W. Kerkmeijer

## ABSTRACT

*Background.* Stereotactic body radiotherapy (SBRT) for primary renal cell carcinoma (RCC) is considered an alternative non-invasive treatment option compared to the standard treatment of surgery and is increasingly used in the last decade. The ARREST study is a single arm prospective phase II study delivering fiducial marker based cone-beam CT-guided SBRT for inoperable RCC making use of MRI for contouring and pretreatment motion assessment. The study investigates whether this SBRT-approach for RCC is technically and clinically feasible. Furthermore, the ARREST study investigates the value of MRI for response assessment and prediction. The ARREST study is a precursor study for the full MRI-based MRI-linac approach, which will be introduced the upcoming years.

*Patients and methods.* The research population consists of 30 inoperable patients with RCC aged  $\geq 18$  years. Before treatment, fiducial markers were implanted, and a custom made abdominal corset was manufactured to diminish breathing motion. A contrast enhanced 4DCT and 4DMRI were obtained, and were used to define the tumor mid-position, to delineate the gross tumor volume (GTV) and organs at risk (OAR).

Delineation of the GTV and OAR were performed on the 20% phase of the 4DCT (best representative of a midventilation phase), and on the co-registered T2 weighted MRI sequence, T1, DWI and ADC MRI sequences. The SBRT fractionation scheme consists of 35 Gy in 5 fractions in two weeks.

*Preliminary results.* Up till now, two inoperable RCC patients were enrolled in the ARREST study. In both patients three fiducial markers were implanted successfully and without complications. An abdominal corset was tolerated well during the planning scans (4DCT and MRI), and treatment. Both patients successfully completed the treatment of 35 Gy in 5 fractions. The follow-up was 6 and 12 months respectively, in which kidney function, quality of life (QoL) and toxicity scores remained unchanged compared to baseline.

*Conclusion.* Although preliminary, the current SBRT approach for inoperable patients with RCC seems to be feasible and safe for the first two patients. The final results of the ARREST study, safety and feasibility are awaited, as well as toxicity and QoL outcomes and feasibility of the use of MRI for response prediction and evaluation.

*Trial registration.* [www.clinicaltrials.gov](http://www.clinicaltrials.gov) (NCT02853162)

## INTRODUCTION

Kidney cancer accounts for 2-3% of all cancers: 90% of these are renal cell carcinoma's (RCC)(1). The standard treatment of RCC is (partial-) nephrectomy. Alternative, less invasive, treatment options are radiofrequency ablation (RFA), cryoablation (CA), microwave ablation (MWA) and stereotactic body radiotherapy (SBRT), although the last two are less frequently used than RFA and CA. A recent review comparing all these minimal invasive techniques showed promising results for SBRT treatments comparable to other alternative treatment modalities (2).

In the last decade, radiotherapy for RCC has improved dramatically and is increasingly used as an alternative treatment modality for RCC. The use of radiotherapy was historically limited due to the assumed radioresistance of RCC. This assumption of radioresistance dated from treatment with external beam radiotherapy (EBRT) with conventional fractionation schemes, low biological effective doses and large radiation fields. Developments towards image guided SBRT allowed for precise delivery of high dose hypofractionated radiotherapy(3). Recent studies (using adequate radiation doses) showed that RCC is radiosensitive(4,5). The studies were relatively small with a number of patients varying between 16 and 40(2). Incidence rates of grade 1 and 2 toxicities ranging between 30 and 60% were reported, severe toxicity grade 3 or higher 3.8%(6), at a median follow-up of 16-31 months, as well as a local control rate of 63-100%, with a cancer specific survival of 100%(2). SBRT delivers a high biological effective dose in one or a few fractions, with a steep dose fall off from the planned target volume (PTV) to surrounding healthy tissues. The introduction of CT-guided SBRT has allowed for margins to be reduced and a more accurate dose delivery. Despite these improvements, also present-day radiotherapy remains a minimal invasive technique, as in most cases implantation of fiducial markers is required to guide treatment(7-10). Further improvements in image-guided SBRT are expected in the next few years, when a non-invasive (without fiducial markers) MRI-guided radiotherapy will become more widely available for RCC, which allows for even more precise radiotherapy with higher tumor doses and lower doses to the surrounding healthy tissues, aiming to increase local control and decrease toxicity(11). An example of a MRI-guided radiotherapy technique is the MRI-linac, which integrates a linear accelerator and a 1.5T MRI(12). Recently, the first clinical study has been executed in patients with bone metastases at the UMC Utrecht(13). The MRI-linac allows for a high precision radiation technique, with the delivery of a high radiation dosage, in one or more fractions, using online MRI-guided radiotherapy and treatment adaptation (during treatment)(14). The MRI-linac has the potential to offer high precision radiotherapy as a non-invasive treatment option for complex and moving tumor sites, such as the kidney(15). The first technical prototype of the MRI-linac has been developed and installed

at the UMC Utrecht and has been used to develop, evaluate and validate clinical procedures. An international MRI-linac consortium (The Atlantic Consortium) has been formed in order to ensure the clinical introduction of the MRI-linac(16).

As described above, recent studies showed promising results in CBCT-guided SBRT of RCC with or without the use of fiducial markers. However, before changing to a treatment of RCC on the MRI-linac, more experience is required in treating RCC with present-day (CT-guided) SBRT. In the present study a fiducial marker, cone-beam CT based SBRT technique is proposed for inoperable patients with RCC. Therefore, the study investigates whether SBRT for RCC is technically and clinically a feasible treatment option. Additional MRI's were included to prepare for future MRI-guided radiotherapy. Radiological treatment response of the tumor was assessed, and measured according to the RECIST criteria(17), in combination with functional imaging parameters (multiparametric MRI). The additional MR imaging will be used for future response prediction (MRI after 2<sup>nd</sup> fraction), and response evaluation (MRI after 6 and 12 months). The ARREST study is a precursor for the full MRI-based MRI-linac approach which will be introduced the coming years.

## **MATERIAL AND METHODS**

The ARREST study is a single arm prospective phase II study delivering fiducial marker based CBCT-guided SBRT for inoperable patients with RCC. Moreover, this study investigates the value of MRI for treatment planning and response assessment of the cone beam CT-guided SBRT treatment.

### ***Patient population***

The ARREST study is an institutional ethics board approved prospective clinical trial (clinicaltrials.gov ID NCT02853162) conducted at the University Medical Center Utrecht, the Netherlands. All patients participating signed informed consent.

The research population consists of 30 inoperable patients with RCC aged  $\geq 18$  years. Patients were considered inoperable if comorbidities posed an unacceptable increased risk of morbidity and mortality following general anaesthesia in these patients. In case an operable patient refuses surgery, participation in this study was also allowed. Adequate kidney function, based on eGFR and a renogram should allow for intervention. Diagnosis of RCC should be pathologically confirmed.

If patients met one or more of the following exclusion criteria, patients were excluded: evidence of metastatic disease, fulfilling one or more of the exclusion criteria for a contrast enhanced MRI scan, patients with one functioning kidney, prior renal surgery (partial



nephrectomy), prior radiotherapy to the abdomen, patients considered unsafe to have fiducial marker implantation, chemotherapy less than 3 weeks before treatment or targeted therapy (i.e. sunitinib)  $\leq 7$  days before treatment, or a WHO performance status  $> 3$ .

After recruiting a patient, treatment within the ARREST study must be discussed and approved by the multidisciplinary urologic oncology board.

### ***Study objectives***

The main objective was to evaluate the safety and feasibility of CBCT and fiducial marker guided SBRT for RCC. The primary outcome was acute toxicity, according to the Common Terminology Criteria for Adverse Events (CTC-AE) version 4.0. Acute toxicity was defined as toxicity occurring within 90 days after the first radiation treatment. The treatment was considered safe if less than three out of the first five patients experienced a grade  $\geq 3$  toxicity. The treatment is considered successful if for all patients all 5 treatments were completed and  $< 15\%$  of the patients reported a toxicity  $\geq$  grade 3. The feasibility of the technique was determined by an adequate dose planning, dose delivery and fiducial marker placement.

The secondary outcome objectives were radiological tumor response, overall survival, local progression free survival, distant progression free survival, disease specific survival and Quality of life, assessed with the EORTC-QLQ-C30. The radiological response was measured according to the RECIST criteria(17), in combination with functional imaging parameters (multiparametric MRI). The response prediction was evaluated by one contrast enhanced MRI after the second fraction. Response evaluation was investigated by a contrast enhanced MRI 6 and 12 months after treatment. In addition, study patients were followed by routine follow-up by the urologist, including CT and renal function.

### ***Study protocol***

#### ***Before treatment***

After giving informed consent, fiducial markers (Gold Anchor marker, Naslund Medical AB, Stockholm, Sweden: 22G x 7.9"needle, with 0.40 x 20 mm marker) were implanted by an interventional radiologist (ultrasound-guided). In case a pathological diagnosis of RCC has not been obtained before, the radiologist performed a biopsy at the same time as fiducial marker implantation. A renogram and evaluation of kidney function was performed. Patients obtained an individual abdominal corset to diminish inter- and intrafraction motion(18). A planning MRI-scan with gadolinium contrast and a contrast enhanced planning CT-scan were acquired in treatment position. Both scans were obtained 4D to evaluate kidney movement and fiducial marker movements. The CT and MRI scans were used to define the tumor mid-position, to delineate the GTV and OAR (surrounding healthy tissues).

MRI scanning was performed on a 1.5 Tesla Philips Ingenia scanner (Philips, Best, The Netherlands), using a 16-channel anterior and 12-channel posterior coil. An intravenous cannula was placed during the MRI-scan and 0.2mM/kg gadobutrol (Gadovist, Bayer Leverkusen, Germany) was administered to perform a dynamic contrast enhanced scan. Pretreatment (baseline) toxicity was assessed using the CTC-AE version 4.0. Furthermore, prior to treatment quality of life (QoL) was assessed using the EORTC-QLQ-C30 questionnaire. To prevent from nausea during or after treatment, patients started prophylactic anti-emetics (ondansetron 2 x 8 mg) the day before the first radiation treatment up to 5 days after the last SBRT fraction.

### ***Treatment planning and delivery***

The CT and MRI scan were registered based on the position of the fiducial markers. Motion characterization was performed with the corset in place by cine MRI scanning in the sagittal direction (150 sec), with the scan plane positioned through the center of the tumor. Cine-MRI was used to determine the midventilation position by combining the planned dose distribution with the 3D motion trajectory. Tumor tracking was performed with a Minimum Output Sum of Squares Error (MOSSE) adaptive correlation filter(18). This allowed to simulate the motion effect on the dose distribution for the GTV, PTV and OAR before the start of the treatment, in order to determine if the estimated PTV margin of 3 mm was sufficient for the individual patient. Delineation of the GTV and OAR were performed on the 20% phase of the 4DCT, supported by the co-registered T2, T1, DWI (diffusion weighted imaging) and ADC (apparent diffusion coefficient) MRI sequences. The 20% phase was the best representative of a midventilation phase on the 4DCT(19).

The radiotherapy was performed by a linear accelerator (Elekta Synergy, Stockholm, Sweden), using Volumetric Modulated Arc Therapy (VMAT). The 4D CBCT before each treatment fraction was automatically registered to the midventilation phase of the planning CT treatment plan, based on the position of the fiducial markers. If necessary, setup corrections were conducted. After set-up correction a 3D CBCT was made in order to verify the position correction. A third CBCT was performed after dose delivery to monitor the intrafraction motion. Furthermore, after the 2<sup>nd</sup> radiotherapy fraction a contrast enhanced MRI-scan was made for future response prediction purposes.

The SBRT fractionation scheme consists of 5 fractions of 7 Gy prescribed to the PTV every other day, over the course of two weeks. The dose prescription to the tumor and the dose constraints are described in detail in Table 1.

**Table 1.** Dose prescription target and Dose constraints organs at risk (OAR)**GTV\_35 target coverage: V100%  $\geq$  99%, Dmax 150%****PTV\_35 target coverage: V95%  $\geq$  99%, V90%  $\geq$  95%, V110%  $<$  1% (within the PTV minus GTV)**

OAR	Constraint
Lung	V19.5 Gy $<$ 35%
Aorta	Dmax 35 Gy
Heart	Dmax $<$ 38 Gy V32 Gy $<$ 15 cc
Spinal cord	V23 Gy $<$ 0.35 cc V14.5Gy $<$ 1.2 cc
Kidney_ipsilateral	Dmean $<$ 11.3 Gy
Kidney_ipsilateral + Kidney_contralateral	V16.8 Gy $<$ 67%
Ureter	Dmax 42 Gy
Duodenum	Dmax $<$ 32 Gy V18 Gy $<$ 5 cc V12.5 Gy $<$ 10 cc
Small bowel	Dmax $<$ 35 Gy V19.5 Gy $<$ 5 cc
Large bowel	Dmax $<$ 38 Gy V25 $<$ 20 cc
Esophagus	V27.5 Gy $<$ 5 cc V35 Gy $<$ 0.035 cc
Stomach	Dmax $<$ 32 Gy V18 Gy $<$ 10 cc
Liver	700cc $<$ 21 Gy Mean Dose $<$ 18 Gy
Pancreas	Dmax 32 Gy
Spleen	Dmean $<$ 11.5 Gy

Dmax; maximum dose, VXX Gy  $<$  XX%/cc – volume of organ receiving at least XX Gy no more than XX%/cc.

### Follow-up

Follow-up was planned during treatment and at 1, 3, 6 and 12 months after treatment in order to evaluate (early- and late-) toxicity (CTC-AE version 4.0), quality of life (EORTC QLQ-C30 questionnaire) and response compared to baseline. An additional contrast enhanced MRI-scan was planned at 6 months and 12 months after treatment for response evaluation purposes. The treatment scheme and study logistics are described in Figure 1. After a year of follow-up in the ARREST-study, routine follow-up of RCC after intervention was conducted by the urologist, including CT and renal function.

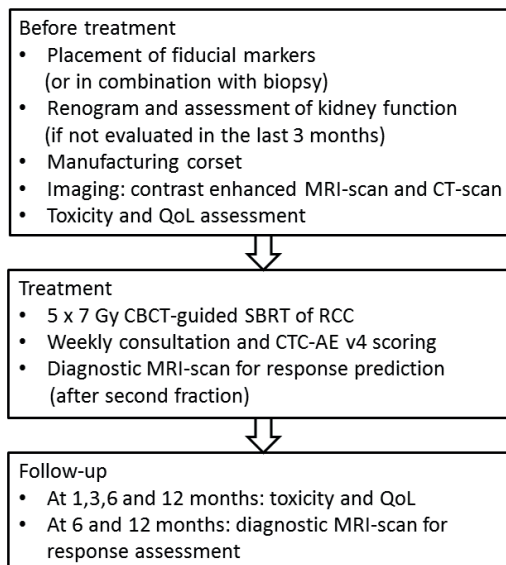


Figure 1. flowchart study procedures.

## RESULTS

In 2017 two inoperable patients with RCC were enrolled in the ARREST study.

### *Case descriptions*

The first patient was a 85 year old male, WHO 1. His medical history included a splenectomy, transient ischaemic attack (TIA), myocardial infarction, percutaneous coronary intervention (PCI), and recently a sigmoid resection (open instead of laparoscopically due to adhesions). Medication included acetylsalicylic acid. The CT-scan showed a growing tumor of 4.4 cm on the upper pole of the left kidney, which was pathologically proven a clearcell RCC, Fuhrman grade I. The patient was considered inoperable based on adhesions resulting from previous surgery; the lesion was considered not suitable for RFA.

The second study patient was a 71 year old male, WHO 1. His medical history included chronic obstructive pulmonary disease (COPD), cerebrovascular accident (complete recovery), and diabetes mellitus type II. Medication included acetylsalicylic acid. CT-scan showed a Bosniak III/IV cyst, 7.6 cm in the upper pole of the right kidney, pathologically proven clearcell/papillary type RCC. The patient was considered inoperable due to poor pulmonary status and the lesion was considered too large for RFA.

### **Feasibility and safety of treatment**

In both patients three fiducial markers were implanted successfully and without complications. Both patients tolerated the abdominal corset well during the planning scans (4DCT and MRI), and treatment.

Both patients successfully completed the treatment of 35 Gy in 5 fractions. In both patients the PTV margin of 3 mm was sufficient, based on the simulation of the motion effect, using the MOSSE adaptive correlation filter. The gold fiducials were clearly visible on the CBCT, and therefore the automatic registration of the 4D CBCT to the midventilation phase was straightforward. Set-up corrections after the first CBCT to verify position correction were minor and could easily be conducted. Mean dose to the GTV was 40.1 and 41.4 Gy respectively, with a maximum dose of 48.6 and 50.8 Gy. The delineation and the dose distribution/ treatment plan of one of the patients is shown in Figure 2.

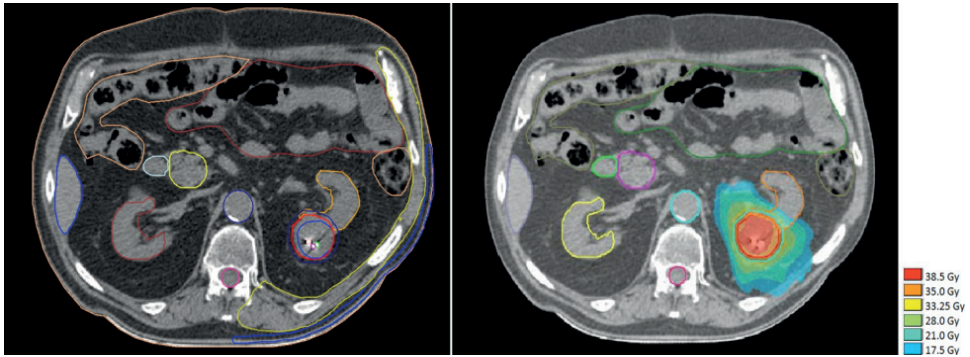


**Figure 2.** delineation(left) and treatment plan(right) of patient 1

### **Clinical outcomes and follow-up after 6 months**

Both patients completed a follow-up of 6 months, the first patient completed a follow-up of 12 months. The kidney function during follow-up remained stable, as well as the Quality of Life (QoL) and toxicity scores. Change in kidney function is visualized in figure 3. Both patients reported a good overall QoL score of 7 (excellent) and 6 (really good). These scores remained stable over time. The CTC score did not change over time. Both patients reported a 1 (mild) in fatigue, and this remained stable during treatment and during the follow-up period.

MRI showed that at baseline, at 6 months (and 12 months) the tumors showed no shrinkage nor growth. A small radiotherapy effect was visible, presenting a necrosis in the central part of both tumors. According to the RECIST criteria, both patients had a stable lesion (no growth nor shrinkage of the tumor), with necrosis in the center of the tumor and no progression in the size of the tumor.

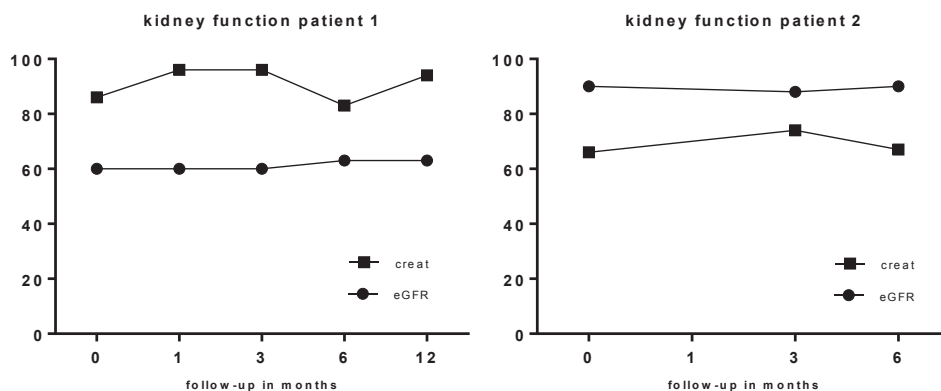


Figure 3. kidney function (creatinine and eGFR) of both patients

## DISCUSSION

The first preliminary results showed that the proposed approach for SBRT of 35 Gy in two inoperable patients with RCC seems to be safe and feasible. A dose of 35 Gy to the PTV was prescribed, however the GTV reached a higher dose of 48.6 and 50.8 Gy (Dmax). Fiducial markers, an abdominal corset and midventilation approach assured good target coverage while sparing the OAR, especially the healthy kidney tissue and duodenum, the most critical OAR.

SBRT is one of the alternative minimal invasive treatment options for RCC, with local control and recurrence free survival rates comparable to the other treatment modalities, with acceptable toxicity(2). Up to now, surgery remains standard of care in primary RCC, and most alternative treatments are reserved for inoperable patients. Previous studies however, showed promising results and suggested a primary treatment of RCC with SBRT in operable patients(5). Most SBRT studies have enrolled a small study population with less than 40 patients, the follow-up is limited to 5-years. And a longer follow-up is required.

Ideally curative treatment of primary RCC would be totally non-invasive and without the use of fiducial markers, which are used in this study and previous studies(7-10). MRI-guided radiotherapy allows for more accurate targeting of radiotherapy rendering fiducial markers obsolete and allowing for smaller margins around the tumor. More accurate targeting will ideally lead to lower toxicity rates, while increasing dose to the tumor and decreasing the number of fractions in future MRI-guided radiotherapy studies.

In the ARREST-study, MRI was used in treatment planning; i.e. in delineation and motion simulation and for response prediction and evaluation. Delineation is still CT-based, although aided by MRI in this CT-based delineation, especially the T2, T1 and DWI sequences. Recommendations allowing for MR-only delineations have been made recently(20).

Besides the role in tumor delineation, cine MRI is also used to accurately detect the intrafraction motion of the tumor, and the determination of the midventilation position. Cine-MRI is adapted especially for RCC in order to precisely follow the respiratory motion over time and therefore a precise estimation of the PTV margin. The PTV margin of 3 mm used in the two described patients is sufficient if compared with other studies(6).

The results of the two RCC patients treated with CBCT guided SBRT are promising and comparable to previously described studies. However, no firm conclusion can be drawn out of these preliminary results of two patients treated, with a limited follow-up. The ARREST study is still open for inclusion and is expected to include a total of 30 patients. This treatment can possibly be applied in all radiotherapy centers in the Netherlands in order to treat more inoperable patients with RCC.

Although preliminary, the current SBRT approach for inoperable patients with RCC seems to be feasible and safe in the first two patients. The final results of the ARREST study will show whether this approach is feasible and safe, and if MRI can be used for response prediction and evaluation.

## REFERENCES

1. Ljungberg B, Bensalah K, Bex A, Canfield S, Dabestani S, Giles RH, et al. Guidelines on Renal Cell Carcinoma. European Association of Urology 2015.
2. Prins FM, Kerkmeijer LGW, Pronk AA, Vonken EPA, Meijer RP, Bex A, et al. Renal cell carcinoma: alternative nephron-sparing treatment options for small renal masses, a systematic review. *J Endourol* 2017 Jul 25.
3. Siva S, Daniels CP, Ellis RJ, Ponsky L, Lo SS. Stereotactic ablative body radiotherapy for primary kidney cancer: what have we learned from prospective trials and what does the future hold? *Future Oncol* 2016 Mar;12(5):601-606.
4. De Meerleer G, Khoo V, Escudier B, Joniau S, Bossi A, Ost P, et al. Radiotherapy for renal-cell carcinoma. *Lancet Oncol* 2014 Apr;15(4):e170-7.
5. Siva S, Kothari G, Muacevic A, Louie AV, Slotman BJ, Teh BS, et al. Radiotherapy for renal cell carcinoma: renaissance of an overlooked approach. *Nat Rev Urol* 2017 Sep;14(9):549-563.
6. Siva S, Ellis RJ, Ponsky L, Teh BS, Mahadevan A, Muacevic A, et al. Consensus statement from the International Radiosurgery Oncology Consortium for Kidney for primary renal cell carcinoma. *Future Oncol* 2016 Mar;12(5):637-645.
7. Sun MR, Brook A, Powell MF, Kaliannan K, Wagner AA, Kaplan ID, et al. Effect of Stereotactic Body Radiotherapy on the Growth Kinetics and Enhancement Pattern of Primary Renal Tumors. *AJR Am J Roentgenol* 2016 Mar;206(3):544-553.
8. Yamamoto T, Kadoya N, Takeda K, Matsushita H, Umezawa R, Sato K, et al. Renal atrophy after stereotactic body radiotherapy for renal cell carcinoma. *Radiat Oncol* 2016 May 26;11(1):72-016-0651-5.
9. Staehler M, Bader M, Schlenker B, Casuscelli J, Karl A, Roosen A, et al. Single fraction radiosurgery for the treatment of renal tumors. *J Urol* 2015 2015/03;193(3):771-775.
10. Ponsky L, Lo SS, Zhang Y, Schluchter M, Liu Y, Patel R, et al. Phase I dose-escalation study of stereotactic body radiotherapy (SBRT) for poor surgical candidates with localized renal cell carcinoma. *Radiother Oncol* 2015 Sep 8.
11. Menard C, van der Heide U. Introduction: Systems for magnetic resonance image guided radiation therapy. *Semin Radiat Oncol* 2014 Jul;24(3):192.
12. Raaymakers BW, Lagendijk JJ, Overweg J, Kok JG, Raaijmakers AJ, Kerkhof EM, et al. Integrating a 1.5 T MRI scanner with a 6 MV accelerator: proof of concept. *Phys Med Biol* 2009 Jun 21;54(12):N229-37.
13. Raaymakers BW, Jurgenliemk-Schulz IM, Bol GH, Glitzner M, Kotte ANTJ, van Asselen B, et al. First patients treated with a 1.5 T MRI-Linac: clinical proof of concept of a high-precision, high-field MRI guided radiotherapy treatment. *Phys Med Biol* 2017 Nov 14;62(23):L41-L50.
14. Crijns SP, Raaymakers BW, Lagendijk JJ. Proof of concept of MRI-guided tracked radiation delivery: tracking one-dimensional motion. *Phys Med Biol* 2012 Dec 7;57(23):7863-7872.
15. Lagendijk JJ, Raaymakers BW, Raaijmakers AJ, Overweg J, Brown KJ, Kerkhof EM, et al. MRI/linac integration. *Radiother Oncol* 2008 Jan;86(1):25-29.



16. Kerkmeijer LG, Fuller CD, Verkooijen HM, Verheij M, Choudhury A, Harrington KJ, et al. The MRI-Linear Accelerator Consortium: Evidence-Based Clinical Introduction of an Innovation in Radiation Oncology Connecting Researchers, Methodology, Data Collection, Quality Assurance, and Technical Development. *Front Oncol* 2016 Oct 13;6:215.
17. Eisenhauer EA, Therasse P, Bogaerts J, Schwartz LH, Sargent D, Ford R, et al. New response evaluation criteria in solid tumours: revised RECIST guideline (version 1.1). *Eur J Cancer* 2009 Jan;45(2):228-247.
18. Heerkens HD, van Vulpen M, van den Berg CA, Tijssen RH, Crijs SP, Molenaar IQ, et al. MRI-based tumor motion characterization and gating schemes for radiation therapy of pancreatic cancer. *Radiother Oncol* 2014 May;111(2):252-257.
19. Wolthaus JW, Sonke JJ, van Herk M, Damen EM. Reconstruction of a time-averaged midposition CT scan for radiotherapy planning of lung cancer patients using deformable registration. *Med Phys* 2008 Sep;35(9):3998-4011.
20. Prins FM, Kerkmeijer LGW, van der Voort van Zyp JRN, Eppinga WSC, Heerkens HD, Lagendijk JJW, et al. Development and evaluation of a MRI based delineation guideline for renal cell carcinoma. Submitted.



## Summary

---



MRI-guided radiotherapy for RCC is a non-invasive state-of-the-art treatment option and will be available on the MRI-linac in the near future. In order to make sure MRI-guided radiotherapy for RCC will be feasible, the present thesis describes various aspects necessary to work towards achieving this goal.

### ***Chapter 2. Renal cell carcinoma: alternative nephron-sparing treatment options for small renal masses, a systematic review***

The standard of care in the treatment of primary RCC is (partial-) nephrectomy. In recent years less invasive alternative treatment options like radiofrequency ablation (RFA), cryoablation (CA), microwave ablation (MWA) and stereotactic body radiotherapy (SBRT) have been used, especially for those patients who are unfit to undergo an invasive treatment. Chapter 2 includes a systematic review describing all of the aforementioned alternative treatment options to be safe and effective, based on phase I and II studies. The adjusted value and advantage of SBRT over the other treatments is that SBRT is not limited to size or location of the tumor, and it is non-invasive (when performed without the use of fiducial markers). Radiotherapy studies using SBRT do have a shorter follow-up and lower patient numbers than RFA and CA, although the number of patients treated is rapidly increasing throughout the last decade. Further improvements in the radiotherapy technique are expected within the next years, when non-invasive MRI-guided radiotherapy will become more widely available.

### ***Chapter 3. Superior target delineation for SBRT of bone metastases from RCC on MRI compared to CT***

A small percentage of primary RCC lesions will develop into metastatic disease. Occasionally metastatic disease is detected during initial presentation. Due to the increasing overall survival in metastatic RCC, there is a need for better local control of the tumor and its metastases. SBRT of RCC bone metastases can be optimized by using MRI for contouring of the metastatic lesion. It seems MRI represents the extent of the gross tumor volume (GTV) in RCC bone metastases more accurately, possibly due to improved visualization of bone marrow infiltration and soft tissue infiltration. Contouring based on CT-only could result in an underestimation of the actual tumor volume, which may cause underdosage of the GTV in SBRT treatment plans. Contouring of RCC bone metastases on MRI results in clinically relevant and statistically significant larger lesions compared to contouring the same lesions on CT.

#### ***Chapter 4. Development and evaluation of a MRI based delineation guideline for renal cell carcinoma***

With the clinical introduction of MRI-guided radiotherapy, the (conebeam)CT-scan is expected to be omitted to plan and guide radiotherapy treatment. For that purpose, a guideline for MRI based delineation was developed in chapter 4. Based on T2 weighted MR imaging, with help of contrast enhanced T1 weighted imaging and diffusion weighted imaging (DWI), a delineation guideline for RCC on MRI was developed and evaluated. The inter-observer delineation variations were small. The recommendations and guideline described in this study can be used for the introduction of MRI-guided radiotherapy for primary RCC in the clinic.

#### ***Chapter 5. Intrafraction motion management of RCC with MRI-guided SBRT***

One of the major challenges in SBRT of RCC is motion of the kidney during treatment, especially breathing motion, which is complex and changes over time at an individual level. In this chapter we focus on the intrafraction motion occurring during treatment time. To deliver MRI-guided radiotherapy for RCC it is necessary to simulate the motion and drift of the kidney over a time period as long as a treatment fraction takes, in order to realistically simulate what happens during treatment. The intrafraction motion is required to determine (and if possible reduce) the planned target volume (PTV) margin. The contributions of both high amplitude respiratory motion and slow drifts led to establish a realistic determination of the PTV margin required. The present results show that with the motion management techniques used, drift compensation (tumor trailing) would be able to reduce the motion margin by up to 75%. This makes tumor trailing an interesting option to consider in future treatment of primary RCC with MRI-guided radiotherapy.

#### ***Chapter 6. Dual-purpose MRI acquisition to combine 4D-MRI and dynamic contrast enhanced (DCE) imaging for abdominal SBRT planning***

In general, SBRT treatments benefit from accurate imaging for precise contouring, localization and image guidance of the tumors and organs at risk (OARs) before and during treatment. In addition to a CT scan, anatomical (T1, T2) and functional (for example DCE, DWI) MRI sequences, can provide supplementary value to delineate the tumor. DCE-MRI is used to enhance contrast between tumor, healthy kidney and other OARs. Furthermore it is used to characterize tumor specific contrast agent uptake values and quantify perfusion parameters. 4D-MRI, on the other hand, can be used to calculate the mid-position of the tumor. Unfortunately, both DCE-MRI and 4D-MRI are lengthy acquisitions. The present study demonstrates a dual-purpose MRI acquisition that combines DCE and 4D-MRI to generate high-spatio-temporal DCE volumes for contrast enhancement characterization and tumor delineation, and characterize motion precisely using an additional 4D-MRI reconstruction.

With this combination, a separate 4D-MRI is not necessary, while patient comfort and reproducibility for the DCE acquisition is increased, since no breath holds are required. An additional 5D reconstruction proved mainly useful for minimization of respiratory-induced blurring for a sharper tumor edge. The combination of three different reconstructions is unique and valuable in the context of MR-guided radiotherapy, for tumor characterization, accurate delineation, and mid-position volume generation.

***Chapter 7. Ablative tReatment of inoperable REnal cell carcinoma using STereotactic body radiotherapy (ARREST-study): study protocol and first clinical experience***

Before we can safely treat patients with RCC on the MRI-linac, we first need to gain more experience in treating RCC with SBRT and prepare for the integration of MRI in the treatment workflow of RCC. In the ARREST-study protocol, a fiducial marker cone-beam CT based SBRT treatment is described for inoperable patients with RCC. The ARREST study is a phase II safety and feasibility study. In addition to previous studies on SBRT for RCC, an abdominal corset to diminish motion will be used, as well as a mid-ventilation based PTV margin calculation, MRI-based motion characterization, MRI- (and CT-)based tumor delineation. Based on the ARREST study results, MRI-based response prediction and evaluation will be developed. The study protocol and first clinical results are described in chapter 7. Up till now, two patients have completed treatment, and the study is open for inclusion. The ARREST-study is a precursor study for the full MRI-based approach for SBRT of RCC, which will be introduced within the coming years on the MRI-linac.





## **General discussion and future perspectives**

---



The present thesis focuses on the preparation of MRI-guided radiotherapy of renal cell carcinoma (RCC). Surgery is the current standard treatment for RCC. Other alternative treatment modalities such as radiofrequency ablation (RFA), cryoablation (CA), microwave ablation (MWA) and stereotactic body radiotherapy (SBRT) with use of fiducial markers are minimally/less invasive. A non-invasive treatment modality is desirable. Current CBCT-guided stereotactic body radiotherapy (SBRT) has good outcome in terms of local control and limited toxicity, but can be further improved by online MRI-guidance of the treatment instead of using CT. The chapters of the thesis describe the different steps necessary to prepare for MRI-guided radiotherapy for RCC. Remaining obstacles to overcome will be described, as well as a perspective on the future of MRI-guided radiotherapy of RCC.

## **IMAGE-GUIDED SBRT: AN EMERGING TREATMENT MODALITY FOR RCC**

The first treatments of RCC were conducted with external beam radiotherapy (EBRT), with conventional fractionation schemes, low biological effective doses and large radiation fields. The disappointing results led to an assumed radioresistance of RCC, which partly explains the former limited role. Nonetheless, over the past decade, radiotherapy has emerged in the treatment of RCC. In primary RCC the transition has been made towards SBRT, including a steep dose fall off from the planned target volume (PTV) to surrounding tissues and a precise delivery of hypofractionated radiotherapy(1). Recent studies using these adequate radiation doses showed that RCC is radiosensitive(2-4). As a result various studies for primary RCC have been conducted, and in several clinics the treatment is implemented as standard of care for inoperable patients(2).

**Chapter 2** describes the modalities of alternative minimal invasive treatment options in the last decade, including SBRT(5). The SBRT studies are all cone beam computed tomography(CBCT)-guided using different devices and different dosages for treatment. Despite the different approaches used, these studies showed an increased use of SBRT in RCC over time. Although the dosage varied largely between the different institutes, the toxicities resulting from SBRT treatment remained acceptable. Limited toxicities between 30-60% have been reported, in which fatigue was the most commonly reported symptom, followed by dermatitis, chest wall pain, and nausea. Severe toxicities were reported in less than 5% of patients. Local control rates vary between 85 - 100%, with a follow-up of up to 5-years, and a cancer specific survival of 100%(5). Last year the phase II study of Siva et al. was presented with similar results(6).

RFA and CA are treatment modalities more commonly used than SBRT for RCC, although the treatment results are comparable for recurrence free survival and cancer specific survival. However, there are a few distinct benefits of SBRT compared to the other minimally invasive techniques. First of all SBRT is not limited to a maximum tumor size, enabling

a larger group of patients to be treated in a non-invasive manner. Secondly, if no gold-fiducials are used SBRT is completely non-invasive, increasing comfort for the patient and reducing the change of possible complications. Most of all, SBRT seems to be a comparable technique to RFA and CA, with minimal severe toxicity, and might (when further improving the technique) become a better treatment option in the future.

The findings in the summary of **chapter 2** are confirmed by a recently published extensive overview of primary treatment of RCC with SBRT(3), and a consensus statement of a worldwide RCC consortium(IROCK)(2). Both groups conclude that SBRT is an emerging treatment modality for patients with inoperable primary RCC. The IROCK-group also suggests to prospectively compare RFA/CA with SBRT in the inoperable setting. These recommendations are all based on research in CT-guided radiotherapy. However, MRI-guided radiotherapy of RCC is believed to enhance the results for patients even further. Potential benefits are improved visibility of the tumor, real time tracking, reducing the margins and therefore establishing lower toxicity, delivering higher dosages in less fractions (possibly a single fraction). MRI-guided radiotherapy could be a totally non-invasive alternative for RCC patients. The future perspective is that in 5-10 years the SBRT treatment approach (CT and/or MRI based) will be the standard of care for inoperable primary RCC.

## **TECHNICAL DEVELOPMENTS TOWARDS MRI-GUIDED SBRT FOR RCC**

A major topic of the present thesis is the use of MRI for radiotherapy, especially the improvement of the different sequences to be used for MRI-guided radiotherapy for RCC. The optimization includes development of a dedicated T1 and T2 weighted and functional MR imaging.

### ***Motion management***

One of the major challenges of SBRT of RCC is motion of the kidney during treatment. Breathing motion is complex and may change over time at an individual level. In order to ensure that the tumor receives an adequate dose, while sparing the surrounding tissues as much as possible, different planned target volume (PTV) margins, margin recipes and immobilization techniques have been applied in different centers. Motion management is conducted differently over centers worldwide. In order to reduce the motion various immobilization devices are used, like abdominal compression(7), or vacuum immobilization(8). To improve visualization of the tumor motion before or during treatment, in some institutions gold fiducials are inserted in the tumor(7,9,10). Image guidance of kidney tumors when using online 3D CBCT-techniques can be challenging without the use of fiducial markers or contrast agents(11). For example, when using a Cyberknife approach, the motion of the tumor can be tracked, but fiducial markers remain necessary.

Interfraction motion management is usually 4DCT-guided and an internal target volume (ITV) principle is used to define the tumor throughout the different breathing phases (2). A mid-ventilation approach is also possible, although not widely used in the treatment of RCC (12). A few studies report respiratory motion management of the kidney based on cine-MRI images, instead of the widely used 4DCT guided approach (13,14). Stam et al. observed the largest movement of the kidney in free breathing in the cranio-caudal direction (14). Kidney movement in the left-right (LR) and anterior-posterior (AP) direction was smaller. Besides respiratory movement, motion drift is another problem that should be taken into account. As seen in preliminary work, some patients show drift which could have a significant impact on dose coverage (15,16).

### ***Determination of the PTV margin***

There is a large variation in the PTV margin used in CT-guided SBRT. The PTV margin of RCC varied between 1 and 10 mm (with PTV coverage goals of 95-100%) amongst the different centers. The center using a Cyberknife (Accuray Inc. Sunnyvale, CA) approach used a PTV margin of 0 mm (2). Although a topic of interest, so far the rationale behind the difference in PTV margins used is unknown.

In this thesis further developments have been made to the rationale behind the PTV margin. Firstly, in **chapter 5**, the motion characterization with cine-MRI and gated 3D spoiled gradient echo (SPGR) acquisitions were shown, in order to determine the high amplitude breathing motion as well as the drift of the tumor. In this study the imaging has been done within the expected actual treatment times, which ensured that the simulation of motion was representative for future treatment of MRI-guided radiotherapy of RCC. Secondly, based on calculations made on respiratory motion (amplitude) and motion drift (trailing) it is possible to reduce the motion margin by up to 75% (6.1 to 1.5 mm, assuming perfect tumor trailing). When all motion management techniques are used to correct for the amplitude and drift (including tracking) it may even be possible to set a future PTV margin at 0 mm. Nevertheless, tracking on MRI-guided radiotherapy devices is not possible yet. However, the clinical introduction of the MRI-linac for RCC could be accelerated when trailing is used, since trailing contributes to the largest difference in PTV margin.

The calculations made in **chapter 5** raised the question if one can determine a PTV margin from only the motion characterization. The PTV margin is often used as a margin to determine that the prescribed dose is actually delivered to the GTV. It should take into account all the uncertainties in planning, patient positioning and beam positioning (17).

In order to go towards a fully non-invasive approach, taking into account the respiratory motion and drift, an MRI-guided approach would be desirable in order to bring the PTV margin close to 0 mm.

### ***Improvement of radiotherapy technique***

**Chapter 6** shows the improvements in 4D-MRI and dynamic contrast enhanced (DCE) imaging. A shift from breath-hold towards free-breathing has been made for DCE imaging, as well as simultaneously acquiring a 4D-MRI and increasing the reproducibility of the DCE scan. The combination of these scans could result in a shorter acquisition time and more accurate images in the planning phase when used for the MRI-linac. A fast 4D-MRI is necessary in order to improve a midposition approach for the treatment.

In the end we want to move towards tracking the tumor, but improvement of the 4DMRI is a necessary step to achieve this. A consensus has not yet been reached if a gating or tracking approach (reducing the PTV margin to 0) would be desirable in the future.

To achieve a fully non-invasive treatment, and still have a comparable or increased dose without extra toxicity to the OAR, the current SBRT treatment of RCC needs to switch to a MRI-only approach. Currently, various MRI-guided radiotherapy systems are available or in development throughout the world. The main differences between these systems are in field strength of the MRI (between 0.35 and 1.5 Tesla), and in the radiation source used (7 MV linac and Co-60)(18), although recently all manufacturers transferred to a 6 or 7 MV linac radiation source. MRI-guided tracking or gating would be necessary to precisely treat the GTV with a high dose, without any PTV margin, and with a lower toxicity. Results of MRI-guided SBRT for primary RCC have not been published to this date.

## **CLINICAL DEVELOPMENTS TOWARDS MRI-GUIDED SBRT FOR RCC**

Besides technical improvements, clinical developments have also been described in the present thesis. Developments in MRI-based contouring and first clinical experience in SBRT of RCC in the UMC Utrecht will be discussed below.

### ***Delineation***

The introduction of MRI-guided radiotherapy allows and requires MRI-based tumor and OAR delineation. As MRI has the benefit of improved soft tissue imaging compared to CT, MRI may have the advantage of better visualization of the extent of primary RCC and RCC (bone) metastases. Adequate contouring for RCC and metastases of RCC is crucial for optimal targeting of the tumor for radiotherapy. However, the MRI sequences used for RCC and metastatic RCC (mRCC) are currently only used in a diagnostic setting and have not been optimized for radiotherapy purposes.

A review by experts in diagnostic imaging of RCC suggests the use of T2 weighted imaging, as a feasible alternative to CT imaging of RCC(19). Recent evidence also shows that MRI might be better to differentiate between renal lesions, which remained inconclusive at first on CT imaging, leading to further utility of renal MRI(20). Diffusion-weighted and perfusion-weighted imaging are also more often used to diagnose renal tumors(21).

Sequence optimization for radiotherapy has been performed before for other abdominal tumor sites(22,23). In pancreas for example, MRI sequences have been optimized and a contrast enhanced T1 weighted MRI based delineation guideline has been developed(22). On healthy subjects abdominal organs at risk (OAR) have been delineated on T2 weighted imaging(23). **Chapter 3** and **chapter 4** describe the optimized MRI sequences used for mRCC and RCC, suitable for delineation and radiotherapy treatment purposes. **Chapter 3** shows a clinically relevant and statistically significant superior target delineation of MRI compared to CT of mRCC. In **chapter 4**, a MRI-only delineation guideline is developed for primary RCC. In contrast to contouring of mRCC bone metastases (performed on T1 weighted TSE), the suggested contouring in primary RCC should be performed on T2 images, aided by T1 and diffusion weighted imaging (DWI) sequences.

In mRCC delineation as well as in primary RCC delineation optimized sequences have been developed. However, it is still debatable whether the target volume delineated on MRI represents the actual target volume. No pathological validation of MRI target volumes has been performed, either in local studies or reported in the literature, as it is not considered to be practically achievable.

### ***The ARREST study***

In **chapter 7** the study protocol and preliminary results of an ongoing single arm prospective phase II trial (ARREST study) have been shown. The ARREST study is specifically designed for inoperable patients or patients refusing surgery. The SBRT treatment is delivered using fiducial markers and an abdominal corset. Furthermore, for the first time for RCC SBRT a mid-ventilation approach was used to ensure good target coverage while sparing the OAR(12). In the ARREST-study, additional MRIs were performed in order to develop a MRI-only approach. MRI was used in delineation and motion simulation. The multiparametric MRI (mpMRI) was also used for response assessment and for response monitoring.

Upon completion, the ARREST study will provide more information on survival, assessment of the toxicity and quality of life (QoL). These results are expected to be in line with the findings of completed primary RCC SBRT studies, as described in **chapter 2** and a recent review of Siva et al.(3). One question remains unresolved in the SBRT trials performed; Do the histological variants of RCC respond differently to radiotherapy? The most common subtype is clearcell RCC, followed by papillary (type I and II) and a chromophobe subtype.

It would be interesting to determine whether the different subtypes respond differently to radiotherapy. If this is the case, adjusting radiotherapy treatment schemes to pathological subtype may be beneficial in future studies in order to enhance tumor response(3).

## **FUTURE PERSPECTIVES**

Before SBRT can be implemented as routine clinical care for operable RCC patients, more patients and longer follow-up will be necessary(24). Improvements in image guided radiotherapy for RCC are expected in the next few years, when instead of CT-guided SBRT, a non-invasive (without fiducial markers) MRI-guided radiotherapy will become more widely available. This will allow for even more accurately targeted radiotherapy facilitating higher tumor doses, and lower doses to the surrounding healthy tissues(18).

### ***How can an improved radiotherapy technique lead to improved outcome for RCC patients?***

In **chapter 3, 4, 5** and **6** improvements in imaging for delineation, margins and motion purposes have been shown. With all these improvements it is possible to deliver the radiotherapy dose more accurately and thus with smaller margins. A suggestion for future research is to validate the sequences with pathological validation, in order to determine the real tumor in vivo and on MR imaging, although it is questionable whether this would be practically achievable.

The most important change will be the transition from a midposition acquisition to a treatment in which the tumor will be fully tracked. By tracking the tumor the margins can be reduced even further, possibly to no margins at all. More accurate targeting of the tumor could eventually result in a higher dose to the GTV and reduced toxicity to the surrounding OAR. With a higher dose given to the tumor, future treatment may lead to better local control and probably better survival in RCC patients.

Another advantage of MRI-guided radiotherapy of RCC is the possibility to treat in one fraction, although the potential superiority of a one-fraction approach above for instance five fractions (like the ARREST study protocol) should first be studied. The potential benefit of a one fraction (non-invasive and within one hour) treatment will be minimizing the burden to the patient. It will be important to precisely establish the position of the tumor during treatment, to prevent underdosing the GTV and overdosing the OAR, leading to toxicity. Current motion management seems at an acceptable level, however it is not clear yet which specific moments in treatment are the most adequate to track, as well as the specific timeframe of this tracking. If the tracking problem is solved it is technically possible to switch safely towards a one fraction treatment, also for larger tumors.



In summary, an improved radiotherapy technique could lead to improved outcomes for RCC patients. A one-day outpatient treatment could reduce the number of hospital visits, as well as improving local control and minimizing toxicity. This will plausibly have a positive effect on the QoL in RCC patients.

***Could functional imaging play a role in assessment of radiotherapy response?***

In the ARREST-study, MRI-scanning is incorporated in the treatment protocol. MpMRI is used for delineation, motion assessment, response prediction and evaluation. The scan on the day of the second fraction aims to visualize changes in the mpMRI, which might correspond with an improved outcome. It will be possible to adjust the dose in later fractions based on changes measured on mpMRI. If the outcome can be predicted with the mpMRI at the second fraction this might influence the dose prescription, with higher doses for non-responders after two fractions. With the aid of functional imaging, like DCE and DWI, the response might be predicted already during treatment, although these results will not be available until the ARREST study has been finished. Response prediction is for example previously successfully conducted in radiotherapy of rectal and esophageal tumors(25-28). Current follow-up after radiotherapy of RCC is CT-based according to the RECIST criteria(29). Future follow-up may be MRI-based. As a precursor for this future assessment, in the ARREST study the follow-up after treatment is performed with mpMRI (in addition to routine follow-up by CT). The main goal of follow-up is to visualize the response of the tumor after treatment and to detect residual/recurrent tumor tissue. Up to a year after radiotherapy it can be difficult to distinguish between residual tumor or radiotherapy effect when a lesion still shows contrast differences, as the response of kidney tumors to radiotherapy occurs relatively late, similar to prostate cancer.

Nowadays, the RECIST criteria are used for the clinical evaluation of the radiotherapy response. The RECIST criteria do not specify whether there is residual tumor or effect of radiotherapy treatment. Within the RECIST criteria, an increase in volume of 20% is considered as disease progression. RCC are known to grow slowly over time(9), and when a tumor progresses, it might take years before the 20% cutoff point will be reached. Within the RECIST working group the question has also been raised whether there should be a shift from volumetric to functional assessment, for example by mpMRI(29). In the present thesis, in **chapter 4, 5 and 6**, multiple improvements in functional imaging for RCC have been shown. As described earlier, further developments are necessary to increase our knowledge and validate the different functional imaging parameters in the follow-up of RCC after radiotherapy treatment. In other tumor sites, FDG-PET-CT imaging is also developed thoroughly in order to monitor treatment response. However, RCC is not clearly visible on PET-CT, especially the most common RCC subtype, clearcell carcinoma(19).

Other options for functional imaging are the use of PSMA-PET-CT to detect recurrent RCC(30). PSMA uptake is more intense than FDG-PET in RCC. Recently a study has been conducted for PSMA-PET imaging for metastatic RCC, in which RCC was more visible. Moreover, the PSMA-PET has the ability to detect more metastases than FDG-PET or CT imaging(30). Thus besides mpMRI, in the future PSMA-PET may also play a role in the distinction between residual/recurrent RCC or radiotherapy effect.

In order to validate all thoroughly developed functional imaging sequences, a pathological validation of MRI and PSMA-PET should be considered in future research.

### ***Shared decision making***

Currently, SBRT for primary RCC is most suitable for fragile, inoperable, mostly elderly patients as is described in **chapter 2 and 7**. It is an equally important treatment option as RFA, CA and MWA, as is described in **chapter 2**. The expectation is, within the next few years, SBRT for primary RCC will also be considered as a treatment option for operable RCC patients, as it is expected to have a comparable cancer specific survival and limited toxicity. However, SBRT of RCC still has to be proven at least equally good to surgery with comparable or less toxicity to make this treatment option available for all patients. Nonetheless, shared decision making between patient and the different professions involved is paramount, as recently advised for prostate cancer patients(31). For localized prostate cancer, radiotherapy, surgery and active surveillance are options with comparable prostate cancer specific mortality rates over 10 years(32). The difference between the treatment modalities is not in oncological outcome but in side-effects. In the treatment of localized prostate cancer, patients and physicians decide together whether surgery or radiotherapy will be the treatment of choice. This approach should also be conducted in the treatment of primary RCC.

Moreover, to successfully implement SBRT of RCC treatment, it will be essential to have a multidisciplinary approach. Physicians in the fields of Urology, Radiotherapy and Radiology should work efficiently together to determine the best treatment option for each individual patient. Ideally RCC care would be implemented in a combined Urology-Radiotherapy outpatient department. A combined consultation assures the most extensive patient information and could prevent patients getting inaccurate ideas about the different treatment options, as noted in a recent study on prostate cancer(33). Implementing this treatment for primary RCC within a multidisciplinary framework could lead to a general improvement in shared decision making and care of RCC patients.

## CONCLUSION

We can now conclude that SBRT of primary RCC is an upcoming treatment modality and the results are comparable to other minimally invasive alternative treatment options like RFA and CA. Image guided SBRT can be further improved by the implementation of MRI-guided SBRT (for example with the MRI-linac), leading to a fully non-invasive curative treatment option, with minimal burden to the patient.

MRI-guided SBRT for RCC will be more widely available in the coming years, delivering higher radiation doses (in less fractions) to increase local control, diminishing toxicity and improving the QoL for patients. To successfully implement SBRT in primary RCC treatment, inevitably a multidisciplinary approach will be required. Physicians in the field of Urology, Radiotherapy and Radiology should collaborate with each other and with the patient to determine the best treatment option.

## REFERENCES

1. Siva S, Daniels CP, Ellis RJ, Ponsky L, Lo SS. Stereotactic ablative body radiotherapy for primary kidney cancer: what have we learned from prospective trials and what does the future hold? *Future Oncol* 2016 Mar;12(5):601-606.
2. Siva S, Ellis RJ, Ponsky L, Teh BS, Mahadevan A, Muacevic A, et al. Consensus statement from the International Radiosurgery Oncology Consortium for Kidney for primary renal cell carcinoma. *Future Oncol* 2016 Mar;12(5):637-645.
3. Siva S, Kothari G, Muacevic A, Louie AV, Slotman BJ, Teh BS, et al. Radiotherapy for renal cell carcinoma: renaissance of an overlooked approach. *Nat Rev Urol* 2017 Sep;14(9):549-563.
4. De Meerleer G, Khoo V, Escudier B, Joniau S, Bossi A, Ost P, et al. Radiotherapy for renal-cell carcinoma. *Lancet Oncol* 2014 Apr;15(4):e170-7.
5. Prins FM, Kerkmeijer LGW, Pronk AA, Vonken EPA, Meijer RP, Bex A, et al. Renal cell carcinoma: alternative nephron-sparing treatment options for small renal masses, a systematic review. *J Endourol* 2017 Jul 25.
6. Siva S, Pham D, Kron T, Bressel M, Lam J, Tan TH, et al. Stereotactic ablative body radiotherapy for inoperable primary kidney cancer: a prospective clinical trial. *BJU Int* 2017 Nov;120(5):623-630.
7. Yamamoto T, Kadoya N, Takeda K, Matsushita H, Umezawa R, Sato K, et al. Renal atrophy after stereotactic body radiotherapy for renal cell carcinoma. *Radiat Oncol* 2016 May 26;11(1):72-016-0651-5.
8. Chang JH, Cheung P, Erler D, Sonier M, Korol R, Chu W. Stereotactic Ablative Body Radiotherapy for Primary Renal Cell Carcinoma in Non-surgical Candidates: Initial Clinical Experience. *Clin Oncol (R Coll Radiol)* 2016 Apr 27.
9. Sun MR, Brook A, Powell MF, Kaliannan K, Wagner AA, Kaplan ID, et al. Effect of Stereotactic Body Radiotherapy on the Growth Kinetics and Enhancement Pattern of Primary Renal Tumors. *AJR Am J Roentgenol* 2016 Mar;206(3):544-553.
10. Staehler M, Bader M, Schlenker B, Casuscelli J, Karl A, Roosen A, et al. Single fraction radiosurgery for the treatment of renal tumors. *J Urol* 2015 2015/03;193(3):771-775.
11. Siva S, Pham D, Gill S, Bressel M, Dang K, Devereux T, et al. An analysis of respiratory induced kidney motion on four-dimensional computed tomography and its implications for stereotactic kidney radiotherapy. *Radiat Oncol* 2013 Oct 26;8:248-717X-8-248.
12. Wolthaus JW, Schneider C, Sonke JJ, van Herk M, Belderbos JS, Rossi MM, et al. Mid-ventilation CT scan construction from four-dimensional respiration-correlated CT scans for radiotherapy planning of lung cancer patients. *Int J Radiat Oncol Biol Phys* 2006 Aug 1;65(5):1560-1571.
13. Bjerre T, Crijns S, af Rosenschold PM, Aznar M, Specht L, Larsen R, et al. Three-dimensional MRI-linac intra-fraction guidance using multiple orthogonal cine-MRI planes. *Phys Med Biol* 2013 Jul 21;58(14):4943-4950.
14. Stam MK, van Vulpen M, Barendrecht MM, Zonnenberg BA, Intven M, Crijns SP, et al. Kidney motion during free breathing and breath hold for MR-guided radiotherapy. *Phys Med Biol* 2013 Apr 7;58(7):2235-2245.

15. Stemkens B, Tijssen RH, de Senneville BD, Lagendijk JJ, van den Berg CA. Image-driven, model-based 3D abdominal motion estimation for MR-guided radiotherapy. *Phys Med Biol* 2016 Jul 21;61(14):5335-5355.
16. Glitzner M, Crijns SP, de Senneville BD, Kontaxis C, Prins FM, Lagendijk JJ, et al. On-line MR imaging for dose validation of abdominal radiotherapy. *Phys Med Biol* 2015 Nov 21;60(22):8869-8883.
17. Burnet NG, Thomas SJ, Burton KE, Jefferies SJ. Defining the tumour and target volumes for radiotherapy. *Cancer Imaging* 2004 Oct 21;4(2):153-161.
18. Menard C, van der Heide U. Introduction: Systems for magnetic resonance image guided radiation therapy. *Semin Radiat Oncol* 2014 Jul;24(3):192.
19. Sankineni S, Brown A, Cieciera M, Choyke PL, Turkbey B. Imaging of renal cell carcinoma. *Urol Oncol* 2016 Mar;34(3):147-155.
20. Willatt JM, Hussain HK, Chong S, Kappil M, Azar SF, Liu PS, et al. MR imaging in the characterization of small renal masses. *Abdom Imaging* 2014 Aug;39(4):761-769.
21. Capitanio U, Montorsi F. Renal cancer. *Lancet* 2016 Feb 27;387(10021):894-906.
22. Heerkens HD, Hall WA, Li XA, Knechtges P, Dalah E, Paulson ES, et al. Recommendations for MRI-based contouring of gross tumor volume and organs at risk for radiation therapy of pancreatic cancer. *Pract Radiat Oncol* 2017 Mar - Apr;7(2):126-136.
23. Noel CE, Zhu F, Lee AY, Yanke H, Parikh PJ. Segmentation precision of abdominal anatomy for MRI-based radiotherapy. *Med Dosim* 2014 Autumn;39(3):212-217.
24. Pryor DI, Wood S. Stereotactic radiotherapy for primary renal cell carcinoma: time for larger-scale prospective studies. *BJU Int* 2017 Nov;120(5):603-604.
25. Habr-Gama A, Perez RO, Nadalin W, Sabbaga J, Ribeiro U Jr, Silva e Sousa AH Jr, et al. Operative versus nonoperative treatment for stage 0 distal rectal cancer following chemoradiation therapy: long-term results. *Ann Surg* 2004 Oct;240(4):711-7; discussion 717-8.
26. Maas M, Beets-Tan RG, Lambregts DM, Lammering G, Nelemans PJ, Engelen SM, et al. Wait-and-see policy for clinical complete responders after chemoradiation for rectal cancer. *J Clin Oncol* 2011 Dec 10;29(35):4633-4640.
27. van Rossum PS, van Lier AL, van Vulpen M, Reerink O, Lagendijk JJ, Lin SH, et al. Diffusion-weighted magnetic resonance imaging for the prediction of pathologic response to neoadjuvant chemoradiotherapy in esophageal cancer. *Radiother Oncol* 2015 May;115(2):163-170.
28. Heethuis SE, van Rossum PS, Lips IM, Goense L, Voncken FE, Reerink O, et al. Dynamic contrast-enhanced MRI for treatment response assessment in patients with oesophageal cancer receiving neoadjuvant chemoradiotherapy. *Radiother Oncol* 2016 Jul;120(1):128-135.
29. Eisenhauer EA, Therasse P, Bogaerts J, Schwartz LH, Sargent D, Ford R, et al. New response evaluation criteria in solid tumours: revised RECIST guideline (version 1.1). *Eur J Cancer* 2009 Jan;45(2):228-247.
30. Siva S, Callahan J, Pryor D, Martin J, Lawrentschuk N, Hofman MS. Utility of 68 Ga prostate specific membrane antigen - positron emission tomography in diagnosis and response assessment of recurrent renal cell carcinoma. *J Med Imaging Radiat Oncol* 2017 Jun;61(3):372-378.

31. Mottet N, Bellmunt J, Bolla M, Briers E, Cumberbatch MG, De Santis M, et al. EAU-ESTRO-SIOG Guidelines on Prostate Cancer. Part 1: Screening, Diagnosis, and Local Treatment with Curative Intent. *Eur Urol* 2017 Apr;71(4):618-629.
32. Hamdy FC, Donovan JL, Lane JA, Mason M, Metcalfe C, Holding P, et al. 10-Year Outcomes after Monitoring, Surgery, or Radiotherapy for Localized Prostate Cancer. *N Engl J Med* 2016 Oct 13;375(15):1415-1424.
33. van Stam MA, van der Poel HG, van der Voort van Zyp, J.R.N., Tillier CN, Horenblas S, Aaronson NK, et al. The accuracy of patients' perceptions of the risks associated with localised prostate cancer treatments. *BJU Int* 2017 Sep 28.







## Addenda

---

Samenvatting

Review committee

List of publications

Dankwoord

Curriculum Vitae



## SAMENVATTING

MRI-gestuurde radiotherapie voor nierceltumoren (RCC) is een niet-invasieve innovatieve behandeloptie en zal beschikbaar zijn op de MRI-linac in de nabije toekomst. Het huidige proefschrift beschrijft verschillende stappen die nodig zijn om MRI-linac radiotherapie voor RCC voor te bereiden.

### ***Hoofdstuk 2. Nierceltumoren: alternatieve nefron-sparende behandelopties voor small renal masses, een systematische review***

De standaard zorg voor de behandeling van primaire RCC is (partiële-) nefrectomie. In de afgelopen jaren zijn minder invasieve behandelingen zoals radiofrequency ablation (RFA), cryoablation (CA), microwave ablation (MWA) en stereotactic body radiotherapy (SBRT) gebruikt, met name voor die patiënten die niet geschikt zijn om een invasieve behandeling te ondergaan. In hoofdstuk 2 wordt in een systematische review beschreven dat alle bovenstaande alternatieve behandelmethoden veilig en effectief zijn, gebaseerd op fase I en fase II studies. De toegevoegde waarde en het voordeel van SBRT boven de andere behandelingen, is dat SBRT grootte en locatie van de tumor niet als beperking heeft, en dat het niet invasief is (wanneer een methode zonder fiducial markers wordt gebruikt). Radiotherapie studies met SBRT hebben een kortere follow-up en een lager patiënten aantal dan studies met RFA en CA, hoewel het aantal patiënten dat behandeld wordt het laatste decennium snel toeneemt. Verdere verbeteringen in de radiotherapie techniek wordt verwacht in de komende jaren, wanneer MRI-gestuurde radiotherapie meer beschikbaar wordt.

### ***Hoofdstuk 3. Verbeterde intekening van RCC botmetastasen op MRI in vergelijking met CT voor stereotactische radiotherapie (SBRT)***

Een klein deel van de primaire RCC laesies zal zich ontwikkelen tot gemetastaseerde ziekte. In sommige gevallen wordt gemetastaseerde ziekte ontdekt bij primaire presentatie. Door de toenemende overleving bij gemetastaseerde RCC is betere lokale controle van de primaire tumor en afstandsmetastasen nodig. SBRT voor RCC botmetastasen kan geoptimaliseerd worden door gebruik te maken van MRI voor het intekenen van de botmetastase. Het lijkt erop dat MRI de uitbreiding van het gross tumor volume (GTV) bij RCC botmetastasen meer accuraat weergeeft dan CT, mogelijk door verbeterde visualisatie van beenmerginfiltratie en weke delen infiltratie. Intekenen alleen gebaseerd op CT zou kunnen resulteren in een onderschatting van het werkelijke volume, wat mogelijk kan leiden tot een te lage dosering in een deel van het doelgebied van de SBRT behandelplannen. Intekenen van RCC botmetastasen op MRI resulteert in klinisch relevante en statistisch significant grotere GTV's vergeleken met het intekenen van dezelfde afwijkingen op CT.

#### ***Hoofdstuk 4. Ontwikkeling en evaluatie van een MRI gebaseerde intekenrichtlijn voor nierceltumoren***

Bij MRI-gestuurde radiotherapie van de nier wordt verwacht dat (conebeam-) CT niet meer nodig zal zijn voor het plannen en uitvoeren van de radiotherapie behandeling. Voor MRI-gestuurde radiotherapie is een richtlijn voor MRI-gebaseerd intekenen van belang. Gebaseerd op de T2 gewogen MRI, met behulp van een T1 gewogen opname met contrast en DWI, is een intekenrichtlijn voor RCC op MRI ontwikkeld en geëvalueerd. De inter-observer intekenvariaties waren klein. De aanbevelingen en richtlijn beschreven in deze studie kunnen gebruikt worden voor de introductie van MRI-gestuurde radiotherapie voor primaire RCC in de kliniek.

#### ***Hoofdstuk 5. Intrafractie beweging van RCC voor MRI-gestuurde SBRT***

Een van de grootste uitdagingen bij SBRT voor RCC is beweging van de nier tijdens de behandeling. Met name de ademhalingsbeweging is complex, verandert over de tijd en verschilt per individu. In dit hoofdstuk ligt de focus op de intrafractiebeweging (tijdens het afstralen van het plan). Om MRI-gestuurde radiotherapie voor RCC voor te bereiden, is het nodig om de beweging en de drift van de RCC laesie voor een groep patiënten tijdens de duur van een behandel fractie te meten, om zo realistisch mogelijk te kunnen simuleren wat er tijdens de behandeling gebeurt. Met de intrafractiebeweging kan een planned target volume (PTV) marge berekend worden (en mogelijk gereduceerd worden). De bijdrage van zowel een hoge amplitude ademhalingsbeweging en trage drifts zijn meegenomen in het bepalen van een benodigde PTV marge. De huidige resultaten laten zien dat bovenop de huidige methoden voor compensatie voor beweging, een toekomstige compensatie voor de drift (tumor trailing) de PTV marge tot 75% zou kunnen reduceren. Dit maakt tumor trailing een interessante optie om te overwegen in de toekomstige behandeling van primaire RCC met MRI-gestuurde radiotherapie.

#### ***Hoofdstuk 6. MRI-acquisitie voor gecombineerde 4D-MRI en dynamic contrast enhanced (DCE) beeldvorming voor abdominale SBRT planning***

Voor SBRT behandelingen zijn accurate beeldvorming voor precies intekenen, lokaliseren van de tumor en beeldsturing van de tumoren en risico-organen (OARs) voor en tijdens de behandeling van groot belang. In aanvulling op een CT scan, kunnen anatomische (T1,T2) en functionele (bijvoorbeeld DCE, DWI) MRI sequenties van toegevoegde waarde zijn voor het intekenen van de tumor. DCE-MRI wordt gebruikt om het contrast tussen tumor, gezond nierweefsel en andere OAR's te vergroten. Daarbij wordt het gebruikt om tumor specifiek contrast te karakteriseren en wordt het gebruikt om perfusie parameters te kwantificeren. 4D-MRI kan gebruikt worden om de midpositie van de tumor te berekenen. Echter, zowel DCE-MRI als 4D-MRI zijn langdurige scans. Deze studie laat een tweeledige MRI-acquisitie

zien, welke DCE-MRI en 4D-MRI combineert om zo hoge spatio-temporele DCE volumes voor contrast vergroting te verkrijgen. Tevens zorgt een aanvullende 4D-MRI reconstructie voor tumor intekening en precies karakteriseren van beweging. Met deze combinatie is een aparte 4D-MRI niet nodig, terwijl het comfort van de patiënt en de reproduceerbaarheid van de DCE acquisitie wordt vergroot, omdat er geen breath-holds nodig zijn. Een extra 5D reconstructie bewijst met name handig te zijn voor het minimaliseren van bewegingsgeïnduceerde vertroebelen van de randen van de tumor. De combinatie van 3 verschillende reconstructies is uniek en waardevol in de context van MRI-gestuurde radiotherapie, voor tumor karakterisatie, accurate intekeningen en het verkrijgen van midpositie volume.

***Hoofdstuk 7. Stereotactische radiotherapie van inoperabele patiënten met een niercelcarcinoom (ARREST studie): studie protocol en eerste klinische ervaring.***

Voordat we veilig patiënten met een RCC kunnen behandelen op de MRI-linac, moeten we eerst meer ervaring opdoen in het behandelen van RCC met SBRT en de integratie van MRI in de workflow voor RCC optimaliseren. In het ARREST studieprotocol wordt een fiducial marker, cone-beam CT gebaseerde SBRT beschreven voor inoperabele patiënten met RCC. De ARREST studie is een fase II studie gericht op veiligheid en haalbaarheid. Anders dan in eerdere studies van SBRT voor RCC zal een abdominaal korset gebruikt worden om de ademhalingsbeweging te verminderen, evenals een midventilatie benadering, MRI-gebaseerde bewegingskarakterisatie en MRI-(en CT-) gebaseerde tumor intekeningen. Tevens kan in de toekomst met de resultaten uit de ARREST studie een MRI-gebaseerde respons predictie en respons evaluatie ontwikkeld worden. Het studie protocol van de ARREST studie en de eerste klinische resultaten zijn beschreven in hoofdstuk 7. Tot nu toe hebben 2 patiënten de behandeling voltooid en de studie is open voor inclusie. De ARREST-studie is een voorbereidende studie voor de volledige MRI-gestuurde SBRT techniek voor RCC, welke naar verwachting de komende jaren op de MRI-linac geïntroduceerd zal worden.



## REVIEW COMMITTEE

Prof. dr. I.H.M. Borel Rinkes, chair  
*Professor of Surgery, University Medical Center Utrecht, The Netherlands*

Prof. dr. B.J. Slotman  
*Professor of Radiation Oncology, VU University Medical Center Amsterdam, The Netherlands*

Prof. dr. B.W. Raaymakers  
*Professor of Experimental Clinical Physics, University Medical Center Utrecht, The Netherlands*

Dr. H.G. van der Poel  
*Urologist, The Netherlands Cancer Institute, Antoni van Leeuwenhoek Hospital Amsterdam, The Netherlands*

Prof. dr. J. Hendrikse  
*Professor of Radiology, University Medical Center Utrecht, The Netherlands*





## LIST OF PUBLICATIONS

Stemkens B, **Prins FM**, Bruijnen T, Kerkmeijer LGW, Lagendijk JJW, van den Berg CAT, Tijssen RHN. A dual-purpose MRI acquisition to combine 4D-MRI and Dynamic Contrast-Enhanced imaging for abdominal stereotactic body radiotherapy planning. *Submitted*

**Prins FM**, Stemkens B, Kerkmeijer LGW, Barendrecht MM, de Boer JCJ, Vonken EPA, Lagendijk JJW, Tijssen RHN. Intrafraction motion management of renal cell carcinoma with MRI guided stereotactic body radiotherapy. *Submitted*

**Prins FM**, Kerkmeijer LGW, van der Voort van Zyp JRN, Eppinga WSC, Heerkens HD, Lagendijk JJW, Tijssen RHN, Vonken EPA, Kotte ANTJ, Barendrecht MM, Chu W, Intven MPW. Development and evaluation of a MRI based delineation guideline for renal cell carcinoma. *Submitted*

**Prins FM**, van der Velden JM, Gerlich AS, Kotte ANTJ, Eppinga WSC, Kasperts N, Verlaan JJ, Pameijer FA, Kerkmeijer LGW. Superior target delineation for stereotactic body radiotherapy of bone metastases from renal cell carcinoma on MRI compared to CT. *Ann Palliat Med* 2017;6: S147-S154.

Stemkens B, Glitzner M, Kontaxis C, de Senneville BD, **Prins FM**, Crijns SPM, Kerkmeijer LGW, Lagendijk JJW, Van den Berg CAT, Tijssen RHN. Effect of intrafraction motion on the accumulated dose for free-breathing MR-guided stereotactic body radiation therapy of renal-cell carcinoma. *Phys Med Biol.* 2017 Sep 1;62(18):7407-7424.

Kontaxis C, Bol GH, Stemkens B, Glitzner M, **Prins FM**, Kerkmeijer LGW, Lagendijk JJW, Raaymakers BW. Towards fast online intrafraction replanning for free-breathing stereotactic body radiation therapy with the MR-linac. *Phys Med Biol.* 2017 Aug 21;62(18):7233-7248.

**Prins FM**, Kerkmeijer LGW, Pronk AA, Vonken EPA, Meijer RP, Bex A, Barendrecht MM. Renal cell carcinoma: alternative nephron-sparing treatment options for small renal masses, a systematic review. *J Endourol.* 2017 Oct;31(10):963-975.

Glitzner M, Crijns SPM, Denis de Senneville B, Kontaxis C, **Prins FM**, Lagendijk JJW, Raaymakers BW. On-line MR imaging for dose validation of abdominal radiotherapy. *Phys Med Biol.* 2015 Nov 21;60(22):8869-83.



## DANKWOORD

Dit proefschrift en de projecten rondom het proefschrift zijn tot stand gekomen door de hulp en steun van vele mensen. Iedereen die zich heeft ingezet wil ik daarom ook hartelijk bedanken! In de eerste plaats de patiënten die hebben meegewerkt in de MRI-RCC en de ARREST studie. Dankzij u hoop ik een bijdrage te kunnen leveren aan het ontwikkelen van een nieuwe behandeling voor patiënten met nierceltumoren. Daarnaast zijn er nog een aantal mensen die ik in het bijzonder wil bedanken.

Prof. dr. J.J.W. Lagendijk en prof. dr. C.H.J. Terhaard, mijn promotoren. Beste Jan, halverwege mijn onderzoek ben je betrokken geraakt, desalniettemin was je meteen enthousiast over dit project. Bedankt voor de enthousiaste begeleiding en voor je kritische houding en blik ten aanzien van het onderzoek. Dank voor de rust en het vertrouwen dat je me hebt gegeven dat alles wel goed ging komen. Beste Chris, als laatste aangesloten bij het promotieteam, bedankt voor het meedenken en meewerken in de afronding van het project.

Dr. L.G.W. Kerkmeijer en dr. M.M. Barendrecht, mijn co-promotoren. Beste Linda, vanaf het eerste moment ben je betrokken geweest bij mijn onderzoek. Deze betrokkenheid heeft geresulteerd in een erg goede samenwerking. De afgelopen 3 jaar heb ik veel van je mogen leren. Dank voor je altijd kritische blik en vragen, jaloersmakende nauwkeurigheid van werken en punctualiteit. Dank voor je enthousiasme over het project en de begeleiding van mij op persoonlijk vlak. Door jou ben ik gegroeid en is mijn wetenschappelijke blik verbreed. Door jouw enthousiasme over de radiotherapie heb je me bijna van gedachten doen veranderen. Ik ben blij dat je in het laatste half jaar precies op tijd terug was voor het afronden van het project. Beste Maurits, nog voor het promotietraject begon was je al betrokken bij dit project. Dank voor je hulp bij het creëren van de mogelijkheid om deze onderzoekslijn op te zetten. Dank voor je enthousiasme, het out-of-the-box denken en de sturing in de focus op de klinische lijn in dit project. Ik heb veel van je mogen leren en ben blij dat we de samenwerking in de kliniek kunnen voortzetten. Linda en Maurits, dank voor de afgelopen jaren, ik ben er trots op jullie eerste promovendus te mogen zijn, opdat er nog een stuk of honderd mogen volgen!

Dr. R.H.N. Tijssen, dr. M. Intven, mijn surrogaat co-promotoren/motoren. Beste Rob, halverwege mijn promotie ben je ingesprongen voor de klinisch-fysische en technische kant van het verhaal. Bedankt voor je intensieve begeleiding, vriendelijkheid, geduld en uitgebreide uitleg over de MR-fysica (aan een promovendus zonder natuurkundige achtergrond). Hoe dit is gelukt naast je drukke werkzaamheden is mij een raadsel, maar ik ben je er erg dankbaar voor. Jij hebt ervoor gezorgd dat mijn proefschrift vorm begon te krijgen en de lastige fysische vraagstukken opgelost werden. Beste Martijn, het laatste jaar van mijn promotie ben je van onmisbare hulp geweest voor klinische lijn van mijn

proefschrift. Bedankt voor de tijd die je erin gestoken hebt naast je drukke klinische werkzaamheden. Dus, Rob en Martijn, bedankt voor de sturing en begeleiding die jullie hebben gegeven in het laatste jaar, hierdoor had ik de mogelijkheid mijn promotietraject te continueren en goed af te ronden.

Prof. dr. I.H.M. Borel Rinkes, Prof. dr. B.J. Slotman, Prof. dr. B.W. Raaymakers, Dr. H.G. van der Poel, Prof. dr. J. Hendrikse, leden van de beoordelingscommissie. Hartelijk dank voor het lezen en beoordelen van mijn proefschrift.

Prof. dr. M. van Vulpen. Beste Marco, bedankt voor het enthousiasme en vertrouwen dat je in me gesteld hebt voor het opstarten van klinische studies op het gebied van de nier en het creëren van een plek die dat mogelijk heeft gemaakt. Helaas hebben we dit traject niet samen kunnen afronden.

Dr.W. Chu. Dear William, thanks for lending me the opportunity to come and visit Sunnybrook Hospital to learn the details of treating renal cell carcinoma with radiotherapy. Thank you for your time to share knowledge and experience. It was a great pleasure to spend time in Toronto, and I am looking forward towards future collaboration.

Alle medewerkers van de afdeling radiotherapie, bedankt dat ik hier de afgelopen 3 jaar heb mogen werken, een betere plek om onderzoek te doen had ik me niet kunnen wensen. Een aantal mensen wil ik hierbij nog in het bijzonder noemen.

Het secretariaat, lieve Leonie, Judith, Yvette en Therese. Jullie zijn fantastisch! Een onmisbare kracht op de afdeling. Dank voor alle hulp die jullie mij geboden hebben en het luisterende oor op zijn tijd.

De laboranten en in het bijzonder Jochem Hes. Dank voor je uitgebreide hulp bij het maken van bestralingsplannen voor de ARREST studie, dank voor het op de (laboranten)kaart zetten van het bestraling van nierceltumoren in Nederland. De MRI-laboranten en in het bijzonder Tuan en Ellart, dank voor jullie hulp bij het uitvoeren van de MRI-RCC en later de ARREST studie. Door jullie meewerken en meedenken hebben we deze projecten tot een succes kunnen maken.

Alexis en Gijs, dank voor het meewerken in de verschillende studies, het last-minute doen van analyses en jullie geduld mij hierover (bij herhaling) uitleg te geven.

Het trialbureau en in het bijzonder Saskia: je bent absoluut onmisbaar geweest voor de twee METC aanvragen die we hebben gedaan en zijn goedgekeurd. Bedankt voor je kritische blik, nauwkeurig werken en gezelligheid. Hierdoor is de samenwerking soepel verlopen en hebben we het binnen afzienbare tijd goed kunnen regelen.

De mannen van de ICT en in het bijzonder Erwin. Bedankt dat ik je voor alle "er is iets met mijn computer" problemen altijd kon storen en dat je altijd snel en vriendelijk met een goede oplossing bent gekomen. Dat maakt het leven van een promovendus een stuk gelukkiger.

De radiotherapeuten, het uro-radiotherapie-team en in het bijzonder Jochem en Wietse. Tijdens mijn semi-artsstage heb ik jullie leren kennen en daarmee is de samenwerking meteen begonnen. Dank voor jullie enthousiasme over de nierprojecten, kritische houding ten aanzien van de studie opzet en includeren van patiënten. Bedankt dat ik met vragen altijd bij jullie terecht kon.

Simon, thank you so much for proofreading my introduction and discussion in order to make this thesis grammatically and linguistically correct.

Alle fysica onderzoekers en in het bijzonder Markus, Bjorn en Charis. Since 2 out of 3 are not Dutch I'll continue in English. Thank you so much for the collaboration in the kidney projects (most of the times with last-minute requests), and helping me understand the basics in MR-physics.

Alle mede-auteurs, bedankt voor jullie inzet en betrokkenheid bij de verschillende onderzoeken. In het bijzonder wil ik hierbij nog bedanken dr. E.P.A. Vonken. Beste Evert-Jan, bedankt voor je radiologische blik op de verschillende projecten, de tijd die je hebt vrijgemaakt om verschillende scans te herbeoordelen en mij er extra uitleg over te geven. Het enthousiasme waarmee je deelneemt aan de ARREST studie waardeer ik zeer. Zeker het moment waarop we de nieuwe goudmakers in gebruik hebben genomen, een memorabel staaltje onderzoek. Tevens een woord van dank aan dr. A. Bex. Beste Axel, bedankt voor de extra tijd die je in het review hebt gestoken om het tot een succes te maken.

Lieve arts-onderzoekers, partners in crime, lotgenoten. We zijn een bijzondere groep waar ik me vanaf het begin erg in thuis heb gevoeld, ook al zijn we in de loop van de jaren al geheel van samenstelling gewisseld. Op onderzoeksvlak heb ik veel van jullie kunnen leren, maar ook op sociaal vlak hebben jullie een onuitwisbare indruk gemaakt. Wat heb ik een mooie tijd met jullie gehad, in de Baai van het Goede, op congressen, met de vrijdagmiddagborrels (die niet echt van de grond kwamen), biertjes gedronken, maar nog veel meer koffie gedronken en taart gegeten. Hoogtepunten gevierd en om dieptepunten samen gehuild. Een turbulente 3 jaar achter de rug, maar dankzij jullie waren die 3 jaar fantastisch, bedankt!

Sieske en Marieke, lieve kamergenoten. Ik wil jullie bedanken voor de steun die jullie mij gegeven hebben, de afleiding wanneer het nodig was en de rust om hard door te werken. Dank voor jullie hulp met mijn proefschrift en de voorbereiding naar de dag van mijn

verdediging. Wat ben ik blij dat jullie mijn paranimfen zijn, onrust zal niet snel ontstaan met twee nuchtere Rotterdammers aan mijn zijde. In de toekomst hoop ik jullie, naast in het sociale leven, ook op de werkvloer nog vaak tegen te mogen komen: zie jullie op de OK!

Lieve vrienden en vriendinnen, jullie maken het leven zo veel leuker! Dank jullie wel voor alle leuke momenten, samen borrelen, sporten, feesten, dansen, kletsen, koken, vakantie vieren, maar ook dank voor jullie steun en begrip in de afrondende fase van mijn promotie. Jullie helpen me herinneren dat we werken om te leven en niet leven om te werken. Op naar een heerlijke zomer met meer tijd samen!

Lieve Anne-To en Ernst, bij het starten van mijn promotietraject waren jullie meteen enthousiast en aanmoedigend om deze kans te nemen. Bedankt voor de oprechte interesse in, kritische vragen en enthousiasme over mijn onderzoek. Dank voor jullie liefde en steun de afgelopen jaren.

Lieve Eefje en Gemma, wat fijn om zulke mooie mensen mijn liefste zussen te mogen noemen. We werken alle drie in een totaal andere wereld en parallellen zijn soms ver te zoeken, maar desalniettemin zijn de adviezen die daaruit voortvloeien soms de beste. Fijn dat jullie zo hebben meegedeeld met mijn onderzoek en afronding ervan, dank voor jullie steun en betrokkenheid, maar met name jullie liefde en gezelligheid.

Lieve Pap en Mam, lieve Henk en Babs, dank voor jullie onvoorwaardelijke liefde en steun. Jullie hebben mij gezegend met doorzettingsvermogen (zo'n koppige Prins), kracht, interesse, aandacht voor je medemens en liefde, wat ervoor heeft gezorgd dat ik nu hier sta. Dank voor jullie aandacht en ondersteuning in de afgelopen periode. Ik ben trots te mogen zeggen dat jullie mijn ouders zijn.

Lieve Rogier, liefde van mijn leven, mijn steun en toeverlaat. Zonder jou was dit proefschrift er nooit geweest. Dank voor je liefde, geduld en onvoorwaardelijke steun. Dank voor de ruimte die je me hebt gegeven om tot in de late uren door te werken, dat je ondanks mijn ongeduld en frustratie me bent blijven helpen en ondersteunen. Het is een voorrecht om mijn leven met zo'n bijzondere man te mogen delen. Ik kijk uit naar een gelukkig leven samen.

*Fieke*







## CURRICULUM VITAE

Fieke Maria Prins was born on the 18<sup>th</sup> of July 1987 in Bedum, the Netherlands. After primary school in Bedum, she attended the H.N.Werkmancollege in Groningen, where she received her VWO-diploma in 2006. That same year she commenced studying Pharmacy at the University of Groningen. In 2007 she decided to switch studies and started with Medicine at the same university. During her internships she developed a special interest in Urology, and therefore the senior internship took place at the department of Urology at the University Medical Centre Utrecht (UMCU). She fulfilled her other senior internship at the Radiation Oncology department. The scientific part of her final year was a collaboration between the Urology and Radiation Oncology department of the UMCU. Following this research project, she started working as a PhD-candidate in April 2015, focusing on radiotherapy for renal cell carcinoma. In October 2015 she visited Sunnybrook Hospital in Toronto, Canada to gain experience in treating patients with radiotherapy for kidney cancer. She combined her final year as a PhD-candidate with a part-time position as urological resident not in training (ANIOS) at the Antonius Hospital in Nieuwegein. Since December 2017 she has been working full-time as a urological resident not in training (ANIOS) at the Tergooi Hospital in Blaricum.



Fieke currently lives in Utrecht and loves to spend her free time playing cello, enjoying different kinds of sports (indoor climbing, running, field hockey), reading, and traveling.